AD-A084 847 ROSENSTIEL SCHOOL OF MARINE AND ATMOSPHERIC SCIENCE --ETC F/G 8/1
PHYSIOLOGICAL OPTICS OF THE EYE OF THE JUVENILE LEMON SHARK (NE--ETC(U)
MAY 80 R E HUETER N00014-75-C-0173
UNCLASSIFIED UM-RSMAS-80003 NL

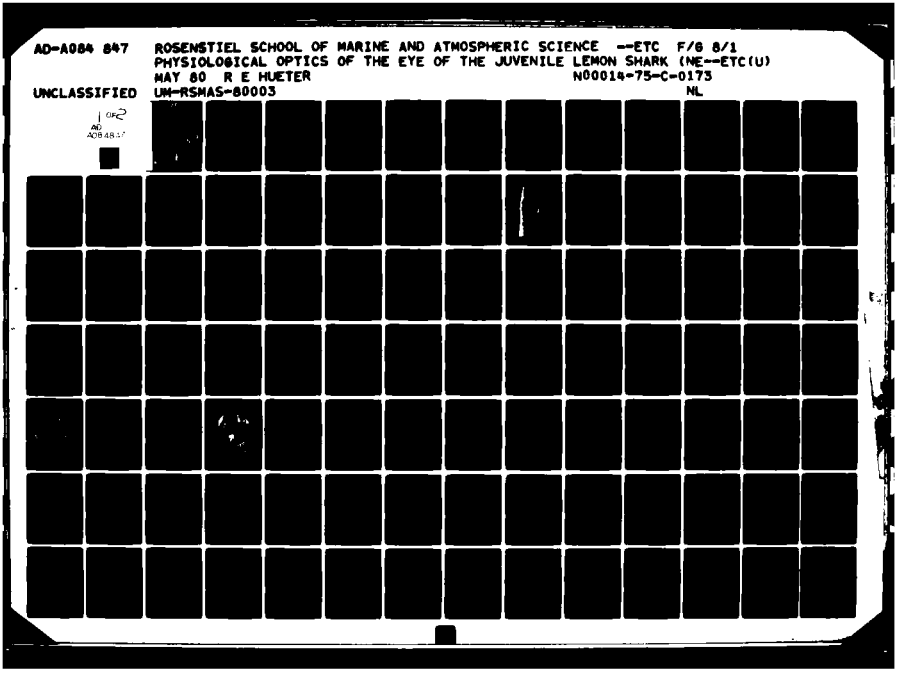

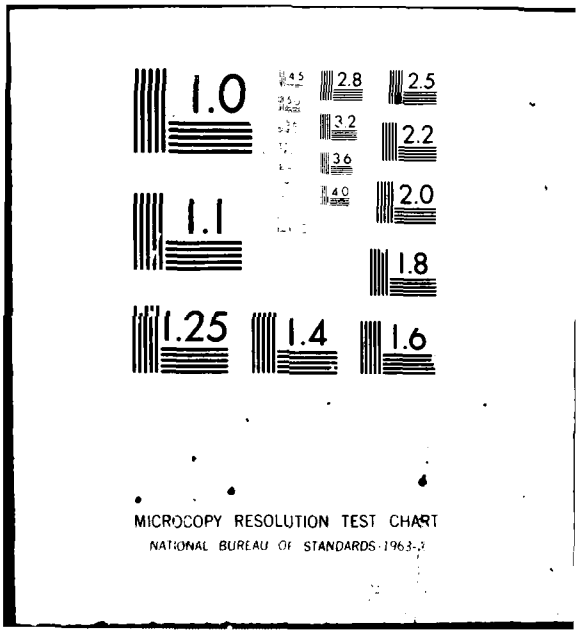
1.0
2.8
2.5
3.2
2.2
3.6
4.0
2.0
1.1
1.8
1.25
1.4
1.6
MICROCOPY RESOLUTION TEST CHART
NATIONAL BUREAU OF STANDARDS-1963-A

LEVEL

UNIVERSITY OF MIAMI

ROSENSTIEL SCHOOL OF MARINE AND ATMOSPHERIC SCIENCE

UM RSMAS-80003

Technical Report

May, 1980

PHYSIOLOGICAL OPTICS OF THE EYE OF THE JUVENILE LEMON SHARK (NEGAPRION BREVIROSTRIS)

by

Robert E. Hueter

The Office of Naval Research
Contract N00014-75-C-0173

MIAMI, FLORIDA 33149

UNIVERSITY OF MIAMI
ROSENSTIEL SCHOOL OF MARINE AND ATMOSPHERIC SCIENCE
4600 Rickenbacker Causeway
Miami, Florida 33149

TECHNICAL REPORT

May, 1980

PHYSIOLOGICAL OPTICS OF THE EYE OF THE JUVENILE LEMON SHARK (NEGAPRION BREVIROSTRIS)

by

Robert E. Hueter

A Report to the Office of Naval Research
of Research Supported by
Contract N00014-75-C-0173

UM RSMAS-80003

William W. Hay
Dean

HUETER, ROBERT EDWARD (M.S., MARINE BIOLOGY)

Physiological Optics of the Eye of the Juvenile Lemon Shark (Negaprion brevirostris). (May, 1980)

Abstract of a master's thesis at the University of Miami.
Thesis supervised by Dr. Samuel H. Gruber.

A schematic eye for the eye of the average juvenile lemon shark inhabiting Florida Bay, a shallow marine environment marked by high turbidity, was constructed. The crystalline lens in this eye is the sole refractive element, with an overall equivalent refractive index of 1.664 and a principal power of approximately +140 diopters. The eye is hypermetropic by nearly +3 diopters in seawater, although retinoscopic measurements of the refractive state of this eye average +7.5 diopters. Sources of this discrepancy are evaluated.

Retinal magnification factor (RMF) in this eye is 164 μm/°visual angle; minimum separable angle (MSA) predicted from the RMF and average intercone distance is approximately 4.1', but this type of visual acuity will be adversely affected by the hypermetropia. Even so, the slight hypermetropia and observed intraocular opacity of eyes are probably secondary to the poor quality of their photic environment.

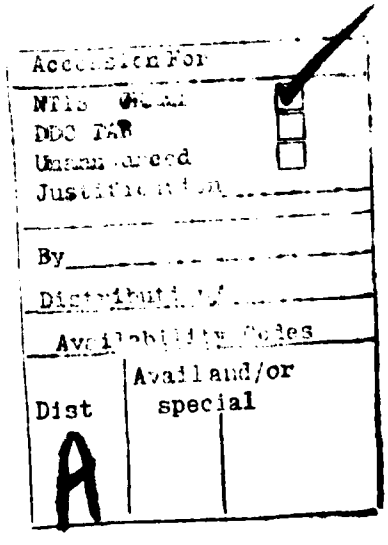

ACKNOWLEDGMENTS

Many persons kindly assisted me in a variety of ways throughout the course of this study. I first thank Dr. Samuel Gruber (University of Miami-RSMAS), who initially directed me into the area of research, served as my committee chairman, and provided substantial support along the way. Drs. Howard Gordon (University of Miami, Department of Physics), Arthur Myrberg (RSMAS), and Thorne Shipley (University of Miami, Department of Ophthalmology) served on my committee, and I thank them collectively for their valuable contributions and their enthusiasm for the project. Drs. Douglas Anderson and Ronald Radius (University of Miami, Department of Ophthalmology) also provided important suggestions and support. Assistance in the initial design of the research, as well as periodic inspiration along the way, was provided by Dr. Jacob Sivak (University of Waterloo, Department of Optometry).

I received an immeasurable amount of guidance from Dr. Duco Hamasaki (University of Miami, Department of Ophthalmology) who, though not officially associated with my research project, made his laboratory, experience, and knowledge completely open to me. I also thank the supporting staff working under Drs. Hamasaki and Anderson, including Mr. Barry Davis and Ms. Barbara French, who provided essential technical materials and assistance. Dr. John Flynn (University of Miami, Department of Ophthalmology) aided me with the retinoscopic work; further assistance and helpful discussions were contributed by practicing ophthalmologist Dr. Stanley Spielman. My thanks are also due to Drs. Harry Schultz and Arthur Keenan (University of Miami, Department of Chemistry), for the use of their Abbé refractometer.

Many friends at RSMAS provided valuable time and assistance through the duration of the project. Mr. Tom Walmsley supervised the collection, care, and

maintenance of the experimental animals, and periodically furnished technical aid. I thank Ms. Marcie Jacobs for so ably typing the final manuscript, and Mr. Don Heuer and his staff for assistance with the printing. Mr. John Reynolds provided tangible as well as intangible support during my sojourn at RSMAS, and I thank him for his friendship and encouragement. My deepest gratitude is extended to Dr. Joel Cohen, presently at the Harvard Biological Laboratories, who generously gave so much in so many ways that it would be impossible to enumerate all of his contributions.

I also thank, for their support and assistance, my friends on the editorial staff at the International Oceanographic Foundation in Miami, as well as a special thanks to Mr. Christopher Migliaccio. All of the members of my family provided constant encouragement and support as always, and to them I am deeply indebted for their faith in me; and to Ms. Susan Markley, who made the various successes and failures worthwhile.

Finally, I acknowledge the generous financial support of the following sources: Office of Naval Research Contract N00014-75-C-0173 to S.H. Gruber (with special thanks to Ms. Ruth Trencher); a Sigma Xi Grant-in-Aid; a UM Bader Research Fund Award; a UM Graduate Fellowship; and private grants from the Walter E. Heller Co. and Mr. Leo Gordon of Key Biscayne, Florida.

TABLE OF CONTENTS

LIST OF FIGURES

LIST OF TABLES

INTRODUCTION

> My nose is sufficiently good. My eyes are large and gray; although, in fact, they are weak to a very inconvenient degree, still no defect in this regard would be suspected from their appearance.
>
> --Edgar Allan Poe, "The Spectacles"

Conspicuously lacking in our understanding of visual function in sharks is a more than cursory analysis of the refractive components of the shark eye. This serious omission of the first-order visual process in these animals has hindered all attempts to explore their capabilities for spatial vision, expressed as visual acuity and discrimination. The well described extreme sensitivity of the shark eye to low illumination, and the resulting characterization of this eye as functioning primarily in the scotopic visual range, have precluded close attention to the dioptrics of the shark eye. With the thorough evidence of photopic visual function in sharks that now exists (Gruber, 1975), the physiological optics of these animals should no longer be ignored.

I. COMPARATIVE PHYSIOLOGICAL OPTICS

Quantitative studies of comparative optics have been concerned primarily with the following areas: (1) description of the individual optical components in the "average" eye of an animal species, including refractive indices of the ocular media, intraocular dimensions, and radii of curvature of refractive surfaces; (2) determination of the animal's refractive state, which denotes the proximity of the eye's back focal point with respect to the retina; (3) demonstration of capability of the species for accommodation, which is the ability of the eye to vary its optical power, so that a focused image can be maintained on the retina for varying distances between the eye and objects in the visual field; and

(4) measurement of the extent of the animal's horizontal and vertical visual fields, both monocular and binocular. Given that the first of these study areas is carried to completion with adequate sample sizes, a mathematical model of the dioptrics of the average eye of the species can be constructed, and this model can subsequently be used to corroborate indirect measurements of refractive state in that species. This quantitative dioptric model is known as a schematic eye; its calculation employs thick-lens theory, derived from geometrical optics, to specify the dioptric behavior of light rays entering the eye.

The first schematic eye models were developed for the human eye. Following Gauss's (1841) elucidation of the conditions for reducing a compound optical system to three pairs of points, known as cardinal points, Listing (1845) produced a reduced eye model for the human eye, representing cornea and lens as a single refractive surface. von Helmholtz's vital contributions between 1856 and 1866, combined with Listing's work and that of Tscherning (1898), allowed Gullstrand to formulate his human schematic eye around 1908 (for von Helmholtz and Gullstrand contributions, see Von Helmholtz, 1924). Gullstrand's schematic eye, though continuously adjusted since its introduction through more precise measurements (Westheimer, 1972), is still basically in use today. Listing's reduced eye is adequate for human dioptric analyses not requiring fine precision.

From this historical development, the formulation of schematic eye models has progressed to its present importance, expressed by Vakkur and Bishop (1963: p. 357):

> A schematic eye is a self-consistent mathematical model of the optical system of the average eye. Its development in man forms the science of physiological optics, and the design of spectacles and the use of optical instruments in ophthalmology have largely depended upon it.

The primary purpose of constructing a schematic eye is to locate the positions of the six cardinal points of an eye's optical system (Hughes, 1977).

These cardinal points are the front and back focal points, first and second principal points, and first and second nodal points. All are located on the optical axis, the line which passes through the optical (and geometric) centers of the principal refractive elements of the eye (cornea front and back surfaces, lens front and back surfaces).

The focal points are located at the positions on the eye's optical axis where light rays from an infinitely distant object are brought into focus; the back focal point is the real point of focus for the eye, whereas the front focal point is the theoretical point of focus if light rays could be passed through the eye in the reverse direction, i.e. from retina to cornea. The principal points locate the planes, perpendicular to the optical axis, at which equivalent thin lenses could be substituted to represent the eye's entire optical system. The first and second nodal points locate the "optical pivots" of the eye: a light ray directed toward the first nodal point will appear to emerge from the second nodal point along the same angle of incidence; these points are essential in defining visual angle and image size for an eye. Further descriptions of the characteristics of the cardinal points can be found in Campbell et al. (1974).

The formulation of a complete schematic eye requires the specification of the position and radius of curvature of each refractive surface and the refractive indices of all optical media of the eye. The theory and mathematical procedures underlying the schematic eye calculations are presented by Bennett and Francis (1962).

The most recent, extensive treatment of the optical systems of vertebrate eyes was that of Hughes (1977). Although his review centered on the visual physiology of mammals, Hughes quite ably addressed himself to the comparative optics of fishes, amphibians, lizards, and birds, as well as mammals. Hughes's paper deserves special note, for it represents the first attempt to bring together

the diverse sources of quantitative information on the physiological optics of many species. Prior to this work, the writings of Franz (1934), Walls (1942), Rochon-Duvigneaud (1943), Polyak (1957), and Duke-Elder (1958) provided the solid qualitative foundation for comparative studies of the visual systems of vertebrates.

According to Hughes (1977), descriptive treatment of animal optics began with Newton's schematic diagram of a sheep eye, published around 1680. The fundamental quantification of the optics of vertebrate eyes, however, did not begin until the works of Matthiessen (1879-1893) and Hirschberg (1882) appeared. Then, for nearly a century, the subject of comparative optics was all but forgotten; the use of this information to formulate schematic eyes for animals awaited the demands of neurophysiological studies of vision, which began to flourish in the early 1960s. Subsequently, a steady stream of schematic eyes has appeared in the past two decades; these include models for the eyes of the cat (Vakkur and Bishop, 1963), rat (Block, 1969; Massof and Chang, 1972; Hughes, 1979a), rabbit (Hughes, 1972), opossum (Oswaldo-Cruz et al., 1979), pigeon (Marshall et al., 1973), and frog (duPont and deGroot, 1976). The only schematic eye developed for a fish was Charman and Tucker's (1973) compromised model of the goldfish eye.

II. PHYSIOLOGICAL OPTICS OF THE FISH EYE

Optical studies of the eyes of fishes have dealt almost exclusively with the determination of "the refractive state of the fish eye," as if the approximately 25,000 species of fishes, occupying a myriad of different ecological niches, should share equal optical demands. Not surprisingly, this quest has been met with confusion and controversy. Present knowledge on the refractive state of the teleost eye was initially drawn from the results of extensive experiments by

Beer (1894), who used an ophthalmoscope for most of his measurements of refractive state. Beer discovered hypermetropia (far-sightedness) in the majority of species that he examined. (A hypermetropic condition means that the dioptric power of the eye is weaker than is required to correctly focus the image of a distant object on the retina; the back focal point of the eye lies behind the photoreceptors, so that no object can be sharply imaged on the retina without some type of accommodatory adjustment. The nearer an object is to the hypermetropic eye, the more accommodation is required for sharp focusing.)

Though his results indicated general hypermetropia in fishes, Beer felt that he was measuring refractive error relative to the vitreal-retinal border rather than the level of the photoreceptors, so he adjusted his readings for the thickness of the retina. This adjustment resulted in myopia (near-sightedness) for most of the teleost species. (Myopia exists when the eye's dioptric power is stronger than that required to bring the back focal point conjugate with the photoreceptors; in the myopic eye, only images of objects located at one point in the near visual field can be sharply focused on the retina without accommodatory compensation.)

Using the technique of retinoscopy to assess refractive state, Verrier (1927, 1928, 1934) reported hypermetropia for various species of teleosts. No adjustment for retinal thickness was made, so her conclusions conflicted with those of Beer. Apparently unaware of Verrier's interpretation (or at least not acknowledging it), Walls (1942) branded the teleost eye as being myopic in general; when subsequent reports of retinoscopically measured hypermetropia in fishes appeared (Rochon-Duvigneaud, 1943; Baron and Verrier, 1951; Baylor and Shaw, 1962; Baylor, 1967), confusion reigned. Walls's words carried that much weight.

Recent investigations along these lines have concentrated on resolving the conflict between retinoscopic measurements and other determinations of refractive state, such as electrophysiological (Meyer and Schwassmann, 1970; Schwassmann and Meyer, 1971). It is now clear that retinoscopic measurements of refractive state in teleost fishes usually result in hypermetropic readings; but whether this hypermetropia is real, or is due to reflection from the vitreal-retinal boundary (Glickstein and Millodot, 1970; Schwassmann, 1975), or is biased because of chromatic aberration of the eye (Sivak, 1974a; Sivak and Bobier, 1978; Nuboer and van Genderen-Takken, 1978; Nuboer et al., 1979), or arises from yet another factor, is still open to debate. When adjustments for these confounding effects are made, the general degree of hypermetropia in the eyes of fishes is significantly reduced, approaching emmetropia (zero refractive error, where the unaccommodated eye's back focal point is located directly on the photoreceptors).

In-depth optical investigations on the refractive components of the fish eye have been less prolific. Matthiessen's studies of focal lengths of the crystalline lenses in fishes (1880, 1882) established a too generally applied rule that lens focal length in teleosts equals approximately 2.55 times the radius of the spherical lens. A useful discussion of elementary physiological optics of the teleost eye was contributed by Pumphrey (1961). The research of Tamura and his colleagues (Tamura, 1957; Tamura and Wisby, 1963; Kimura and Tamura, 1966; Somiya and Tamura, 1973) centered on the theoretical resolving power and axis of accommodation of teleosts, but their work was encumbered by heavy dependence on generalities such as Matthiessen's ratio and Walls's model of vision for all fishes. Sadler (1973) finally drew attention to these weaknesses, and, in recent years, there has been less tendency to generalize and more research on particular species, including considerations of specific habitats (e.g. Sivak, 1973).

Slightly more sophisticated approaches have been stimulated by the work of Charman and Tucker (1973), Sivak (1974a, 1976a), Sroczyński (1976a, 1976b, 1977), and Penzlin and Rönicke (1976). The optical analyses in this research, however, have lagged far behind the precedents established by schematic eye work on mammal eyes (see Hughes, 1977).

III. PHYSIOLOGICAL OPTICS OF THE SHARK EYE

A. Historical Background

Detailed investigations on the physiological optics of elasmobranchs (sharks, skates, and rays) are even more scarce than the work on teleosts. Sivak (1978a) has recently reviewed this paltry body of literature. According to Sivak, Beer included a small section on refraction of elasmobranchs in his 1894 study of the eyes of teleosts. Beer reported slight hypermetropia for the elasmobranch eye, but apparently did not indicate whether he had adjusted his readings for retinal thickness as he had for the teleosts.

Subsequent studies by Franz (1905, 1931) and Verrier (1930) dealt with attempts to induce accommodative changes in the eyes of a number of elasmobranch species, including sharks (e.g. Mustelus spp.), skates (e.g. Raja spp.), and rays (e.g. Torpedo spp.). Both workers reported consistent findings of hypermetropia for these various species, averaging around 7 to 10 diopters (D) of hypermetropia. [Diopter is a unit of measurement for lens power as well as refractive error; for lens power, the number of diopters equals the reciprocal of the lens focal length in meters. For example, a lens with a 50 cm focal length is a 1/0.5 = 2D lens. Diopters are also used in measurements of refractive state of an eye, to denote the equivalent lens power that must be added to (for hypermetropia) or subtracted from (for myopia) the optics of the eye to achieve emmetropia. A hypermetropic eye, therefore, has a +D refractive error; a myopic eye has a −D error.]

Despite Franz's (1931) report of accommodative movement in the eye of a torpedo ray, and Sivak's (1974b) and Sivak and Gilbert's (1976) retinoscopic studies of accommodation in three species of sharks (Negaprion brevirostris, Ginglymostoma cirratum, and Carcharhinus milberti), little attention has been paid to the optical properties of the refractive components of the elasmobranch eye. Incomplete data have been presented by Sivak (1976b, 1978a, 1978b) and Nicol (1978); aside from these reports, no attempt has been made to generate the types of quantitative measurements required to produce a schematic eye for an elasmobranch species. On the other hand, some quantitative work has been done on the spectral absorption of the lenses of elasmobranchs (Kennedy and Milkman, 1956; Zigman and Gilbert, 1978; Nicol, 1978).

Lengthy reviews by Franz (1934), Walls (1942), Rochon-Duvigneaud (1943), Gilbert (1963), and Gruber and Cohen (1978) have provided the groundwork for understanding the anatomical nature of the optical components of shark eyes; but no comprehensive analysis of the physiological optics of those components exists. Such an analysis must concentrate initially on the optical properties of one shark species; only after a complete description for one species has been established should interspecific comparisons between different sharks, elasmobranchs, or fishes in general be undertaken.

B. Objectives of this Study

1. Describe and define the dioptric properties of the refractive components in the eye of one shark species, to provide sufficient quantitative data so that a complete schematic eye for the species can be constructed;

2. Utilize alternative, indirect techniques of assessing refractive state in sharks, such as retinoscopy, to analyze the methodology of these indirect techniques and to draw comparisons between the results of the different methods;
3. Predict the optical limitations on spatial vision of the selected shark species, using the final adopted model of the optics of the species and incorporating any other relevant experimental data that are available;
4. Draw comparisons where possible between optical properties of the shark species and those reported for other aquatic vertebrates.

C. The Juvenile Lemon Shark

There are approximately 300 species of living sharks presently described (Compagno, 1977). My choice of the juvenile lemon shark (Negaprion brevirostris) as the model species for a description of the physiological optics of the shark eye was based on several factors. Most important of these was that extensive psychophysical and electrophysiological studies of vision in this animal have been conducted (e.g. Gruber, 1967, 1975; Cohen et al., 1977). A combination of the results of these types of studies, together with a mathematical model of the optics of the lemon shark eye, may ultimately allow a thorough description of this shark's visual system. A further consideration was that there were some preliminary data in the literature regarding the refractive state of juvenile lemon sharks (Sivak, 1974b).

In addition to these advantages, the juvenile lemon shark was deemed highly suitable for laboratory work due to two additional factors. Because many animals would be required for my overall study, it was necessary to select a species that would be available throughout the year; juvenile lemon sharks are

frequently the most abundant species of shark in the shallow coastal waters of Florida Bay and the Florida Keys at least half of the year (Springer, 1950), and are present in satisfactory quantities the remainder of the year. In addition, these animals are well adapted for experimental conditions, because of their ability to pump water over the gills and continue to respire during confinement, a rare trait among shark species.

A final consideration in choosing the lemon shark was its phyletic position among the selachians: as a carcharhinid, it is a member of the dominant group of the superorder Galeomorphi, which comprises 73% of all living shark species (Compagno, 1977). Thus, the lemon shark is not a bad choice as representing a "typical" shark for which a description of the refractive components of the shark eye could begin.

An additional trait of the lemon shark which deserves mention is that, by virtue of its large size (approximately 11 feet maximum total length), its predatory nature, and its residence in shallow coastal waters, this species is potentially dangerous to man. Out of the 267 cases from the world-wide Shark Attack File (SAF) in which the species of shark could be identified, six cases cited a lemon shark as the attacker (Baldridge, 1974).

Externally visible features of the ocular apparatus of the juvenile lemon shark include a nictitating membrane (Fig. 1), a vertical slit pupil that is mobile, and a slight degree of eye movement. Internal features of this eye are diagrammed in Fig. 2. The sclera is supported by a thick cartilagenous layer, and the nutritive choroid contains an occlusible tapetum lucidum, a reflective layer that is exposed under scotopic conditions. The retina is not vascularized and contains no known landmarks other than the optic disc. There is no fovea, and no area centralis has been reported for the species. The ellipsoidal lens is supported by a dorsal suspensory ligament and the ventral pseudocampanule (protractor

Fig. 1. Head of a juvenile lemon shark (Negaprion brevirostris) with the nictitating membrane partially extended and the mobile pupil approaching maximum constriction. The nictitating membrane does not normally extend in response to photic stimuli.

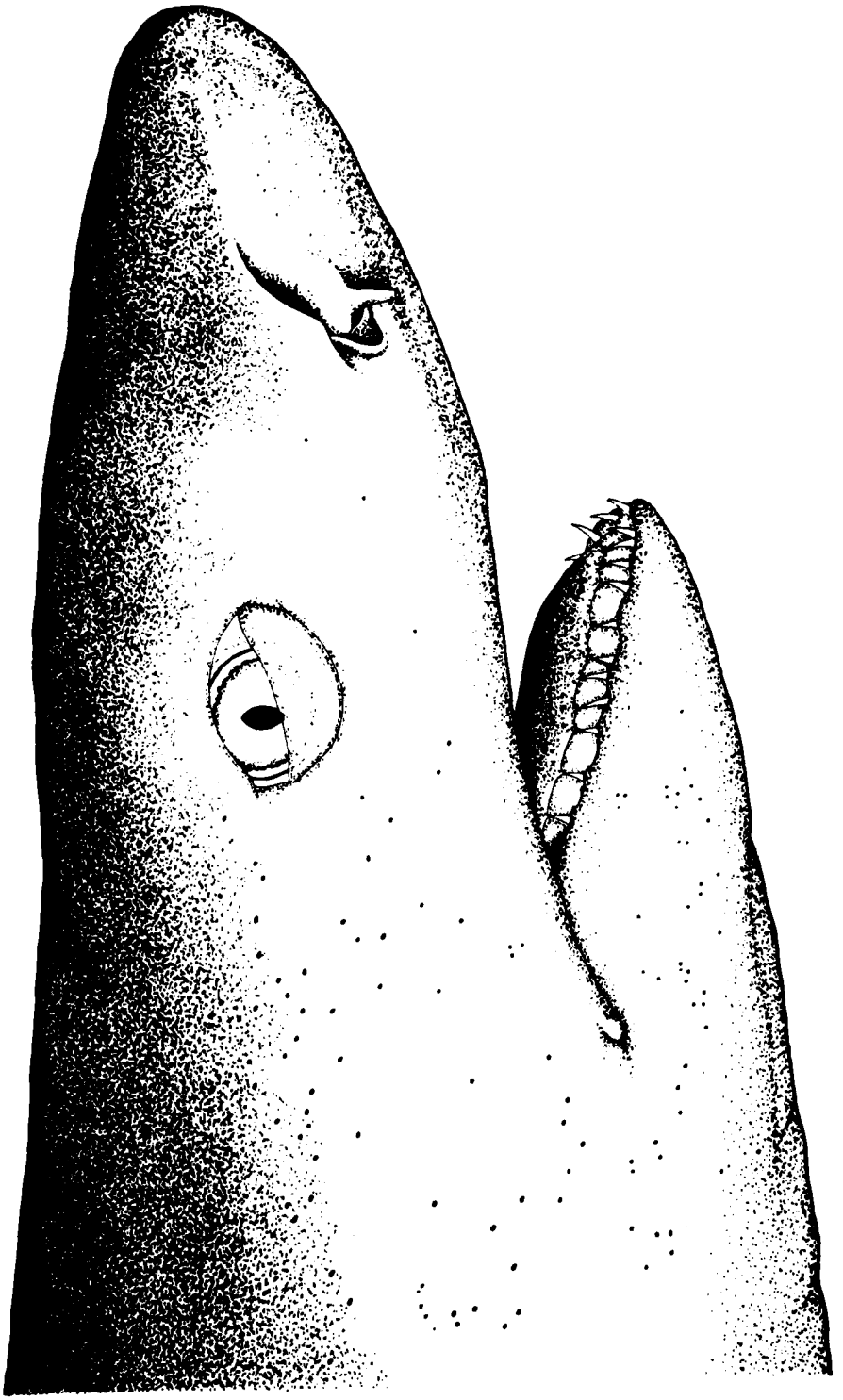

Fig. 2. Diagrammatic transverse section through the shark eye. The lens is not perfectly spherical as in the teleost eye. The optical axis is the line passing through the geometric centers of the surfaces of the refractive elements.

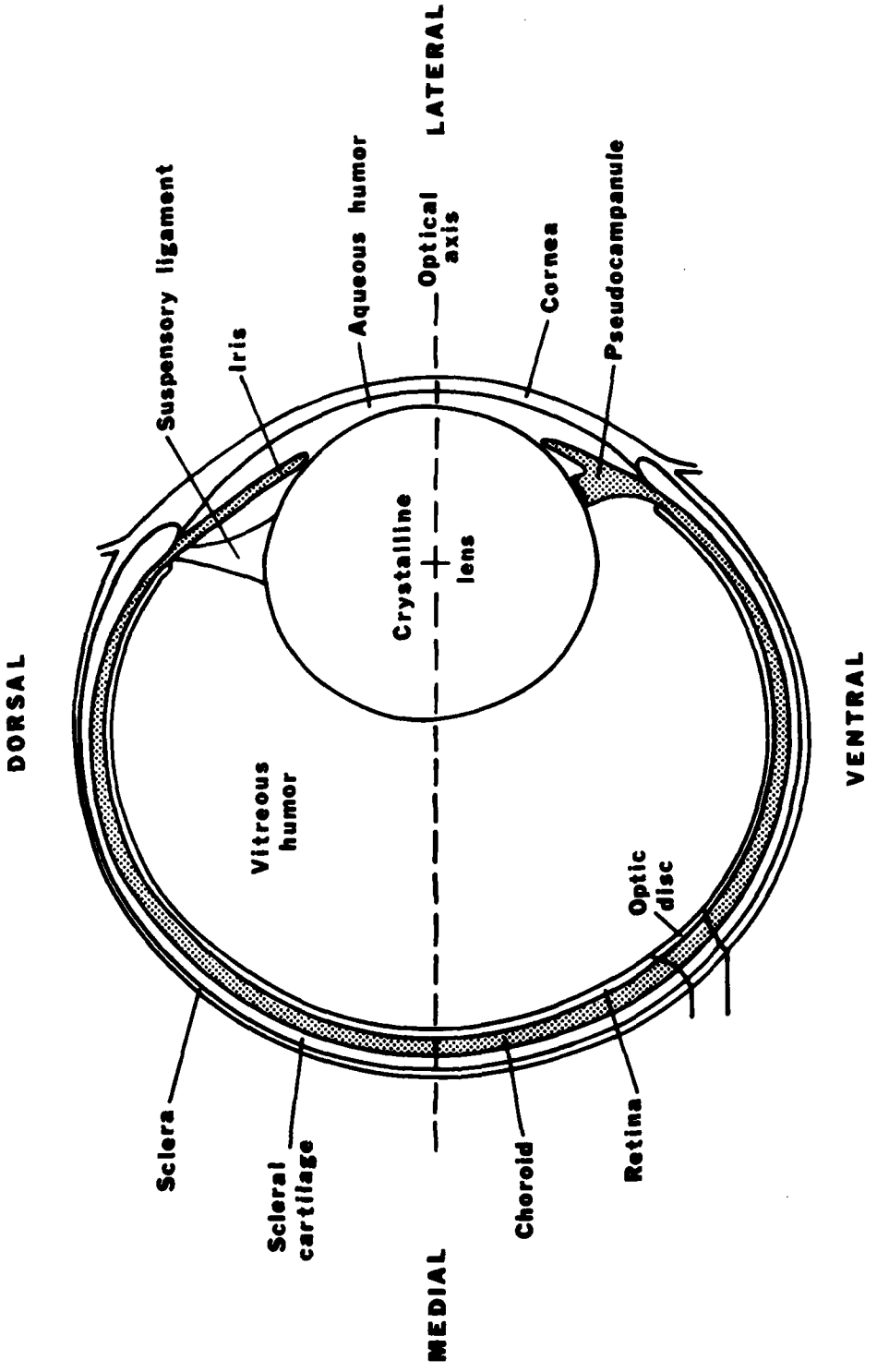
DORSAL
VENTRAL
LATERAL
MEDIAL
Suspensory ligament
Iris
Aqueous humor
Optical axis
Cornea
Pseudocampanule
Crystalline lens
Vitreous humor
Optic disc
Sclera
Scleral cartilage
Choroid
Retina

lentis) arising from the ciliary zone; the latter structure has been implicated in possible accommodatory movements of the shark lens (see Sivak and Gilbert, 1976).

Extensive laboratory studies of visual function in the lemon shark have involved spectral sensitivity (O'Gower and Mathewson, 1967; Gruber, 1969; Cohen et al., 1977), dark adaptation (Gruber, 1967), color vision (Gruber, 1969), nictitating membrane response (Gruber and Schneiderman, 1975), and pupillary and tapetal response (Kuchnow and Gilbert, 1967). Thorough reviews of this research can be found in Gruber (1975, 1977) and Gruber and Cohen (1978).

Reports of field studies of the lemon shark are practically nonexistent; the ecological role of this species in the tropical marine ecosystem is currently under study by Gruber (1979). Compagno and Vergara (1978) describe Negaprion brevirostris as a sluggish benthic species found in coastal waters throughout the western central Atlantic, feeding mainly on fishes (catfish, mullets, mojarras) and rays, as well as on crabs, shrimps, and carrion. Further notes on the lemon shark are presented by Bigelow and Schroeder (1948); a more thorough, useful report of the natural history of this species, particularly in the waters of Florida Bay, has been provided by Springer (1950).

MATERIALS AND METHODS

I. EXPERIMENTAL ANIMALS

Data were collected from a total of 23 juvenile lemon sharks, 11 males and 12 females, during the course of the entire study. The size of the animals ranged from 50 to 74 cm fork length (or about 60 to 90 cm total length). The mean fork length was 59 cm, which corresponds to an estimated age of less than one year from birth (Gruber, 1979, derived from Holden, 1974).

All animals were acquired from a charter fisherman who relied mainly on a cast net to capture juvenile sharks. The animals were netted in shallow waters (not exceeding 1 m in depth) of Florida Bay, in the vicinity of Matecumbe Key in the Florida Keys. According to Springer (1950), this area constitutes a pupping and nursery ground for the lemon shark, assuring a fairly reliable supply of juvenile animals throughout the year.

The sharks were transported live and unanesthetized from the Florida Keys to the laboratory in Miami via automobile, each animal packed in a plastic bag containing seawater, ice, and oxygen. At the laboratory, the animals were maintained in good condition for indefinite periods of time in closed natural seawater systems. Water temperature in the holding tanks was kept at a constant 26°C, and salinity was maintained at a low 30°/oo as a method of resisting parasitic infestation of the sharks. Constant germicidal treatment of the system seawater with ultraviolet light, as well as monthly addition of Dylox [dimethyl (2,2,2-trichloro-1-hydroxyethyl) phosphonate], was also used to control infection in the captive animals. Further details of maintenance of juvenile lemon sharks in the laboratory are discussed by Gruber (1980).

II. EXPERIMENTAL METHODS

Formulation of a simple mathematical model of the optics of an eye is based upon the description of three fundamental variables: refractive indices of the ocular media; intraocular dimensions of the important optical elements; and radii of curvature of the surfaces of those elements (Westheimer, 1972). In order to derive these as well as other attributes of the schematic eye for the shark, a number of optical and anatomical techniques were required. In some cases, data obtained through two or more techniques were combined for subsequent calculation of specific values in the mathematical model. The various techniques used in this study will therefore be described individually, and the explanation of how the results of each technique contributed towards the schematic eye model will be reserved for the Results section.

A. Refractometry

A direct method of measuring the refractive index (n) of the optical media of an eye is by use of an Abbé refractometer (Hughes, 1977). This instrument utilizes the principle of a total reflection borderline between media of different refractive index; the borderline, once determined, is used to derive the sample n. In practice, the refractive index of a liquid medium is measured by directing a thin film sample of the liquid between the upper (illuminating) prism and the lower (measuring) prism of the Abbé. The refractive index of a solid, on the other hand, is measured by positioning a sample in optical contact with the surface of the lower prism, using a suitable contact liquid. In both cases, the sample-prism interface produces a total reflection borderline which is observed through the instrument eyepiece. A detailed explanation of refractometry can be found in Bauer et al. (1960).

I used a Bausch & Lomb Abbé-3L refractometer to measure refractive index of the shark's ocular media. This instrument is precise to 4 decimal places,

with a standard working range of 1.3000-1.7100 n. My technique utilizing the Abbé was conducted as follows, using a total of eight juvenile lemon sharks (16 eyes). The refractometer was first calibrated with a test glass (n = 1.5125) positioned on a drop of 1-bromonaphthalene, a standard contact liquid. Each experimental animal was refracted with a retinoscope, and the eyes were examined for opacities or other irregularities via direct ophthalmoscope (see Retinoscopy and Ophthalmoscopy, below). If the ocular media appeared to me to be healthy and relatively clear, the animal was anesthetized by spraying over the gills approximately one liter of a 1 g/l seawater solution of MS-222 (tricaine methanesulfonate), a standard elasmobranch anesthetic and immobilizing agent (Gilbert and Wood, 1957). Following cessation of respiratory movements by the animal, the eyes were removed using scissors and forceps, and were placed in a dish containing elasmobranch Ringer's solution (Table 1) to maintain good physiological condition of the ocular media. Measurements of refractive index on the Abbé were then conducted at room temperature.

Aqueous humor. Samples of aqueous humor were extracted from the anterior chamber by hypodermic syringe, using a 25 gauge needle inserted at the sclero-corneal junction. Care was taken to avoid contacting the internal surface of the cornea. Several drops of aqueous were applied to the Abbé lower prism, and refractive index was read using the refractometer technique for "liquid samples" as previously described.

Vitreous humor. A slightly larger needle (20 gauge) was employed to withdraw vitreous humor by entering the back of the eye through the sclera; care was taken to remain clear of the crystalline lens. Refractive index of the vitreous sample was determined on the Abbé in the same manner as with the aqueous.

Table 1. Elasmobranch Ringer's solution (n = 1.3392 as measured on an Abbé refractometer)*.

	g/l
NaCl	16.38
KCl	0.89
$CaCl_2$	1.47
$NaHCO_3$	0.38
Dextrose	1.00
Urea	21.60
$NaH_2PO_4 \cdot H_2O$	0.07

* Formula of Woods Hole Marine Biological Laboratory, adapted from Babkin et al. (1933).

Cornea. By virtue of its relatively large radius of curvature, the shark cornea could be treated as a flat solid sample on the Abbé. A small square section from the central cornea approximating a 5 by 5 mm square was dissected out with scalpel and positioned on the Abbé measuring prism. Readings were taken using the "solid sample" refractometer technique.

Crystalline lens. Contrary to other workers investigating optical characteristics of vertebrate eyes in the past (e.g., Sivak, 1976a), I decided that a valid measurement of lens overall equivalent refractive index (n_{EL}) could not be obtained by squeezing the entire, non-homogeneous lens between the prisms of the Abbé instrument (see also Sivak, 1978c). The contributions of Abbé refractometry towards determining lens refractive index are restricted, at the present itme, to a gross estimate of the overall indices of the major lenticular fractions: the outer gelatinous cortex, and the inner, more solid nucleus of the crystalline lens. Subdividing the lens into its two major components at least eliminates some of the considerable error introduced by working with the whole lens; and, as Hughes (1977) has pointed out, such mechanical disruption does not alter the refractive index of specific regions within the lens, since this attribute is strictly determined by local protein concentration (Phillipson, 1969). However, the relationship between the n_{EL} of a multi-element vertebrate lens and the refractive indices of the individual layers within the lens is complex, such that the n_{EL} actually exceeds the maximum refractive index that is measured from local samples (Westheimer, 1972).

This complex relationship can be described using more sophisticated techniques, such as scanning refractometry (Nakao et al., 1968), to measure the actual gradient of refractive index across the optical axis of the lens. This measured gradient can then be mathematically fitted to an iso-indicial curve, and dioptric characteristics of the eye can be defined using this curve. In any case, Abbé refractometer measurements of lens cortex and nucleus refractive index can, at best, be used only as corroborative data, to simply predict a rough estimate of the n_{EL} for the whole lens. The actual value of this variable must ultimately be determined using other techniques.

With these limitations in mind, I used the Abbé to obtain refractive index readings for lens cortex and nucleus. Following measurements of aqueous, vitreous, and cornea n, the lens was dissected out of each globe, and the zonule (the suspensory ligament surrounding the lens) was stripped off with forceps. The cortex and nucleus were then treated as follows:

Lens cortex. The gelatinous outer material was removed using a cotton swab and was dabbed onto the Abbé measuring prism. A refractive index was obtained by treating the cortex material using the "liquid sample" refractometer technique.

Lens nucleus. The remaining lens nucleus was positioned on a drop of 1-bromonaphthalene contact liquid on the Abbé measuring prism, and slight pressure was maintained on the nucleus with a probe to assure proper contact. A reading was taken using the "solid sample" technique, with the top prism in the up position.

These crude methods and the vulnerability of the lens to mechanical damage allowed successful readings only about 50% of the time. In view of the many problems associated with these procedures, another technique was required to indirectly derive the n_{EL} for the schematic eye (see Measurement of Lens Focal Length, below). The Abbé lens measurements were subsequently used to corroborate results from this other technique.

Sectioning

ezing, sectioning, and photographing excised eyes has developed as a method for estimating intraocular dimensions and curvatures in the (Sivak, 1974a, 1976a). A natural concern with this method is distortion dimensions due to expansion of the ocular fluids, primarily the vitreous, freezing. The reported effects of freezing on size of optical features –0.015% (Sivak, 1974a) to as much as +9% (Hughes, 1975). Once this determined for a given eye, however, the method is preferable to other which involve, for example, handling the pliable unfrozen globe in (e.g., Vakkur and Bishop, 1963). Furthermore, the effects of particular study were minimal since the elasmobranch eye, by cartilagenous sclera, undergoes less distortion during freezing than a soft eye such as a mammal's (Sivak, 1976b).

Although most other researchers have utilized rapid freezing with liquid nitrogen or acetone and dry ice, I found that such methods caused extensive cracking of the globe, rendering it useless for measurements. Repeated attempts to use rapid freezing led to the same result. I therefore reasoned that slow freezing of the juvenile shark eye, over the course of about one minute, might overcome this problem. This slow freezing technique provided the following

advantages: (1) the eye could be directly frozen on the microtome stage, saving a step in handling between excision and sectioning; (2) freezing on the microtome stage allowed greater accuracy in positioning the eye in the proper orientation for sectioning; (3) cracking or gross distortion of the globe never occurred; and (4) boundaries between optical features retained the high contrast and sharpness necessary for photographic analysis.

Freezing, Sectioning, and Photography

Experimental animals chosen for freeze-sectioning were refracted with a retinoscope, examined by direct ophthalmoscope, and anesthetized with MS-222 as previously described. One eye was removed, and globe and corneal dimensions prior to freezing were estimated with vernier calipers, as a check on distortion that might be introduced by freezing the eye. The animal was then returned to a seawater container and revived.

The excised eye was positioned on the stage of an American Optical Spencer 888 sliding bench microtome connected to a Scientific Products Histo-Freeze unit, and freezing was begun. The eye was oriented such that the microtome knife entered at the posterior of the globe, cutting through on a plane parallel to the optical axis; nine eyes were sectioned "vertically" (i.e., on a transverse plane), with the leading edge of the knife parallel to the dorso-ventral long axis of the pupil, and three eyes were sectioned "horizontally" (i.e., on a frontal plane), with the knife cutting perpendicularly to the pupillary axis (Fig. 3). Positioning of the globe was judged by eye, using calipers to verify symmetrical orientation with respect to the globe's optical axis. A pedestal of distilled water was fashioned around the point of contact between the eye and microtome stage, so that the resulting ice collar supported the eye during sectioning.

Fig. 3. Sectioning planes and directions for vertical and horizontal sections of the juvenile lemon shark eye.

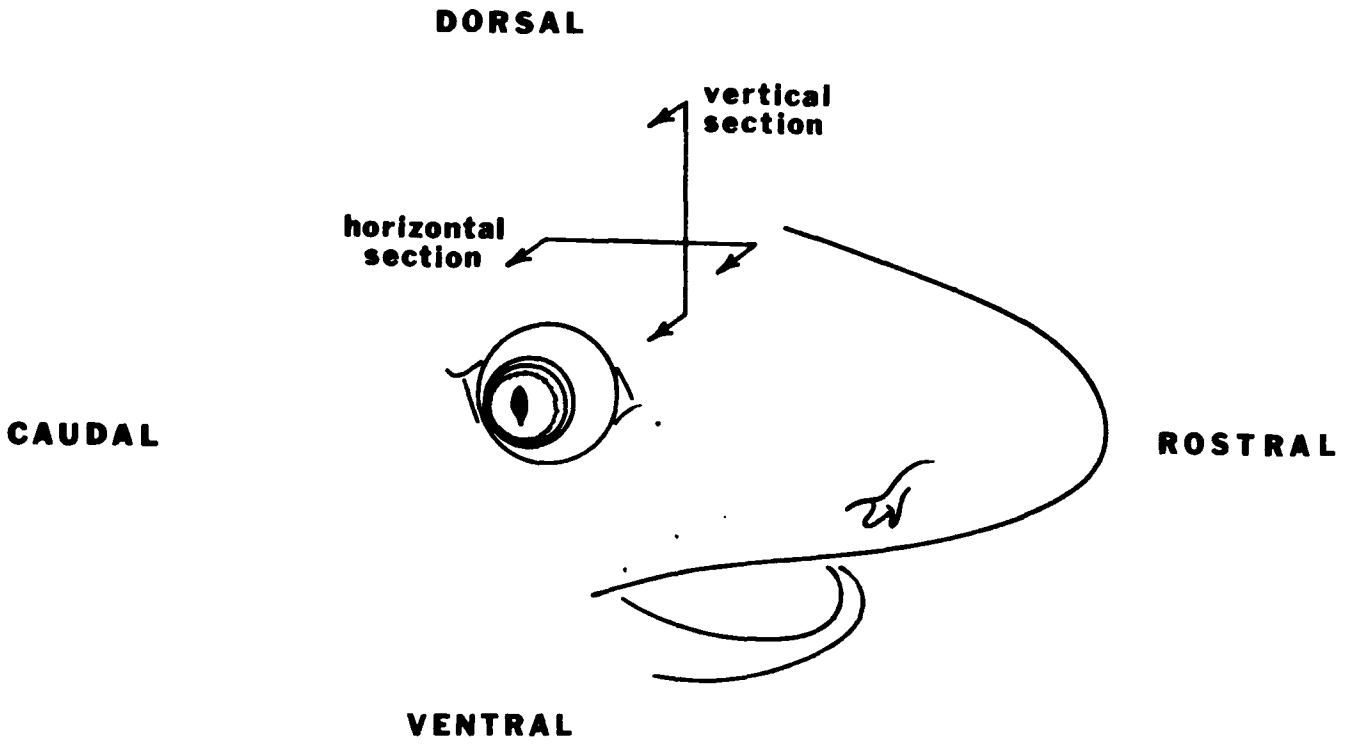
DORSAL
vertical section
horizontal section
CAUDAL
ROSTRAL
VENTRAL

While the globe was freezing, a 35 mm single lens reflex camera was positioned overhead and adjusted. A Nikkormat camera body equipped with a 200 mm Medical-Nikkor lens was used. The lens contained a built-in flash ring, and was modified for fixed focus at 1.5 X magnification. An f40 aperture and 1/60 sec shutter speed were selected, and the flash and shutter were activated by a remote cable release. Kodak Panatomic-X film for black/white prints, ASA 32 with 36 exposures, was used. Prior to the start of sectioning, the camera focus was set, and an information card identifying the eye number was photographed. Several photos were then taken of a micrometer rule, to provide an accurate scale to which the ocular measurements off the black/white prints could be calibrated.

Sectioning of the globe was begun about 10-15 minutes after the Histo-Freeze unit was turned on. "Thin" sections of 25 μm were cut, and the knife and eye block surface were kept cold by frequent application of Quik-Freeze (Miller-Stephenson Chemical), a freezing aerosol. As the sections were removed, photographs were taken of the remaining exposed eye block in the manner employed by Sivak (1974a, 1976a, 1976b). Close to the optical axis, photographs were taken after every other section until it was apparent that, as the size of the remaining block diminished, the geometric center of the eye had been passed. The Histo-Freeze unit was then switched off, and the entire procedure beginning with excision was repeated for the animal's other eye, using a new roll of film.

Printing and Measurement

The film record of each eye was developed and printed on Kodak 8 by 10 inch Ektamatic paper, using an Automega D3 enlarger and a Kodak Ektamatic processor. All 36 exposures for each eye were printed, at a final absolute magnification of between 10 and 15X. After a short fixing in hypo agent, rinse, and drying, the photographs were ready for measurement.

The print series for each eye was surveyed, and that print with the maximum lenticular thickness was selected as portraying the optical axis plane of that eye, since lenticular dimensions decrease on either side of the geometric center. Because photographs were taken after every other section, the maximum error of this procedure was 25 μm off-axis.

A total of 28 different measurments was taken off each optical axis photograph. Vernier calipers (NSK) accurate to .01 mm were used to make the measurements; with the 10-to-1 or greater magnification on the photographs, the intraocular dimensions could be measured to the .001 mm level. The optical axis of each eye was located by connecting the geometric centers of the optical components (front and back surfaces of cornea and lens, lens center), and this line was drawn onto a clear plastic sheet overlaying the axial photograph.

Boundaries of the cornea, aqueous, lens, vitreous, retina, choroid, and sclera divided the optical axis into seven measurements; the eighth measurement was total globe depth from front surface of the cornea to back surface of the sclera. Additional measurements included radii of curvature of seven ocular surfaces: front and back surfaces of cornea and lens, dorsal and ventral surfaces of lens, and retinal-choroidal boundary. Perpendicular chords subtending the ocular surfaces and axial depths of the chords were measured from the photographs, and the radii of curvature were calculated using the formula

$$r = (x^2 + y^2)/2x$$

where r = radius of curvature, x = axial depth of a chord perpendicular to the optical axis, and y = 1/2 length of the chord (Fig. 4). (I attempted to measure corneal curvature in a living animal with a clinical keratometer; however, the flatness of the shark cornea exceeded the capability of the clinical instrument.)

Fig. 4. Determination of radius of curvature of an optical surface from section photographs. Once the optical axis is located, radius of curvature can be calculated using a chord perpendicular to the axis. C, center of curvature; r, radius of curvature; x, axial depth of the perpendicular chord; y, 1/2 length of the chord.

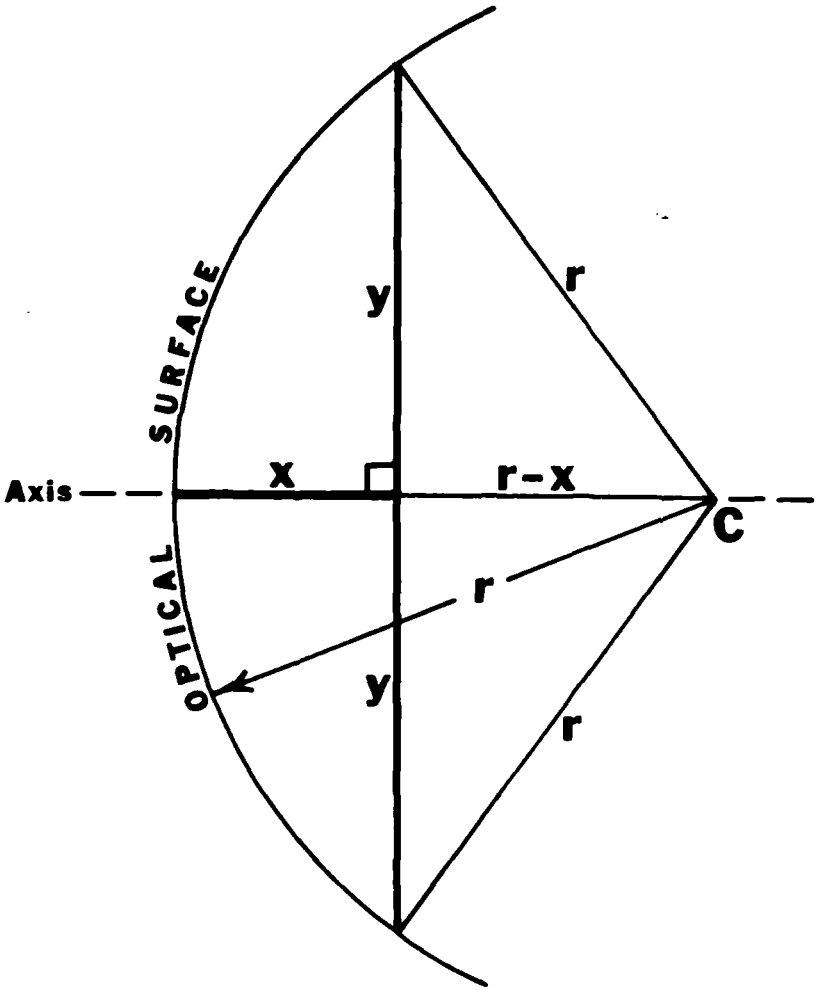

Pythagorean Theorem:

$$r^2 = (r - x)^2 + y^2$$

$$\boxed{r = \frac{x^2 + y^2}{2x}}$$

The remaining 13 measurements taken from the optical axis photographs were concerned with locating other landmarks within the eye, such as the ora terminalis (the peripheral limit of the retina). A final measurement for each eye was taken from the off-axis photograph which showed the bisected optic disc: the angular location of the disc with respect to the lens center and optical axis plane was noted, to provide a reference for ophthalmoscopic examinations of the eyes in living sharks (see Retinoscopy and Ophthalmoscopy, below).

C. Measurement of Lens Focal Length

Due to the failure of refractometry to provide a direct measurement of the f_L for the schematic eye, it was necessary to derive this essential value from measurements of another lens variable, the vertex focal length (f_V), defined as the distance between the vertex (i.e., vitread) surface of the lens and the back focal point. Given the vertex focal length, lens curvatures, and lens thickness, the f_L for a non-homogeneous thick lens, such as in the elasmobranch eye, can be calculated (Vakkur and Bishop, 1963; Block, 1969). Since frozen sectioning destroys particular curvatures and thicknesses, measurements of the focal length of the lens in vitro were called for.

A number of workers have followed a similar course. Using the examples of Hughes (1972), Charman and Tucker (1973), Sadler (1973), duPont and deGroot (1976), and Sroczyński (1976b), I constructed a simple optical system utilizing a vertical collimated light source and a compound microscope (Fig. 5). I measured vertex focal lengths of fresh shark lenses in vitro with this apparatus, using the following procedure. Experimental animals were first refracted with a retinoscope, examined by ophthalmoscope, and then dark-adapted for 15 minutes to dilate the pupil. All subsequent steps were conducted under dim red illumination to keep the pupil dilated (Kuchnow, 1970). During dark-adaptation

Fig. 5. Apparatus for measurements of crystalline lens focal length in vitro. The preparation is shown with the vertex surface of the lens in air and the cornea bathed in elasmobranch Ringer's solution. See text for measurement procedure.

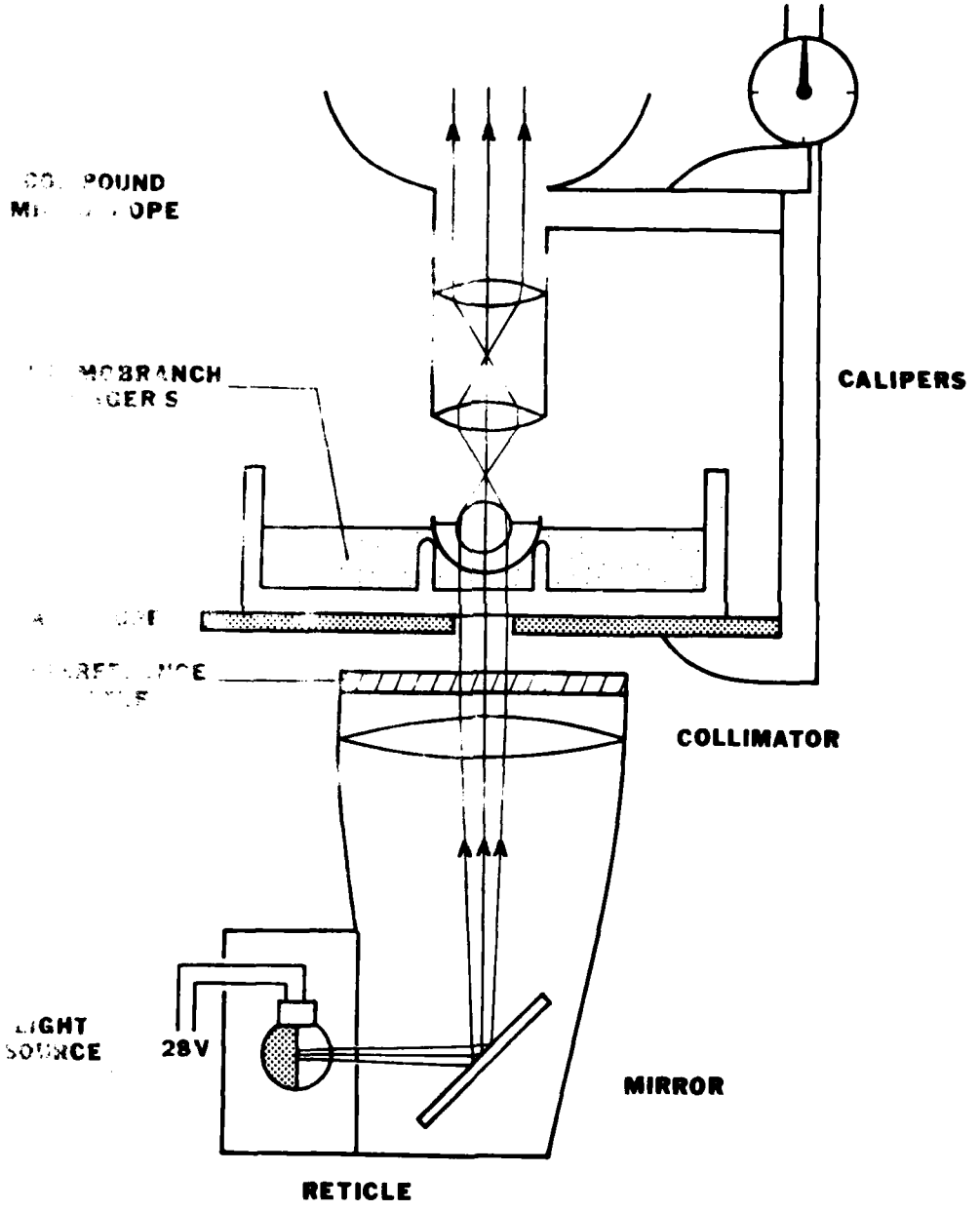
CALIPERS
COLLIMATOR
28V
MIRROR
RETICLE

of the animal, I calibrated the optical system using a 6.5 mm-diameter glass lens (Edmund Scientific) with a known focal length of 12.43 mm. The accuracy of the apparatus was within $\pm$0.05 mm of the true vertex focal length; this was confirmed using several small glass lenses of varying power.

After adequate dark-adaptation, one eye was removed, and the globe was hemisected with a sharp blade by cutting rearward of the lens vertex surface, along a plane perpendicular to the optical axis. The anterior hemisphere, including cornea, aqueous, and undisturbed lens, was placed in a specially constructed glass chamber containing elasmobranch Ringer's solution. The vertex surface of the lens was carefully cleaned of any vitreous material with a cotton swab and was rinsed with Ringer's solution. I positioned the eyecup in the chamber, corneal surface down, so that its optical axis aligned with the axis of my optical system. Once the eyecup was in place, I adjusted the level of Ringer's solution to the point at which the eyecup was adequately bathed without introducing Ringer's into the interior of the hemisphere.

A 28 V lamp operated at .68 amps provided a source of white light, which was projected horizontally from the half-silvered bulb though a bull's-eye reticle, and reflected 90^{o} off of a mirror towards a glass collimating lens (see Fig. 5). The 142 mm achromatic lens (Edmund Scientific) refracted the light beam into vertical parallel rays carrying the image of the reticle. The collimated light then passed through an interference filter (Baird-Atomic), a 1 cm aperture, and into the chamber containing the shark eyecup. Since the refractive index of elasmobranch Ringer's (n = 1.3392 as measured on an Abbé refractometer) closely matches that of the shark cornea and aqueous (n = 1.34; see Results section), no refraction of the collimated light occurred until the lens was encountered. Thus the subsequent focusing of the reticle image was a result of the dioptric power of

the crystalline lens alone, similar to the case of the living shark eye in seawater (n = 1.34; Jerlov, 1976).

Focal Length of the Lens in Air

A Leitz-Wetzlar compound binocular microscope, with a 4X objective and 12X ocular lenses, was focused on the vertex surface of the shark lens. This surface, illuminated by scattered light departing from the collimated beam, was slightly visible in a fresh lens; a damaged lens appeared crackled and dehydrated, and such a lens was rejected from the tests. If the lens appeared healthy, the relative position of the vertex surface as focused through the microscope was recorded, using vernier calipers that measured vertical movements of the microscope objective with respect to the stage.

The scope was then racked up and down until the point of best focus of the reticle image, as converged by the shark lens, was seen. (Again, in a seemingly healthy eyecup, the reticle image appeared fairly sharp, but in a damaged eye the image was very diffuse.). The level of best focus was noted on the calipers, and the vertical distance between the lens surface and the position of the reticle image was taken as the vertex focal length of the crystalline lens with its back surface in air. Using the approach described by Sivak (1974a), I interchanged interference filters of 490 nm and 670 nm wavelength maximum transmission (1/2 bandwidth = 10 nm) in the collimated optical system, as a test for chromatic aberration of the shark lens. Differences in the position of the focused reticle image due to changes in wavelength were recorded.

Focal Length of the Lens in Ringer's

A second series of measurements of vertex focal length was conducted next, this time with the vertex surface of the shark lens in Ringer's solution (Fig. 6). Following the in-air tests, the level of solution in the chamber was

Fig. 6. Measurement of crystalline lens focal length in vitro with the vertex surface of the lens in elasmobranch Ringer's solution. See text for measurement procedure.

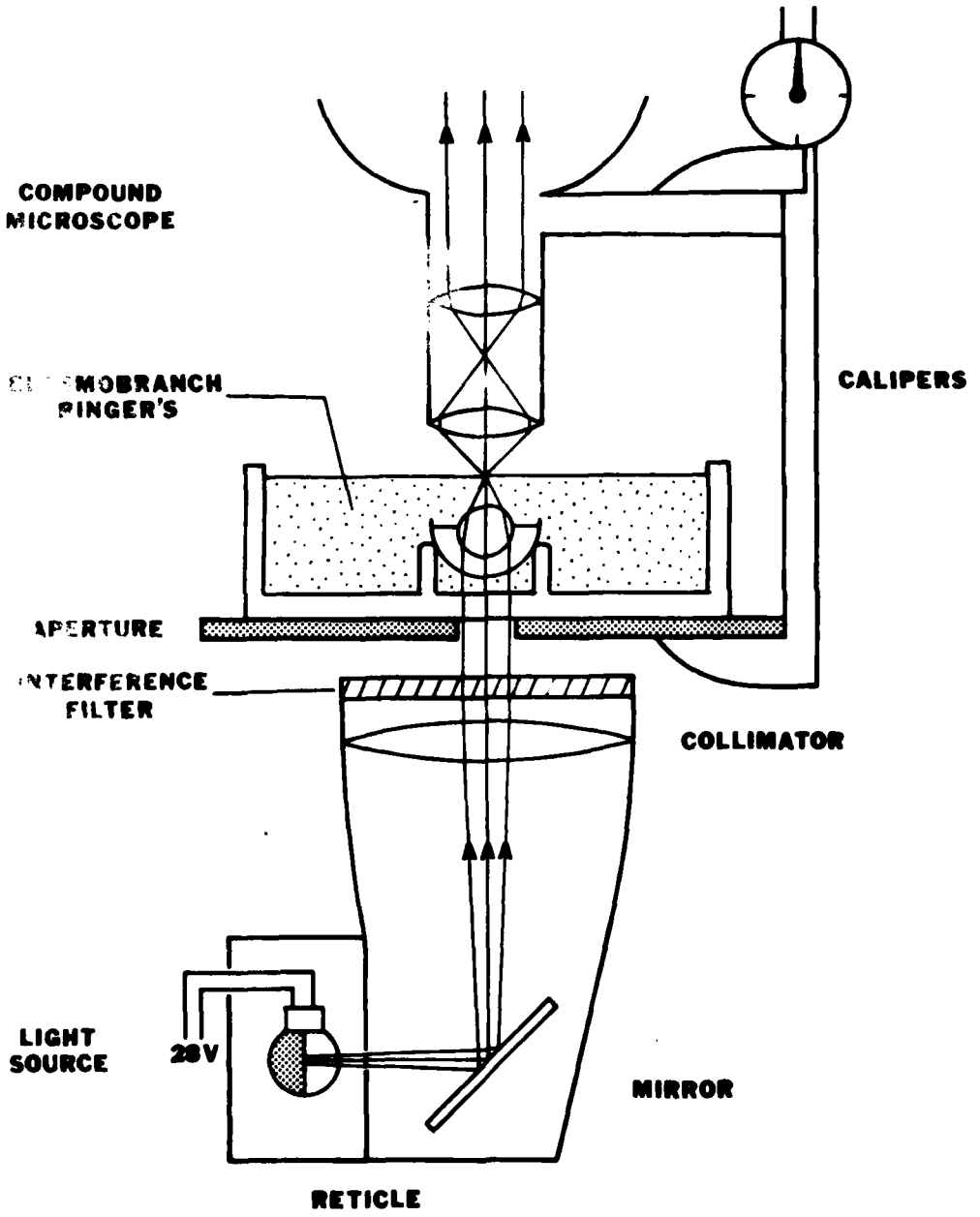
COMPOUND MICROSCOPE
MOBRANCH RINGER'S
CALIPERS
APERTURE
INTERFERENCE FILTER
COLLIMATOR
LIGHT SOURCE
28V
MIRROR
RETICLE

slowly raised using a syringe filled with Ringer's, through a surgical tube connection between syringe and chamber. Introduction of Ringer's into the post-lens space considerably lengthened the vertex focal length of the lens, since the higher refractive index of the Ringer's cut the refractive power of the lens vertex surface (apex surface power remained unchanged).

As the level of Ringer's was raised, the microscope was racked up until the reticle image came into best focus at a position coincident with the surface of the Ringer's solution. This was accomplished by manipulating the scope objective simultaneously with the level of Ringer's, and was important to assure that no error was introduced by spurious refraction at the Ringer's-air interface (note divergence of beam at this interface in Fig. 6). Vertex focal length of the lens in Ringer's was thus measured, and chromatic aberration was again checked using 490 and 670 nm interference filters.

Following the focal length measurements, a final reading was made to determine the thickness of the excised lens. The lens was removed from the eyecup with forceps, cleaned, and positioned on its side in a dry glass chamber. Lenticular thickness was then measured through the microscope to the nearest 0.1 mm, using the stage micrometer.

A total of five shark lenses endured the entire procedure, yielding vertex focal lengths for "in-air" and "in-Ringer's" conditions. Lens thicknesses were subsequently used to extrapolate estimated surface curvatures of the experimental lenses, from a thickness-curvature regression line which was derived from the frozen section data. Given vertex focal lengths, surface curvatures, lens thickness, and refractive indices of surrounding media, an iterative solution for the n_{EL} of each lens was found, using formulas from thick lens theory (see Parrish, 1972).

D. Pupillary Measurement

The entrance pupil and real pupil of the shark's eye are identical, since the cornea has virtually no refractive power underwater (see Results section). The diameter of the entrance pupil can thus be measured directly by examining the real pupil. Three juvenile lemon sharks were dark-adapted overnight to allow maximum pupillary dilation. Pupil sizes of allsix eyes were then measured in air, with a dim red light providing illumination without affecting pupillary size. For each eye, any added refractive power of the cornea in air was eliminated by flattening the pliable cornea with a glass cover slip; vernier calipers were then used to measure the real pupil as it appeared through the cover slip. The major (dorso-ventral) and minor (rostro-caudal) axes of the elliptical real pupil were measured for each eye. Computations of exit pupil characteristics were subsequently made using the procedures of Bennett and Francis (1962), and Hill and Fry (1974).

E. Retinoscopy and Ophthalmoscopy

The most common method of objectively measuring refractive error in the living, intact eye is by the technique of retinoscopy (Bennett and Francis, 1962; Hughes, 1977). Borrowed from ophthalmologists who use the method with children and handicapped adults, retinoscopy requires no communication between subject and examiner, and is therefore applicable for measuring refractive error in animals. The technique beasically involves the lateral movement of a small beam of light directed into the subject's eye, and the behavior of the resulting light "reflex" on the subject's retina, as observed by the examiner through the subject's pupil. The retinoscopist determines the subject's refractive error by placing appropriate lenses in front of the eye, until the reflex is "neutralized": in this sense, neutrality is the point at which the apparent rate of movement of the

reflex becomes infinite. At that point, the refractive error of the subject equals the power of the lenses required for neutrality, minus an amount corresponding to the working distance between subject and examiner. Complete explanations of retinoscopy are presented by Bennett and Francis (1962) and Parrish (1972). (Further aspects of the retinoscopic technique and its ramifications for my study are dealt with in the Discussion section and the Appendix).

Retinoscopy was performed on experimental animals throughout many phases of the study as previously mentioned. A Keeler J21223 streak retinoscope was used in conjunction with a set of trial lens bars containing lenses graduated at 0.5 Diopter (D) steps. The range of the trial lens set extended from −16.5 to +16.5 D.

For retinoscopy, each juvenile shark was placed in a glass aquarium containing enough seawater to cover the eyes and gills. The shark was positioned so that the eye being refracted was less than 5 mm from the glass, with the optical axis aligned perpendicular to the glass and on target with the examiner's line of sight. Working distance between the shark's eye and the retinoscopist's eye was noted; a distance of 50 cm was usually used.

Trial lenses were placed in front of the shark's eye, about 2 mm from the outside of the aquarium glass, i.e., about 1 cm in front of the shark's cornea. The retinoscope was operated with the focusing control in the position that produced a divergent plane mirror effect (see Bennett and Francis, 1962). Cycloplegic drugs such as pilocarpine do not affect the independent elasmobranch iris (Sivak, 1974b), so the animal's pupil was kept dilated by using a low illumination setting on the retinoscope and no background light.

Upon neutralization of the retinoscopic reflex, the dioptric power of the required trial lens was recorded. The refractive error of the animal was calculated as the trial lens power, minus the reciprocal of the working distance

expressed in meters, divided by 1.34 (the ratio of the refractive indices of seawater vs. air). The last step is a necessary adjustment when retinoscopy is performed on an aquatic eye immersed in water, due to spurious refraction at the seawater-air interface (see Appendix).

As an example, the retinoscopically determined refractive error of a shark eye requiring a +10 D trial lens, at a working distance of 50 cm (= 0.5 m), would be calculated as:

$$\begin{aligned} K &= [+10\ D - (1/0.5)D]/1.34 \\ &= (+10\ D - 2\ D)/1.34 \\ &= (+8\ D)/1.34 \\ &= +6 \text{ Diopters refractive error.} \end{aligned}$$

The best precision that I could attain given the juvenile shark's small eye and slit pupil combined with background reflection off of the tapetum was $\pm$0.5 D. Attempts to confirm retinoscopic measurements with a Keeler direct ophthalmoscope were unsuccessful, since the avascular shark retina contains no clear landmarks on which to focus. The ophthalmoscope was therefore used to simply inspect the clarity of the optical media, and to locate the general area of the optic disc.

RESULTS

I. MEASUREMENTS

A. Refractive Indices

Results of Abbé refractometer measurements are presented in Table 2. The 95% confidence limits around the mean refractive indices for aqueous, vitreous, and cornea are broadly overlapping. A Model I Analysis of Variance (Zar, 1974) demonstrated that no significant difference could be detected between the mean refractive indices of these three media ($P > .25$). Therefore, the refractive indices of aqueous, vitreous, and cornea can be treated as equivalent in the schematic eye, and the best estimate of this equivalent index is the grand mean for the data in all three categories. This number is 1.3404, with 95% confidence limits as follows: $P(1.3399 \leq \mu_{a,v,c} \leq 1.3409) = .95$.

Since the refractive index of seawater is approximately 1.340 (Jerlov, 1976), the potential contribution of the cornea to the overall refractive power of the eye is very small ($\ll 1$ D). In the interest of simplicity, therefore, I fixed the refractive index values of all media except the crytstalline lens (seawater, cornea, aqueous, and vitreous) at $n = 1.340$ for the schematic eye. The cornea in this eye model is optically absent, and the crystalline lens is the sole refractive element.

The refractive indices of the lenticular components as measured on the Abbé are high in comparison with similar measurements for other vertebrate lenses (Hughes, 1977); however, high refractive index is consistent with the necessity for a high power lens in an aquatic eye. The values of 1.4624 for the lens cortex and 1.6551 for the lens nucleus can not be used directly in the schematic eye for reasons previously discussed (see Refractometry section in Materials and Methods). However, I can estimate that the n_{EL} of the equivalent lens in the schematic eye should be slightly greater than 1.655, since, in other

Table 2. Abbé refractometer measurements of refractive indices of juvenile lemon shark's ocular media.

Shark Sex	Ford Length (cm)	Eye #	Aqueous	Vitreous	Cornea	Lens Cortex	Lens Nucleus
M	64	1		1.3408			
		2	1.3412	1.3402			
F	52	3	1.3413	1.3400			
		4	1.3418	1.3401	1.3408		
F	53	5	1.3413	1.3407	1.3393		
		6	1.3420	1.3409			
M	55	7			1.3418	1.4623	
		8			1.3407		
M	53	9		1.3400	1.3404		
		10	1.3430		1.3419		
F	53	11	1.3390				
		12	1.3385	1.3389			1.6555
M	51	13	1.3395	1.3393	1.3398	1.4600	1.6553
		14	1.3373	1.3385	1.3420	1.4616	1.6518
M	53	15				1.4670	1.6568
		16				1.4611	1.6563
		n	10	10	8	5	5
		$\bar{X}$	1.34049	1.33994	1.34084	1.46240	1.65514
		s	0.001809	0.000810	0.001004	0.002705	0.001963

Table 3. Abbé refractometer data summary.

	REFRACTIVE INDEX		
	$\bar{x}$	s	n
Cornea	1.34084	.001004	8
Aqueous	1.34049	.001809	10
Lens Cortex	1.46240	.002705	5
Lens Nucleus	1.65514	.001963	5
Vitreous	1.33994	.000810	10

Cornea, Aqueous, Vitreous = 1.340 = seawater
Lens overall equivalent refractive index > 1.655

studies of vertebrate optics, the calculated n_{EL} of the equivalent homogeneous lens has been found to be somewhat greater than the highest measured value obtained from the real lens nucleus. This is due to the additive refractive effects of the individual layers within the nonhomogeneous lens (Westheimer, 1972; Hughes, 1977).

A summary of the results from the Abbé data is presented in Table 3.

B. Intraocular Dimensions

Descriptions of the sizes and locations of ocular components will follow the terms of orientation illustrated in Fig. 3. In addition to the rostro-caudal and dorso-ventral axes, a third axis of direction must be defined. This is the axis that coincides with the optical axis of each eye. Along this line, the term "lateral" will refer to the direction that is towards the cornea and projecting out of the eye, while the term "medial" will be used for the direction that is towards the sclera and projecting into the head (see Locket, 1977).

A typical frozen section cut vertically through the optical axis of the juvenile lemon shark eye is shown in Fig. 7. Several features are notable. The globe appears relatively symmetrical about the optical axis. The crystalline lens is not spherical as in teleosts; neither is it "nearly" spherical, as Walls (1942) characterized the elasmobranch lens in general, a characterization that unfortunately surfaces on occasion in more recent descriptions (e.g. Gilbert, 1963). The lens of the juvenile N. brevirostris eye is in fact lenticular in shape, with the dorsal and ventral surfaces broadly rounded, giving an impression of sphericity relative to a terrestrial mammal's lens. The dorso-ventral height of the lens is, on the average, about 13% longer than the medio-lateral thickness (n = 9 vertically sectioned eyes). This figure falls within the range of values reported by Sivak (1976b) for the elasmobranchs Dasyatis sayi (18%), Dasyatis

Fig. 7. Typical vertical section through the optical axis of a frozen right eye of a juvenile lemon shark. The interruption in the sclera is the edge of the optic disc. The photoreceptor layer is located at the retinal-choroidal boundary, which is the interface between the thick, dark choroid and the thinner, lighter retina. Axes of orientation: top, dorsal; bottom, ventral; left, medial; right, lateral.


1 mm

sabina (7.5%), and Gymnura micrura (11%). Approximating the elasmobranch lens to a sphere will result in significant errors in a dioptric model of the eye.

The diverse structures of the ciliary zone extend between the lateral limits of the scleral cartilage and the crystalline lens. Lateral to the ciliary zone, the anterior chamber appears as a relatively narrow separation between lens and cornea. The multi-layered nature of the cornea is evident, and the flatness of this element compared with a mammalian cornea is apparent.

The retinal-choroidal boundary, marking the approximate level of the photoreceptors, appears as a medium-contrast border between the dark choroid and the more lateral, lighter retina. The scleral tunic, with its thick cartilagenous layer, surrounds the choroid. The beginning of the optic nerve's insertion through the sclera is seen as an opening in the ventral scleral cartilage, located at an angle of about 30° from the optical axis relative to the lens center.

The important optical features of the juvenile lemon shark eye in vertical section are illustrated diagrammatically in Fig. 2.

A typical photograph of a horizontal section through the optical axis of this eye is shown in Fig. 8. (Figs. 7 and 8 depict eyes from animals of approximately the same size.) The more flattened configuration of the globe along the horizontal plane compared with the vertical plane is evident in the horizontal section. The globe again appears relatively symmetrical about the optical axis in this plane. The same features which were noted in the vertical section photograph are evident in the horizontal section photograph, with the exception of the optic nerve insertion, which does appear in the horizontal section through the optical axis (lower off-axis horizontal sections reveal the optic disc to be located approximately 10° rostral to the optical axis). The iris is especially visible in Fig. 8 as two flaps resting against the apex (lateral) surface of the lens;

Fig. 8. Typical horizontal section through the optical axis of a frozen right eye of a juvenile lemon shark. The optic disc is not visible at this level. Axes of orientation: top, rostral; bottom, caudal; left, medial; right, lateral.

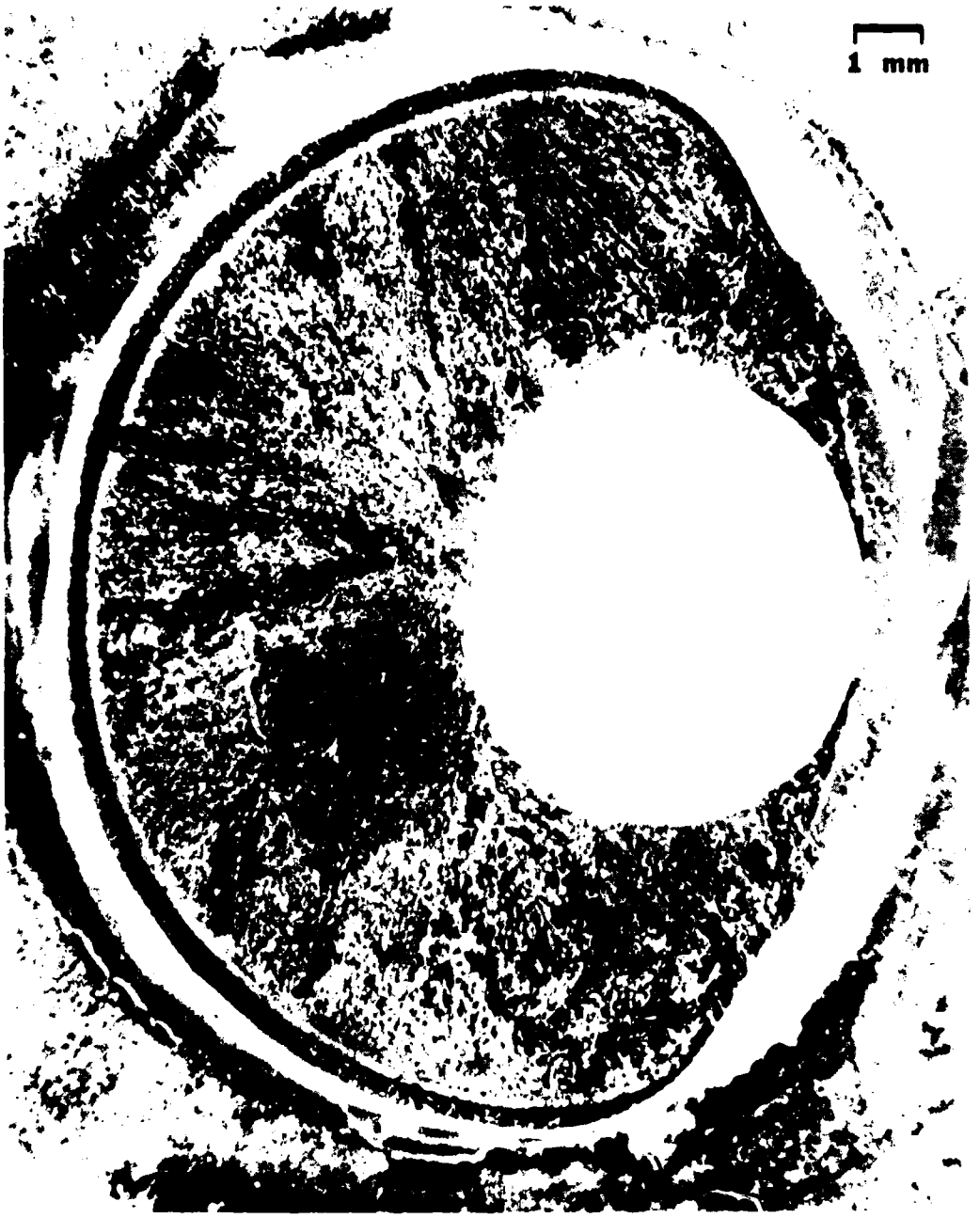
1 mm

the space between the flaps represents a cross-section through the minor (rostro-caudal) axis of the slit pupil.

Caliper measurements from the vertical and horizontal section photos are presented in Tables 4 and 5. Nine eyes, from a total of seven different sharks averaging 61.6 cm fork length, were sectioned vertically. Three eyes from two sharks averaging 55.7 cm were sectioned horizontally. Means and standard deviations were computed for the grouped data in each category.

The possible effects of freezing can be assessed by comparing the caliper measurements of the whole eye before freezing with the corresponding measurements taken from the photographs of frozen sections. The percentage change from pre-freezing measurements to post-freezing measurements was calculated for: (1) the dorso-ventral height of the globe in the nine vertically sectioned eyes; and (2) the rostro-caudal width of the globe in the three horizontally sectioned eyes. The average change in these measurements from unfrozen eye to frozen section was +0.64% ($s = 1.4217\%$, $n = 12$). A slight expansion of the ocular dimensions is therefore indicated, and this must be taken into consideration in the schematic eye analysis.

A number of high correlations between several key dimensions are evident in the frozen section data. These correlations are depicted in Figs. 9 through 12. The importance of the correlations is twofold. First, they indicate that growth of the ocular components is isometric with increase in body length throughout the range of juvenile sharks that were examined. Second, the correlations allow the use of medio-lateral thickness of the crystalline lens as a central reference dimension in the juvenile lemon shark eye. This particular function was essential for the subsequent determinations of the n_{EL} of the lens, because, in the tests of lens focal length, surface curvatures of the experimental lenses had to be indirectly extrapolated using direct measurements of lenticular thickness. For

Table 4. Measurements on [illegible] (Continued)

SUBJECT ANIMAL GENERAL DATA			Shaft [illegible]	[illegible]	3R	R	4L	[illegible]	[illegible]	[illegible]	[illegible]	[illegible]	(4L/3R) (RF/LR)	
			Sex		F	F		[illegible]	F	F	F		[illegible]	
			Body length (cm)		69	69	59	[illegible]	[illegible]	50	55		61.0	5.974
FROZEN SECTION PHOTOGRAPH MEASUREMENTS	"On-Axis" Photographs	Intraocular Dimensions Along Optical Axis		Cornea thickness	[illegible]	0.426	0.465	0.466	[illegible]	0.395	0.404	0.441	0.394	0.436	0.02663
				Cornea to lens	[illegible]	0.538	0.549	0.563	0.454	0.528	0.542	0.496	0.478	0.441	0.08031
				Lens thickness	[illegible]	6.699	6.743	6.891	[illegible]	6.117	5.864	5.868	5.899	6.361	0.51286
				Lens to retina	6.970	6.560	6.188	6.046	[illegible]	5.927	5.615	5.581	5.574	6.030	0.48560
				Retina thickness	0.196	0.191	0.195	0.184	[illegible]	0.215	0.190	0.203	0.215	0.199	0.01078
				Choroid thickness	0.357	0.301	0.332	0.330	0.255	0.230	0.229	0.216	0.281	0.281	0.05170
				Sclera thickness	0.566	0.563	0.492	0.507	0.554	0.578	0.487	[illegible]	0.497	0.529	0.03603
				Total globe depth	16.086	15.496	14.964	14.767	13.748	13.790	13.209	13.283	13.338	14.298	1.06031
			Radii of Curvature	Lateral corneal sfc	8.488	9.278	7.145	7.321	[illegible]	6.056	[illegible]	6.892	7.154	7.304	1.02283
				Medial corneal sfc	6.727	7.685	6.541	6.945	5.300	5.985	5.195	5.930	5.452	6.134	0.89263
				Lateral lenticular sfc (lens apex)	4.074	4.023	3.982	3.900	[illegible]	3.655	3.496	3.495	3.521	3.758	0.23770
				Medial lenticular sfc (lens vertex)	4.299	4.282	4.183	4.271	3.947	3.940	[illegible]	[illegible]	3.846	4.046	0.20982
				Dorsal lenticular sfc	2.659	3.105	2.953	3.106	[illegible]	2.920	[illegible]	[illegible]	2.735	2.898	0.15995
				Ventral lenticular sfc	2.977	3.346	3.127	2.817	2.625	2.962	[illegible]	[illegible]	2.950	2.954	0.18691
				Retinal-choroidal boundary	7.737	7.878	6.958	6.534	6.381	6.544	[illegible]	5.413	6.295	6.623	0.80250
			D-V Deans	Lens height (at center)	7.887	7.879	7.684	7.697	6.924	6.921	6.644	6.636	[illegible]	7.212	0.52872
				Retina vertical max	15.760	15.481	14.376	14.125	13.215	13.245	12.567	12.455	12.968	13.802	1.21747
				Total globe height	17.360	16.970	15.866	15.563	14.675	14.547	13.881	[illegible]	14.147	15.162	1.34115
			Ora Terminalis Location	Dorsal o.t.-ventral o.t. separation	14.039	13.530	12.974	13.079	11.832	11.965	11.360	11.565	11.637	12.445	0.97415
				Dorsal ora terminalis to lens center	[illegible]	[illegible]	[illegible]	[illegible]	[illegible]	5.993	[illegible]	[illegible]	[illegible]	[illegible]	[illegible]
				Dorsal o.t.-optical axis angle at lens center (°)	95	94	92	103	98	97	98	98	96	96.8	3.114
				Ventral ora terminalis to lens center	6.844	6.970	6.969	6.670	5.724	6.036	5.822	5.836	6.009	6.320	0.53099
				Ventral o.t.-optical axis angle at lens center (°)	91	88	93	88	91	95	92	94	91	91.4	2.404
			Scleral Cartilage Lateral Limits	Dorsal s.c.-ventral s.c. separation	10.416	10.606	10.344	9.983	9.642	9.554	9.017	8.967	9.355	9.765	0.60600
				Dorsal scleral cartilage to lens center	5.384	5.152	4.865	4.829	4.763	4.560	[illegible]	[illegible]	4.564	4.736	0.38075
				Dorsal s.c.-optical axis angle at lens center (°)	66	67	67	76	72	72	72	73	72	70.7	3.346
				Ventral scleral cartilage to lens center	5.636	6.111	5.961	5.580	5.186	5.298	5.077	4.982	5.096	[illegible]	0.40688
				Ventral s.c.-optical axis angle at lens center (°)	76	73	78	70	80	82	80	79	78	[illegible]	3.775
	"Off-Axis" Photo			Angle between optic disc & optical axis plane at lens center plane (°)	--	29	[illegible]	29	29	30	29	32	32	30.0	1.309
WHOLE EYE CALIPER MEASUREMENTS				Total globe depth	16.04	15.15	14.22	13.98	13.12	12.98	12.51	12.23	12.30	13.53	1.1768
				Total globe height	17.74	16.71	15.65	15.36	14.55	14.34	13.44	13.53	14.27	15.06	1.4443
				Total globe width (rostro-caudal)	20.75	19.22	18.60	18.25	16.79	16.56	16.19	15.66	16.30	17.58	1.6610
				Corneal dimensions (dors-vent x rost-caud)	--	10.88x 12.94	9.83x 10.72	9.52x 10.65	8.19x 9.60	8.17x 9.43	8.25x 9.30	8.40x 9.51	8.81x 9.36	9.01x 10.19	0.9854x 1.2492

Table 5. Measurements from frozen lemon shark eyes sectioned horizontally. (All measurements in mm unless otherwise specified.)

					Eye #	10	11	12	X̄	s
SUBJECT ANIMAL GENERAL DATA					Shark # -- Left/Right eye	7L	8R	8L	(2L/1R)	
					Sex	F	F	F	(3F)	
					Fork length (cm)	55	56	56	55.7	0.577
FROZEN SECTION PHOTOGRAPH MEASUREMENTS	"On-Axis" Photographs	Intraocular Dimensions Along Optical Axis			Cornea thickness	0.360	0.383	0.394	0.379	0.01735
					Cornea to lens	0.706	0.612	0.709	0.676	0.05516
					Lens thickness	6.089	6.009	5.891	5.996	0.09961
					Lens to retina	5.331	5.915	5.633	5.626	0.29206
					Retina thickness	0.195	0.187	0.209	0.197	0.01114
					Choroid thickness	0.361	0.285	0.265	0.304	0.05065
					Sclera thickness	0.579	0.563	0.573	0.572	0.00808
					Total globe depth	13.621	13.954	13.674	13.750	0.17893
		Radii of Curvature			Lateral corneal sfc	9.086	8.418	9.736	9.080	0.65902
					Medial corneal sfc	7.626	7.283	7.657	7.522	0.20756
					Lateral lenticular sfc (lens apex)	3.694	4.008	4.047	3.916	0.19353
					Medial lenticular sfc (lens vertex)	3.759	4.178	4.235	4.057	0.25993
					Rostral lenticular sfc	2.854	3.023	3.798	3.225	0.50338
					Caudal lenticular sfc	2.796	2.878	2.830	2.835	0.04120
					Retinal-choroidal boundary	7.914	8.006	8.053	7.991	0.07070
		Intraocular Dimensions Not Along Optical Axis	R-C Dmsns		Lens width (at center)	6.827	6.926	6.867	6.873	0.04980
					Retina horiz. max	15.192	15.536	15.414	15.381	0.17441
					Total globe width	16.451	16.760	16.705	16.639	0.16483
			Ora Terminalis Location		Rostral o.t.-caudal o.t. separation	13.894	14.158	13.857	13.970	0.16415
					Rostral ora terminalis to lens center	7.023	7.194	6.948	7.055	0.12608
					Rostral o.t.-optical axis angle at lens center (°)	88	86	84	86.0	2.000
					Caudal ora terminalis to lens center	6.909	6.964	6.986	6.953	0.03966
					Caudal o.t.-optical axis angle at lens center (°)	84	89	89	87.3	2.887
			Scleral Cartilage Lateral Limits		Rostral s.c.-caudal s.c. separation	10.001	10.575	10.175	10.250	0.29432
					Rostral scleral cartilage to lens center	5.420	5.663	5.429	5.504	0.13777
					Rostral s.c.-optical axis angle at lens center (°)	71	70	68	69.7	1.528
					Caudal scleral cartilage to lens center	5.267	5.434	5.391	5.364	0.08671
					Caudal s.c.-optical axis angle at lens center (°)	67	74	72	71.0	3.606
	"Off-Axis" Photo				Angle between optic disc & optical axis plane at lens center plane (°)	10	09	10	09.7	0.577
WHOLE EYE CALIPER MEASUREMENTS					Total globe depth	12.76	13.36	13.22	13.11	0.3139
					Total globe height (dorso-ventral)	14.02	14.58	14.62	14.41	0.3355
					Total globe width	16.30	16.84	16.78	16.64	0.2960
					Corneal dimensions (dors-vent x rost-caud)	8.70x 9.31	8.56x 9.80	8.76x 9.73	8.67x 9.61	0.1026x 0.2650

Fig. 9. Simple linear correlation between body length and axial thickness of the crystalline lens in the juvenile lemon shark. Correlation coefficient = +.9627. Lens thickness data from photographs of frozen sections.

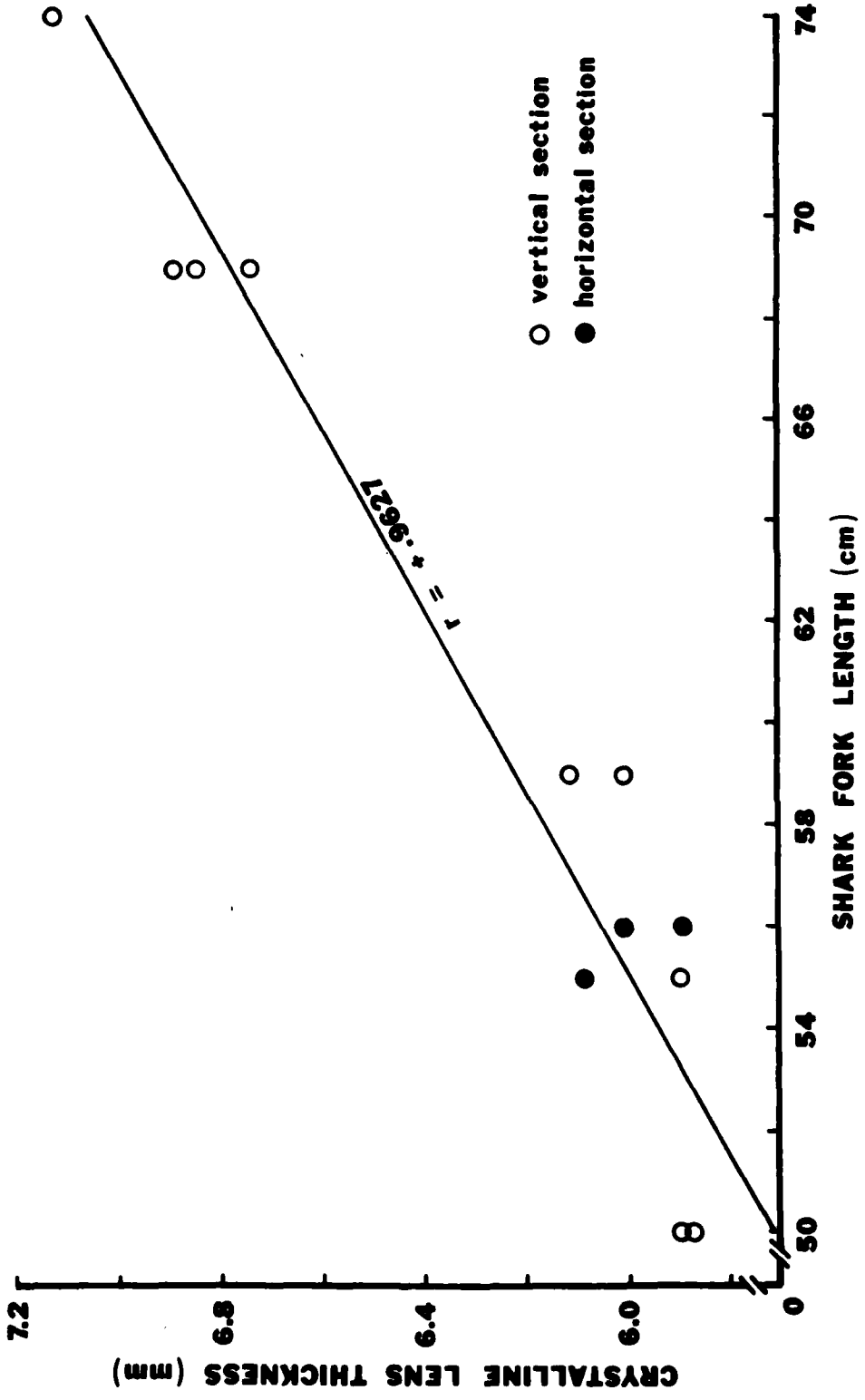
CRYSTALLINE LENS THICKNESS (mm)
7.2
6.8
6.4
6.0
0
50
54
58
62
66
70
74
SHARK FORK LENGTH (cm)
r = +.9627
vertical section
horizontal section

Fig. 10. Simple linear correlation between eye size (depth of globe from corneal front surface to scleral back surface) and axial thickness of the crystalline lens in the juvenile lemon shark. Correlation coefficient = +.9675. Data from photographs of frozen sections.

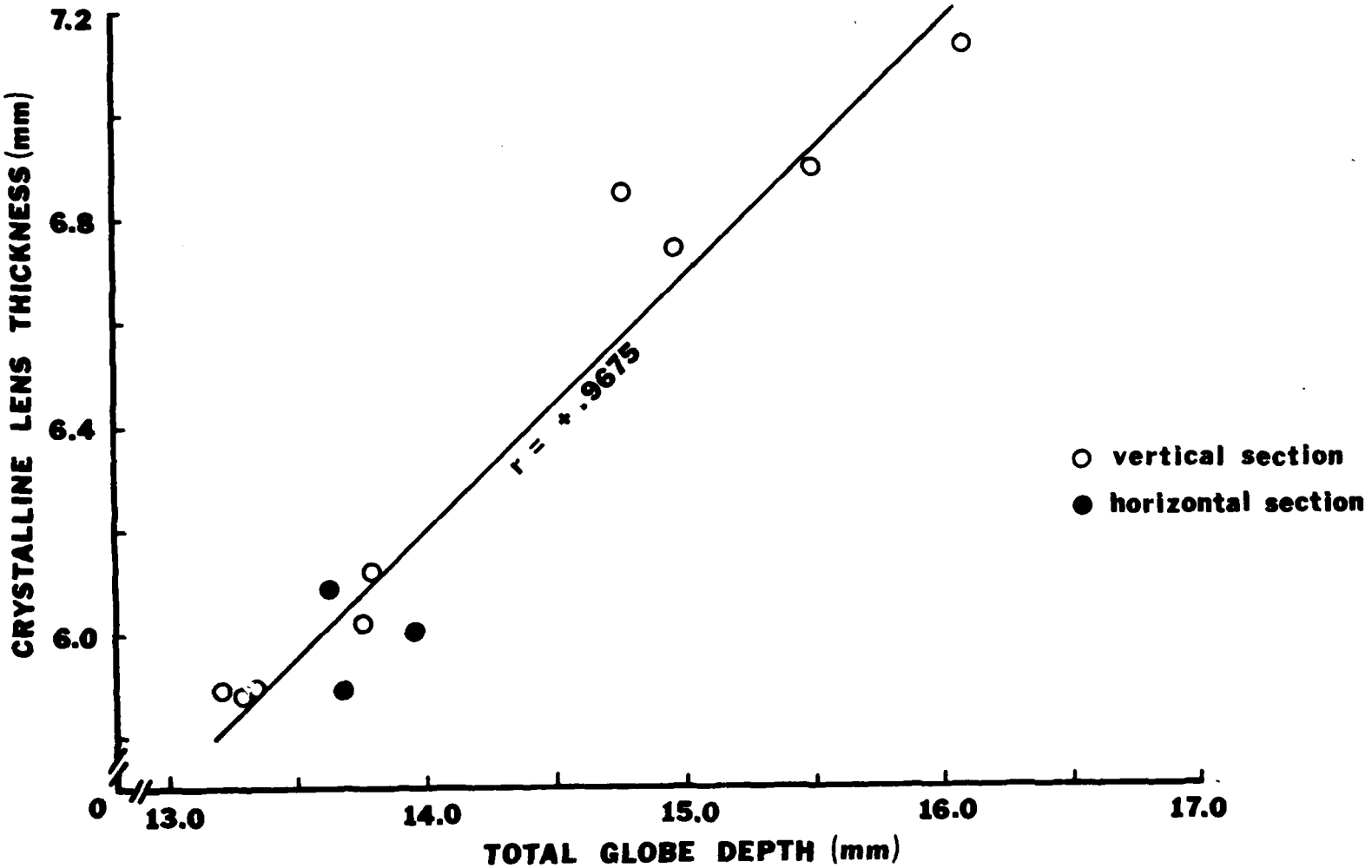
7.2
6.8
6.4
6.0
0
CRYSTALLINE LENS THICKNESS (mm)
r = + .9675
13.0
14.0
15.0
16.0
17.0
TOTAL GLOBE DEPTH (mm)
vertical section
horizontal section

Fig. 11. Simple linear correlation between axial thickness of the crystalline lens and axial lens-to-retina distance (lens vertex to vitreal-retinal boundary) in the juvenile lemon shark. Correlation coefficient = +.9144. Data from photographs of frozen vertical sections.

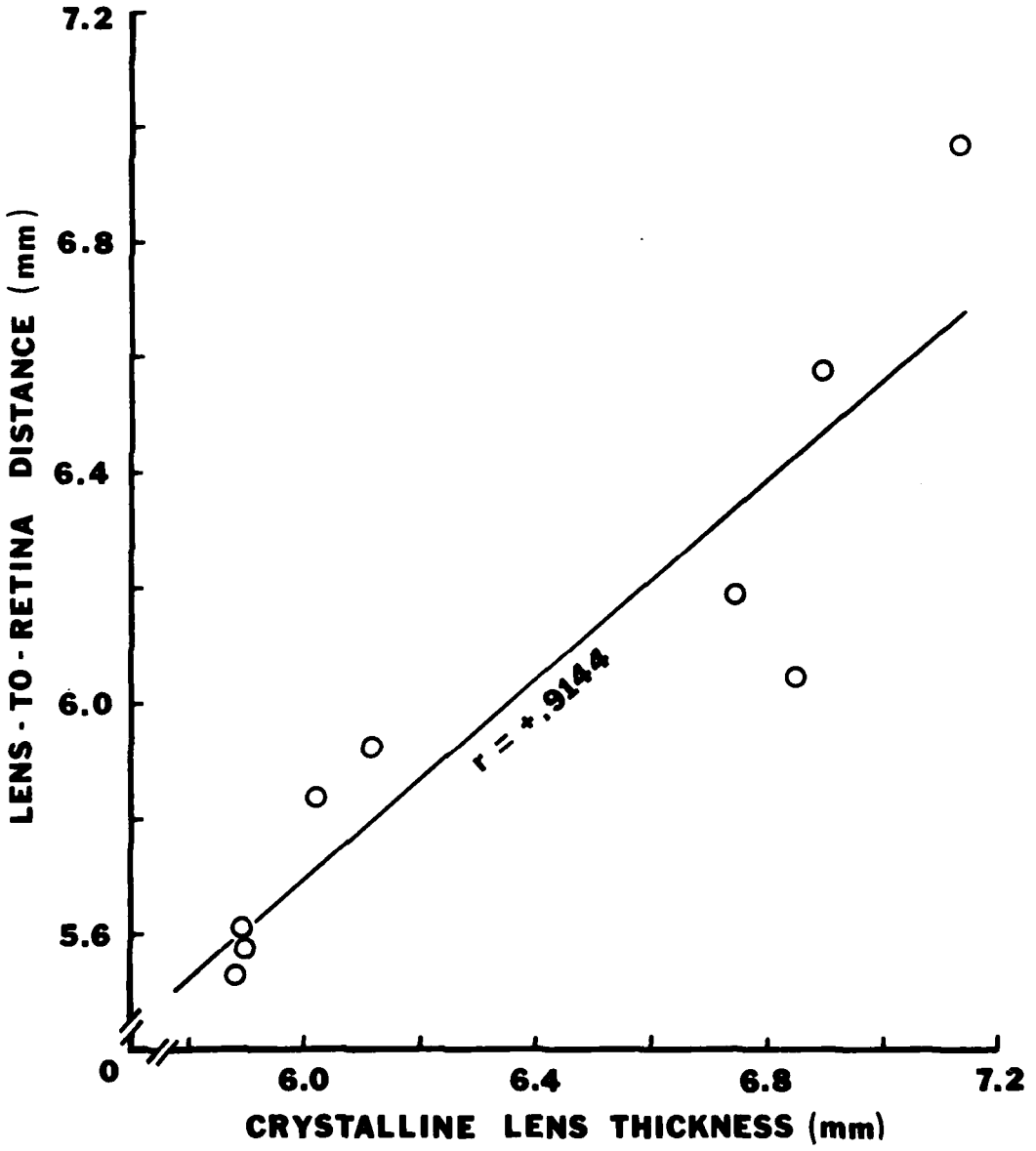
7.2
6.8
6.4
6.0
5.6
0
LENS - TO - RETINA DISTANCE (mm)
r = +.9144
6.0
6.4
6.8
7.2
CRYSTALLINE LENS THICKNESS (mm)

Fig. 12. Simple linear correlation between axial thickness of the crystalline lens and radii of curvature of the lens surfaces in the juvenile lemon shark. Lens apex curvatures are sharper than lens vertex curvatures. Apex correlation coefficient = +.9769; vertex correlation coefficient = +.9871. Data from photographs of frozen vertical sections.

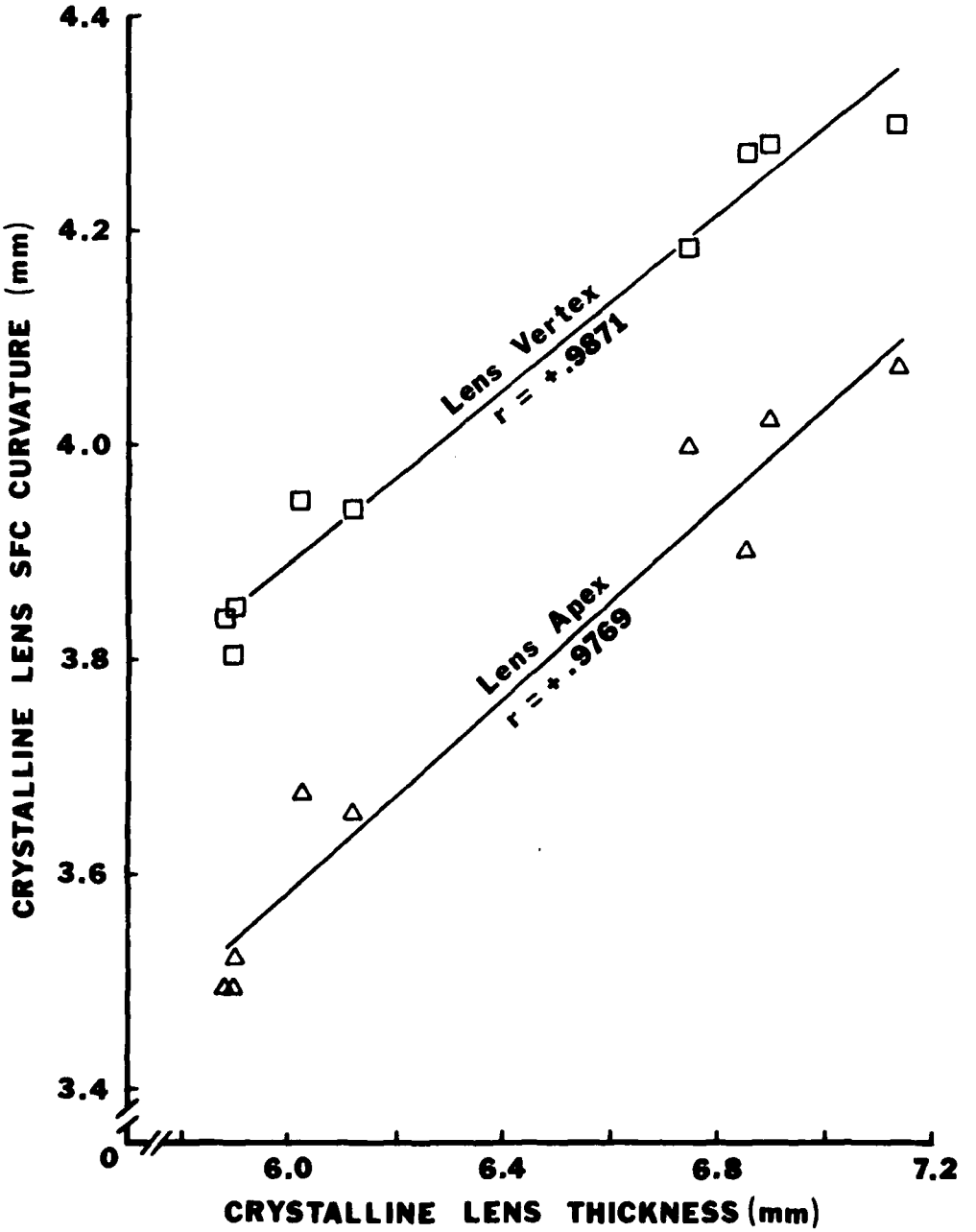
4.4
4.2
4.0
3.8
3.6
3.4
0
6.0
6.4
6.8
7.2
CRYSTALLINE LENS SFC CURVATURE (mm)
CRYSTALLINE LENS THICKNESS (mm)
Lens Vertex
r = +.9871
Lens Apex
r = +.9769

this reason, linear regression lines were fitted by the least-squares method to the correlated data, solely for the purpose of deriving values needed for the focal length tests from measurements of lens thickness.

Fixed values for the schematic eye model were mainly derived from the vertical section data. There is clear precedence for this procedure in the literature (Hughes, 1977); in addition, under photopic conditions, the slit pupil of the lemon shark eye limits the entering axial illumination to a horizontally compressed bundle of rays.

C. Lens Focal Length and n_{EL}

Results of the measurements of vertex focal lengths for five juvenile lemon shark lenses are shown in Table 6. Apex curvatures of the lenses were calculated using the formula

$$r_A = 0.8689 + 0.4528t \quad (1)$$

and vertex curvatures were obtained with the formula

$$-r_V = 1.4685 + 0.4038t \quad (2)$$

where r_A, r_V = apex and vertex radii of curvature of the lens, and t = lens thickness (all measurements in mm). These relationships were derived from the frozen section data by the least squares method of linear regression.

No significant changes in vertex focal length of the shark lenses were observed by interchanging the blue interference filter (490 nm), red interference filter (670 nm), and no filter (white light) in the optical measuring system. Noticeable shifts in focal length from blue to red light for any particular lens were always less than +0.05 mm, which was the measuring accuracy of my apparatus. These shifts could therefore not be construed as reliable measurements of chromatic aberration. A 0.05 mm shift would represent an in vivo change in focal length of less than 1%. To detect chromatic aberration

Table 6. Measured vertex focal lengths (f_V) and calculated n_{EL} for five crystalline lenses from juvenile lemon sharks.

Shark Sex	Fork Length (cm)	Measured Lens Thickness (mm)	Calculated Apex Curvature (mm)	Calculated Vertex Curvature (mm)	Measured Vertex Focal Length in Air (mm)	Measured Vertex Focal Length in Ringer's (mm)		Calculated n_{EL}
M	71.5	7.2	4.129	-4.376	3.70			1.664
						7.05		1.660
F	62.0	6.4	3.767	-4.053	3.41			1.665
						6.49		1.662
M	59.0	6.5	3.812	-4.093	3.43			1.666
						6.60		1.660
F	58.0	6.3	3.721	-4.013	3.35			1.668
						6.33		1.665
F	58.5	6.2	3.676	-3.972	3.34			1.665
						6.32		1.663
							n	10
							$\bar{X}$	1.664
							s	0.00257

effects which are less than the 1% level, a more precise optical system with a higher accuracy than that of my apparatus is required.

The n_{EL} for each lens in both the in-air and in-Ringer's conditions was therefore calculated using vertex focal lengths for white light. In these calculations, the following notation and terms apply:

Definition	Symbol	Derivation	Units
Vertex power of lens	D_V	Equation 3	Diopters
Principal power of lens	D_P	$D_1 + D_2 - eD_1D_2$	Diopters
Power of lens first surface	D_1	$(n_{EL} - n_1)/r_A$	Diopters
Power of lens second surface	D_2	$(n_3 - n_{EL})/r_V$	Diopters
Vertex focal length of lens	f_V	$\overline{VF_2}$	meters
Reduced thickness of lens	e	t/n_{EL}	meters
Real thickness of lens	t	$\overline{AV}$	meters
Radius of curv. of lens apex sfc	r_A	Equation 1	meters
Radius of curv. of lens vertex sfc	r_V	Equation 2	meters
Refr. index of pre-lens medium	n_1	Abbé refractometry	(unitless)
Lens overall equivalent refr. index	n_{EL}	Equation 4	(unitless)
Refr. index of post-lens medium	n_2	Abbé refractometry	(unitless)

According to thick-lens theory (Parrish, 1972), the vertex power of the crystalline lens can be expressed as follows:

$$D_V = \frac{n_3}{f_V} = \frac{D_P}{1 - eD_1} \qquad (3)$$

This relationship can be shown to be equivalent to the following:

$$\frac{n_3}{f_V} = \frac{D_1}{1 - eD_1} + D_2$$

By expanding the terms and simplifying the resulting fractions, I derived the following formula:

$$\frac{n_3}{f_V} = \frac{n_{EL} - n_1}{r_A + t(n_1/n_{EL} - 1)} + \frac{n_3 - n_{EL}}{r_V} \qquad (4)$$

I could not isolate for the unknown (n_{EL}) in this equation, so I used the formula to obtain an iterative solution for n_{EL} by successive approximation. All other values in the equation were accessible from my data.

From a total of ten measurements on five shark lenses, I obtained a mean n_{EL} of 1.664, with 95% confidence limits as follows: $P(1.6630 \leq \mu_{EL} \leq 1.6646) = .95$. An n_{EL} of 1.664 is comparable to the value of 1.65 derived for the goldfish eye (Charman and Tucker, 1973); on the other hand, it is not consistent with the value of 1.481 reported by Sivak (1976b) for the bluntnose stingray (Dasyatis sayi), another elasmobranch. However, Sivak has since noted that the 1.481 value was considerably lower than the true value due to experimental and calculating errors (Sivak, 1978c), and suspects that the n_{EL} of the stingray eye actually approaches the much higher value of 1.66 which he has measured for the lens of Squalus acanthias, the spiny dogfish (Sivak, personal communication). Thus, a high n_{EL} of around 1.66 appears to be the case in the selachian eye in particular, and probably in the elasmobranch eye in general.

Although not measured quantitatively, image quality of the juvenile shark lenses in the focal length tests was noticeably inferior to that produced by glass lenses of similar size to the crystalline lenses. The reticle image focused by the shark lenses appeared to me as significantly lacking in resolution and brightness compared with the image from a glass lens. This may have been due to post-mortem effects in the eyecup, most likely manifested as opacity of the cornea; but if the relatively poor image quality was not artifactual, this would indicate severe constaints on the resolving power of these eyes.

D. Pupillary Characteristics

Measurements of the fully dilated real pupils in three juvenile lemon sharks averaging 61 cm fork length are shown in Table 7. Mean dorso-ventral extent and rostro-caudal extent of the six dilated pupils were 7.16 and 6.69 mm, respectively. This mean size corresponds to a pupillary ellipse with an area of approximately 38 mm^2.

During studies of dark adaptation in Negaprion brevirostris, Gruber (1967) as well as Kuchnow and Gilbert (1967) found that pupillary area increased tenfold from the intensely light-adapted eye, with its slit pupil, to the completely dark-adapted eye, with its nearly circular pupil. The constricted slit pupil of the "average" juvenile lemon shark of about 61 cm fork length will thus contain a minimum pupillary area of about 4 mm^2 in bright light. Under these conditions, the rostro-caudal width of the pupil will decrease to close to 1 mm under intense light adaptation, assuming that the dorso-ventral height of the pupil does not constrict much beyond 2/3 of its maximum size. (This estimate was made by approximating the slit pupil to two identical isosceles triangles with a common base, the base being equal to the rostro-caudal axis of the pupil.)

E. Retinoscopy and Ophthalmoscopy

Refractive Error

Results of retinoscopic measurements of axial refractive error (K) in juvenile lemon sharks are presented in Table 8. Mean refractive error for 20 sharks (33 eyes refracted) was +7.5 D, with a range extending from a low of +4.5 D to a high of +11.5 D. The refracted animals averaged 58.8 cm in fork length, the smallest animal being 50 cm and the largest being 74 cm fork length. There was no clear correlation between shark size and refractive error within the range of animals examined ($r = -.0654$).

Table 7. Real pupil size in three juvenile lemon sharks (all males) dark-adapted overnight for maximum pupillary dilation.

Shark Fork Length (cm)	Left/Right Eye		Pupil Size (mm) Dorso-Ventral Axis	Pupil Size (mm) Rostro-Caudal Axis
61	L		7.10	6.88
	R		7.23	6.49
63	L		7.22	6.73
	R		7.36	6.98
59	L		7.11	6.61
	R		6.91	6.47
		$\bar{X}$	7.16	6.69
		s	0.1529	0.2081

Table 8. Retinoscopic measurements of refractive error (K) of juvenile lemon shark eyes in seawater. (Readings are adjusted for working distance between retinoscopist and shark, and are corrected for spurious refractive error introduced at air-seawater interface.)

Shark Sex	Fork Length (cm)	Refractive Error in Seawater (D)	
		Left Eye	Right Eye
M	64	+5.0	+5.5
F	52	+8.5	+7.5
F	53	+8.0	+8.5
M	55	+7.0	+6.5
M	53	+8.0	+6.0
F	53	+8.5	+8.0
M	51	+11.5	+10.5
M	53	+9.5	+8.0
F	74	+8.5	+11.0
M	69	+6.0	+6.0
F	69	+8.5	+7.0
F	59	+6.5	+7.5
F	50	+9.0	—
F	55	—	+8.5
F	56	—	+8.0
F	62	—	+5.0
M	72	+5.0	—
M	59	+5.0	+6.0
F	58	+4.5	—
F	59	—	+8.0
	58.8 cm	$\bar{X}$	+7.5 D refractive error
		s	+1.77 D
		n	33 eyes; 20 sharks

Sivak (1974b) measured the refractive error of one male and one female juvenile lemon shark with a retinoscope, and reported lateral (= axial) errors of +9.0 and +8.0 D for these two animals, which were approximately 65 cm in fork length. Sivak did not correct his measurements for the air-seawater problem, however (see Appendix); his readings become +6.7 and +6.0 D with the correction. These measurements clearly fit within the range of refractive errors that I observed for this species.

The animals that I refracted were, in general, dark-adapted for 10-15 minutes prior to retinoscopy. This was done to allow moderate dilation of the shark's pupil, so that I could more easily observe the behavior of the retinoscopic reflex from the animal's retina. Since an artificial pupil was not used, I could not judge the possible contribution of pupillary aperture size to refractive error, as measured by retinoscopy, in these animals; nevertheless, every shark that was refracted showed the same degree of dark-adaptation by virtue of "moderate" pupillary dilation.

The role of the tapetum during retinoscopy is additionally important. Kuchnow and Gilbert (1967) reported that complete dark adaptation of the occlusible Negaprion tapetum requires only 20 minutes. By their data, the tapetum of a lemon shark adapted for 10-15 minutes in the dark will exhibit a reflectivity that is about 75% of maximum. Thus the tapeta of the animals that I refracted were probably not completely unoccluded, but were certainly at least partially open. This is confirmed by the golden shine that I observed in refracting these animals.

In summary, I found that juvenile lemon sharks with moderate pupillary dilation and tapetum exposure exhibited a significant degree of spectacle hypermetropia in seawater, averaging +7.5 D as determined by streak retinoscopy. This literally means that, based on the results of retinoscopy, these

animals require underwater spectacles with +7.5 D lenses to correct their vision for maximal optical resolution. It does not mean that the dioptric power of the eye is exactly 7.5 D short; however, this number is a close estimate of the ocular hypermetropia, defined as the additional dioptric power (+ or −), required at the eye's second principal plane, to correctly focus an image from an infinitely distant source onto the photoreceptor layer (Bennett and Francis, 1962).

Observations of the Optical Media in Vivo

The optical media of juvenile lemon shark eyes (cornea, aqueous, lens, vitreous) collectively appeared through the retinoscope and ophthalmoscope as surprisingly translucent. This statement is based not only on my observations, but also on those of two ophthalmologists highly experienced at retinoscopy (J. Flynn, S. Spielman, personal communications). Irregular opacities, apparently in the cornea and lens, were commonly seen, and the media as a whole appeared distinctly non-transparent. This is similar to my observations on the excised eyecup in the measurements of lens focal lengths. The effect of this apparent translucence of the media on optical quality of these eyes is unknown, but it is significant that one of the ophthalmologists has observed much clearer media in preliminary studies of adult lemon shark eyes (S. Spielman and S. Gruber, personal communication). This indicates that the optics of the juvenile lemon shark eye may be in an uncompleted state of development.

With the aid of data from the frozen section measurements, I was able to locate the optic disc in the living shark eye by direct ophthalmoscope. The disc is situated in the rostro-ventral quadrant of the retina, on a line that is directed about 30° below and 10° forward of the optical axis. This fixes the lemon shark's blind spots in the dorso-caudal quadrant of the visual field of each eye.

The optic disc appeared through the ophthalmoscope as a darkened, more or less elliptical patch, with its major length directed dorso-ventrally. Small dark

processes projected for a short distance from the dorsal and ventral aspects of the disc. Attempts to focus the image of the disc with the ophthalmoscope lenses failed; the translucence of the optical media would not permit a clear view of the disc or any other retinal landmark.

Accommodative Movements

No attempt was made to actively induce accommodation in the experimental animals, although a few animals were refracted before and after administration of tricaine anesthetic in an effort to monitor changes in refractive error. Clear evidence of accommodative change was not discovered during these tests, corroborating the negative results obtained by Sivak (1974b), who used intraperitoneal injections of pilocarpine as well as tricaine anesthesia in an unsuccessful attempt to induce accommodation in two juvenile lemon sharks.

On two occasions, however, I witnessed a curious apparent movement of an optical component within two eyes of different juvenile lemon sharks. These movements were seen during retinoscopy, and one of these events was observed and described to me by an ophthalmologist (J. Flynn). On both occasions, an optical surface, seemingly the ventral surface of the crystalline lens or lens nucleus, appeared to spontaneously shift its position in the eye such that it seemed to move dorsally (medially?) during examination. The effect of this movement on axial refractive error measured retinoscopically was not significant, but the possibility that it represented a type of non-axial accommodation can not be ruled out. There is presently no anatomical evidence for such a mechanism.

II. THE SCHEMATIC EYE

A. Conventions

Due to the unimportance of the cornea as a dioptric element in the shark eye, I have taken a number of liberties with the traditional systems of notation utilized in aerial schematic eyes, which normally locate optical surfaces relative to the first corneal surface.

Light rays enter the schematic eye of the shark from left (lateral) to right (medial). Refractive indices are designated by n with a subscript. Important axial landmarks are designated as follows: corneal lateral and medial surfaces, C_1 and C_2; lens apex and vertex, A and V; retina lateral surface (vitreal-retinal boundary), R_1; retinal medial surface (retinal-choroidal boundary = photoreceptor layer), R_2; scleral lateral and medial surfaces, S_1 and S_2. Total depth of the globe, therefore, extends from C_1 to S_2. Intraocular distances are given as vectors from point to point, e.g., lens thickness is $\overline{AV}$, lens vertex to photoreceptor layer is $\overline{VR}_2$, etc.

Radii of curvature are designated by r with a subscript indicating the relevant surface, e.g., radius of curvature of the apex surface of the lens is written as r_A. Surfaces convex to the direction of light rays have positive radii of curvature; concave surfaces have negative radii of curvature.

Dioptric powers are designated by D with a subscript, and are measured in units of diopters (abbreviated as D with no subscript). Focal lengths are designated by f with the appropriate subscript. First and second principal points and nodal points are P_1 and P_2, N_1 and N_2. Ocular refractive error in the schematic eye is designated by K, and, like the dioptric powers, is measured in units of diopters.

B. Schematic Eye Calculations

The principal features of the schematic eye for the "average" juvenile lemon shark of about 62 cm fork length are summarized in Table 9. Most calculations were carried out using data from the nine vertically sectioned eyes. Hughes (1977) has stated that, for such calculations, separate schematic eyes should first be derived for each individual globe that is measured, with averaging being conducted only on the final dioptric dimensions from the individual schematic eyes. This method, according to Hughes, is preferable to averaging all of the measured ocular dimensions first, and then computing a single schematic eye from the grouped data. The problem with Hughes's preferred method of averaging is that it leads to a final schematic eye in which the dioptric powers are not precisely consistent with the model's physical dimensions, such as radii of curvature and intraocular distances.

I computed nine individual schematic eyes for the vertically sectioned shark globes, and compared the overall model obtained from these schematic eyes with the one schematic eye model computed from the grouped raw data. No difference was found in the majority of landmark positions between the two eye models, the only differences being $\pm$0.001 mm in some dimensions. Positions of principal planes and nodal points, as well as medial nodal distance ($\overline{N_2R_2}$), were identical in the two models. Dioptric powers in the model derived from separate schematic eyes were consistently about 0.4 D (or about 0.3%) less than the powers computed in the other model, but this difference did not significantly affect the positions of cardinal points between the two models. Therefore, for the sake of total consistency within the final schematic eye, I chose to base my mathematical model on the averaged raw data, contrary to Hughes's (1977) preference. [A more recent paper by Hughes (1979a) forsakes his 1977

Table 9. Principal features of the schematic eye for the juvenile lemon shark.

(a) Refractive index		
Seawater, Cornea, Aqueous	n_1	1.340
Lens (equivalent)	n_{EL}	1.664
Vitreous	n_3	1.340
(b) Optical axis dimensions (mm)		
Corneal thickness	$\overline{C_1C_2}$	0.436
Cornea to lens apex	$\overline{C_2A}$	0.441
Lens thickness	$\overline{AV}$	6.381
Lens vertex to retina	$\overline{VR_1}$	6.030
Retina thickness	$\overline{R_1R_2}$	0.199
Choroid thickness	$\overline{R_2S_1}$	0.281
Sclera thickness	$\overline{S_1S_2}$	0.529
Total globe depth	$\overline{C_1S_2}$	14.298
(c) Radii of curvature (mm)		
Lateral corneal sfc	r_{C_1}	7.304
Medial corneal sfc	r_{C_2}	6.134
Lens apex sfc	r_A	3.756
Lens vertex sfc	r_V	-4.046
Retinal-choroidal boundary	r_{R_2}	-6.623
(d) Dioptric powers (D)		
Cornea		0
Lens		
Apex sfc	D_1	66.22
Vertex sfc	D_2	80.08
Principal	D_P	139.62
Vertex	D_V	208.88
(e) Cardinal point positions (mm)		
Principal focal lengths (f_P)	$\overline{F_1P_1}$, $\overline{P_2F_2}$	9.583
Lens vertex focal length (f_V)	$\overline{VF_2}$	6.415
Lens apex to 1st princ. pt.	$\overline{AP_1}$	2.944
Lens apex to 1st nodal pt.	$\overline{AN_1}$	
2nd princ. pt. to lens vertex	$\overline{P_2V}$	3.169
2nd nodal pt. to lens vertex	$\overline{N_2V}$	
Principal planes separation	$\overline{P_1P_2}$	0.269
	$\overline{N_1N_2}$	
Nodal nodal distance	$\overline{N_2R_2}$	9.398
(f) Refractive error		
Out-of-focus distance	$\overline{R_2F_2}$	0.185 mm
Ocular refractive error	K	+2.76 D

recommendations and adopts the calculating procedure using the averaged raw data.)

Refractive Indices

Refractive indices of the ocular media were derived from the Abbé refractometer data and from the measurements of lens focal length in vitro. The optical absence of the cornea, due to its equivalence in refractive index with seawater and aqueous, negates its importance in the dioptric model.

Intraocular Dimensions and Radii of Curvature

These variables were obtained from the averaged measurements taken from the photographs of frozen sections.

Dioptric Powers

Dioptric powers of the equivalent crystalline lens were calculated using standard formulas from thick-lens theory (Parrish, 1972; Bennett and Francis, 1962). These formulas are as follows:

a) Surface powers:

$$D_1 = \frac{n_{EL} - n_1}{r_A}$$

$$D_2 = \frac{n_3 - n_{EL}}{r_V}$$

b) Principal power:

$$D_P = D_1 + D_2 - eD_1D_2$$

where $e = \frac{\overline{AV}}{n_{EL}}$ (lens reduced thickness)

c) Vertex power:

$$D_V = \frac{D_P}{1 - eD_1}$$

Radii and distances in these equations are expressed in meters, and powers are expressed in diopters. Principal power is a measure of the dioptric power of the lens relative to the second principal plane; vertex power measures dioptric power relative to the lens vertex, and is always greater than the principal power in a biconvex lens (Bennett and Francis, 1962). The reciprocal of the principal power, multiplied by the refractive index of the medium surrounding the lens, equals the principal focal length f_P, which is the distance between the second principal plane and the back focal point ($\overline{P_2F_2}$):

$$f_P = \frac{n_3}{D_P}$$

The reciprocal of the vertex power, times the refractive index of the post-lens medium, is equal to the vertex focal length f_V, the distance from the vertex surface of the lens to the back focal point ($\overline{VF_2}$):

$$f_V = \frac{n_3}{D_V}$$

Cardinal Points

Since the refractive indices of the pre- and post-lens media are equal (1.340), the system is termed symmetric or equifocal, and the first and second nodal points will lie at the same locations as the first and second principal points (Bennett and Francis, 1962). This simplifies the determination of these four points to two equations:

a) Lens apex to first principal point:

$$\overline{AP_1} = \frac{n_1 e D_2}{D_P}$$

b) Second principal point to lens vertex:

$$\overline{P_2V} = \frac{n_3 e D_1}{D_P}$$

The first and second nodal points are then located coincident with the first and second principal points.

A small error in the location of the principal planes is introduced by substituting a homogeneous lens for the real multi-refractive lens (von Helmholtz, 1924). This substitution leads to a slightly greater separation between the principal planes, with a resulting higher principal power than in the real lens. The effect of this error on location of focal points and on out-of-focus distance is negligible; it has a small effect on the calculation of refractive error, adding about 0.5 D to the refractive error in the cat eye, for example (Vakkur and Bishop, 1963).

Refractive Error

Ocular refractive error (K) is a measure of the number of diopters by which the principal power of an eye undershoots or overshoots the dioptric power required to focus an image from an infinitely distant source onto the photoreceptor layer. A positive K means that the principal power is too weak for the eye, with the focused image falling behind the photoreceptors; this condition is termed hypermetropia, or far-sightedness. Myopia, or near-sightedness, is the opposite case: the focused image falls in front of the photoreceptors, so that the principal power is too strong for the eye, and a negative K will result. In both cases, the image of a distant object will be blurred at the level of the photoreceptors.

Ocular refractive error is calculated using the dioptric power equivalent of the distance between the second principal point and the photoreceptors, minus the eye's principal power, as follows (derived from Hughes, 1972, and duPont and deGroot, 1976):

$$K = \frac{n_3}{\overline{P_2R_2}} - D_P$$

C. Schematic Eye Summary

Fig. 13 depicts the physical and optical elements of the schematic eye for the juvenile lemon shark. The key attributes of this eye are as follows:

Principal power of the eye	D_P	139.82 D
Medial nodal distance	$\overline{N_2R_2}$	9.398 mm
Out-of-focus distance	$\overline{R_2F_2}$	0.185 mm
Ocular refractive error	K	+2.76 D

Although the out-of-focus distance appears very small, the results of a paired-sample t-test (Zar, 1974) rejected the null hypothesis of no significant difference between the principal focal length f_P ($= \overline{P_2F_2}$) and the second principal plane-to-photoreceptors distance $\overline{P_2R_2}$ ($.01 < P < .025$). The out-of-focus distance $\overline{R_2F_2}$ must be significant, as is the positive refractive error.

The schematic eye is therefore hypermetropic by +2.76 D. This schematic value agrees qualitatively but not quantitatively with the average refractive error of +7.5 D measured by streak retinoscopy in living animals.

D. Pupillary Characteristics

Dark-adapted

From the photographs of frozen sections, it is apparent that the location of the real pupil closely matches the position of the lens apex A. The size of the real pupillary opening in the totally dark-adapted shark eye is an ellipse measuring 7.16 x 6.69 mm (dorso-ventral x rostro-caudal axes). This approaches the overall size of the lens itself, which is 7.212 mm high by 6.873 mm wide in the frozen sections.

Fig. 13. Schematic eye of the juvenile lemon shark. The crystalline lens is the sole refractive element in seawater. A, lens apex; D_P, principal power of the eye in diopters; F_1 and F_2, front and back focal points; K, refractive error in diopters; N_1 and N_2, first and second nodal points; n_1 and n_2, refractive indices of aqueous and vitreous humors; n_{EL}, overall refractive index of equivalent homogeneous lens; P_1 and P_2, first and second principal planes; R_1, vitreal-retinal boundary; R_2; retinal-choroidal boundary (photoreceptor layer); V, lens vertex. The eye is slightly hypermetropic in seawater. (See Table 9 for principal numerical features of the schematic eye.)

SCHEMATIC EYE OF THE JUVENILE LEMON SHARK

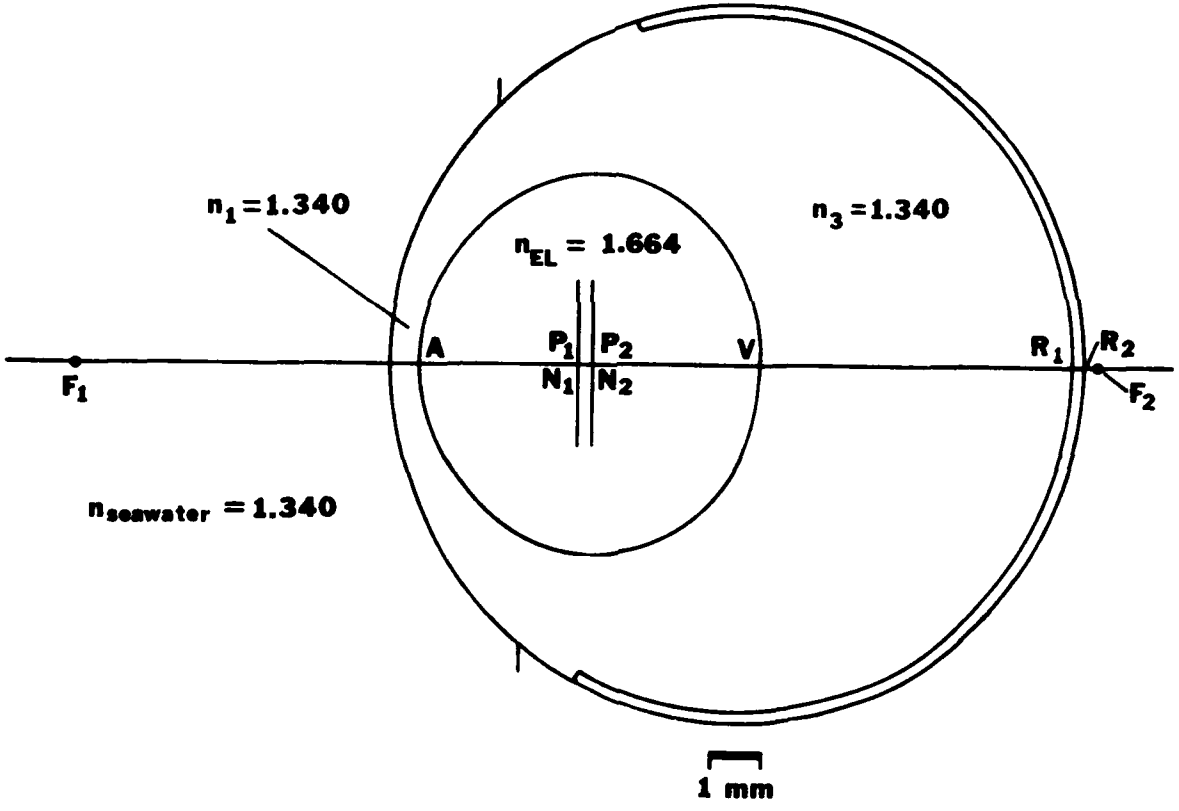

$D_P = +139.82$ D

$K = +2.76$ D

The entrance pupil, which is the image of the real pupil formed by refraction through the cornea, is equivalent to the real pupil in the shark eye because the cornea is optically absent. The exit pupil, on the other hand, does exist separately from the real pupil in this eye. The exit pupil is defined as the image of the real pupil formed by refraction through the crystalline lens, and it is used in the computation of retinal blur circle sizes associated with a given refractive error.

Using the procedures of Bennett and Francis (1962), I calculated that the exit pupil in the dark-adapted shark eye is located at an apparent distance of 1.035 mm in front of the lens apex. Its size is 1.44 times that of the real pupil, making it 10.31 x 9.63 mm.

Light-adapted

Exit pupil characteristics were computed for a theoretical real pupil measuring 5.00 x 1.00 mm. This represents a pupillary size for an eye that is near maximum light adaptation. The exit pupil in these circumstances would measure 7.20 x 1.44 mm, with its position being unchanged from dark-adapted conditions.

DISCUSSION

A mathematical model that is static, that cannot be tested to answer further questions about the system which it simulates, is of little use to the biologist beyond descriptive purposes and for comparison with other static models. Biological systems are far more interesting for their functional and adaptive properties, rather than as mere subjects for a mathematical exercise. To this end, a schematic eye for a particular species should be treated as a result and not a conclusion.

The discussion that follows will utilize the now derived schematic eye for the juvenile lemon shark to arrive at a number of statements about the visual system of the species. The possible applications of this schematic eye are not restricted to the addressed topics; I have chosen to discuss those questions that I consider to be among the most important in the physiological optics of elasmobranchs. These topics will touch upon the areas of physical optics, visual physiology, and ultimately, visual behavior in sharks.

I. SCHEMATIC OPTICAL CHARACTERISTICS OF THE JUVENILE LEMON SHARK EYE

A. Image Formation: Optical Design

The size and sharpness of images produced by a dioptric system are governed by a number of optical characteristics of that system. These include:

(1) Diffraction limitations associated with small apertures.

(2) Lens aberrations.

(3) Clarity of the optical media.

(4) Image size as a result of eye size.

(5) Refractive error.

The first three of these characteristics were not investigated in depth in this study, but they warrant brief consideration in a discussion of image

formation in the schematic eye. The last two characteristics will be more closely examined for their effects on visual acuity in the juvenile lemon shark.

Diffraction Effects

The resolution of a diffraction-limited image is determined by the distance from the energy maximum at the image's center to the first energy minimum resulting from interference effects (Campbell et al., 1974). With a circular aperture, such as the human pupil, this distance is equal to the radius of the so-called Airy disc. For a given wavelength of light, the disc's radius is directly proportional to the F number of the eye (the principal focal length of the lens divided by the aperture diameter). Therefore, smaller pupillary diameters lead to larger Airy discs, and resolution, otherwise determined by refractive and neural factors, becomes diffraction-limited. Diffraction effects in the human eye influence visual acuity up to pupillary sizes of about 2 mm; with larger pupil diameters, the effects of diffraction become secondary to the increasing spherical aberration of the human dioptrics (Riggs, 1965).

The interference pattern produced by an elliptical pupil, such as in the juvenile lemon shark eye, will deviate from an Airy disc-type pattern, but the diffraction limitations on resolution in this eye can be approximated using Airy disc calculations. The formula for computing the size of the Airy disc is:

$$R = \frac{1.22\lambda f_P}{d}$$

where R = radius of Airy disc in μm, 1.22 = constant (which approaches 1.00 for an elliptical aperture), λ = wavelength of light passing through the aperture in μm, f_P = principal focal length of the schematic eye in mm, and d = diameter of the pupillary aperture in mm (Campbell et al., 1974). With the f_P of 9.583 mm for the juvenile lemon shark lens, and choosing 541 nm light which corresponds to

the peak sensitivity of the light-adapted lemon shark retina (Cohen et al., 1977), this equation becomes:

$$R = \frac{(1.22)\,(.541)\,(9.583)}{d}$$

$$= \frac{6.32}{d}$$

where d is expressed in mm and R is expressed in μm. For a 1 mm-wide entrance pupil, such as in the light-adapted eye of the juvenile lemon shark, the radius of the equivalent Airy disc would therefore equal 6.32 μm. (The actual value for an elliptical pupil will be less, not greater, than this value). This number will be compared with other optical specifications, such as retinal intercone spacing, to assess the importance of diffraction effects from small pupil size on visual acuity.

Lens Aberrations

It is generally agreed that visual acuity in fishes (i.e. teleosts) is not limited by optical aberrations (Northmore et al., 1978), and this probably holds true for elasmobranchs as well, as follows:

Spherical aberration. Though not measured in this study, spherical aberration in the lemon shark lens is probably negligible due to the increasing refractive index from cortex to nucleus (Pumphrey, 1961; Weale, 1974). If any spherical aberration exists within the lemon shark lens, it will be minimized in the horizontal meridian by the slit pupil under photopic conditions.

Chromatic aberration. I could not detect significant shifts in lens focal length, due to chromatic aberration effects, at the 0.05 mm level of measurement. Since the out-of-focus distance in the schematic eye is 0.185 mm, I must reject the notion that chromatic

aberration of the juvenile lemon shark lens might compensate for all of the refractive error calculated for white light. This is consistent with the view that teleost lenses are also relatively free of chromatic aberration (Pumphrey, 1961).

With a technique known as chromoretinoscopy, which is retinoscopy performed through colored filters, Sivak (1978b) reported that the eye of the spiny dogfish, Squalus acanthias, exhibited a total chromatic aberration of four to five diopters (around a mean refractive state of +6 D) from blue to red light. However, Sivak did not correct his retinoscopic measurements for the air-to-seawater problem (see Appendix to this thesis), which is further compounded by using different wavelengths of light, and therefore the significance of his results with respect to my study is unclear.

Light Transmission of the Optical Media

I have noted the apparent opacity of the juvenile lemon shark's ocular media in tests of lens focal length and in retinoscopic and ophthalmoscopic examinations. The quantitative effect of this factor on image degradation was not measured, but it can only serve to reduce the intensity and sharpness of the retinal image by absorption and scattering of light within the eye.

Yellow pigments have been detected by spectrophotometry in the ocular media of carcharhinid and sphyrnid sharks (Zigman and Gilbert, 1978), as well as in the smooth dogfish Mustelus canis (Kennedy and Milkman, 1956). The possibility that such a pigment exists in the eyes of lemon sharks, and that it may contribute to the observed opacity in the juvenile eye, cannot be discounted. Spectrophotometric studies of the ocular media of the juvenile and adult lemon shark eyes would help to resolve this matter.

Eye Size and Retinal Magnification

The size of dioptric features in an eye directly affects visual resolution by determining the absolute size of the retinal image. The eyes of sharks have been characterized in general as being small in relation to body size (Gilbert, 1963; the converse was stated by Walls, 1942). In the juvenile lemon shark, however, the axial depth of the eye (14.298 mm) is not small for the animal's size (1-2 kg) when compared with the general relationship between eye size and body weight in various vertebrate species, as described by Hughes (1977). However, juvenile vertebrate eyes tend to be larger in proportion to body size than adult eyes.

The key dimension governing size of an image on the retina (disregarding the further affects of ametropia) is the distance between the second nodal point and the photoreceptor layer. This dimension is known as the posterior nodal distance (PND) in animals with frontally situated eyes; in the lemon shark, I use the term medial nodal distance ($\overline{N_2R_2}$), because the eyes are situated laterally on the head. $\overline{N_2R_2}$ governs retinal magnification by determining the retinal area which is subtended by the image of an object occupying a particular visual angle in the field of view. This visual angle is determined by the size of the object and its distance from the eye's first nodal point. Thus, knowledge of the position and size of an object, and the magnitude of the eye's nodal distance, are both required to calculate the size of the retinal image for that object.

The distance i subtended on the retina by an image with a given visual angle θ can be found with the following relationship, which assumes that θ is small and the subtended retina is relatively flat:

$$\tan(\theta/2) = \frac{0.5i}{\overline{N_2R_2}}$$

This can be rearranged to yield the following:

$$i = 2(\overline{N_2R_2})\,[\tan(\theta/2)]$$

For the juvenile lemon shark schematic eye, $\overline{N_2R_2}$ equals 9.398 mm. Thus, for a 1^{o} visual angle, the corresponding distance subtended on the retina is 0.164 mm; a 1 mm retinal image would likewise correspond to an object that occupies a visual angle of 6.09^{o} (Fig. 14).

This attribute is commonly expressed as retinal magnification factor (RMF) in terms of mm/^{o} visual angle (Hughes, 1977) or μm/^{o} visual angle (Easter et al., 1977) at the photoreceptor layer. RMF for the juvenile lemon shark is therefore 0.164 mm/^{o}, or 164 μm/^{o}. This equals (25.7 x lens thickness)μm/^{o}mm, where lens thickness is 6.381 mm. In comparison, the goldfish RMF equals (20.5 x lens thickness)μm/^{o}mm, or about 60 μm/^{o} (Easter et al., 1977); the bottlenosed dolphin RMF, on the other hand, is around 240 μm/^{o}, or about (25.0 x lens thickness)μm/^{o}mm (derived from Dawson et al., 1972). It appears that the factor relating RMF to lens thickness is approximately equal for the goldfish (20.5), lemon shark (25.7), and dolphin (25.0); differences in absolute magnitude of retinal magnification in the three species must be due primarily to simple differences in ocular size.

One final note on eye size and resolving power concerns the use of "Matthiessen's ratio" to estimate visual acuity. Matthiessen (1882) discovered that the ratio between focal length and radius of the spherical fish lens was relatively constant between several species, being about 2.55. Since this discovery, some workers investigating visual acuity in fishes (e.g., Tamura, 1957; Tamura and Wisby, 1963) have invoked the use of Matthiessen's ratio as an estimate of focal length of the lens from lens radius, regardless of species. That this liberty is not acceptable for calculating visual resolution in many species of

Fig. 14. Visual angle (θ) and retinal magnification factor (RMF) for the eye of the juvenile lemon shark. N_1 and N_2, first and second nodal points; R_2, retinal-choroidal boundary (photoreceptor layer). A 1 mm distance on the retina corresponds with a visual angle of 6.09^{o}; a 1^{o} visual angle corresponds with a retinal subtense of 164 μm.

AD-A084 847 ROSENSTIEL SCHOOL OF MARINE AND ATMOSPHERIC SCIENCE --ETC F/G 8/1
PHYSIOLOGICAL OPTICS OF THE EYE OF THE JUVENILE LEMON SHARK (NE--ETC(U)
MAY 80 R E HUETER N00014-75-C-0173
UNCLASSIFIED UM-RSMAS-80003 NL

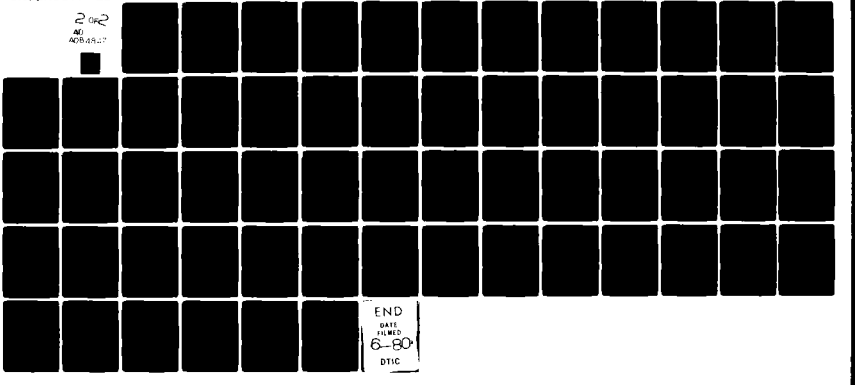

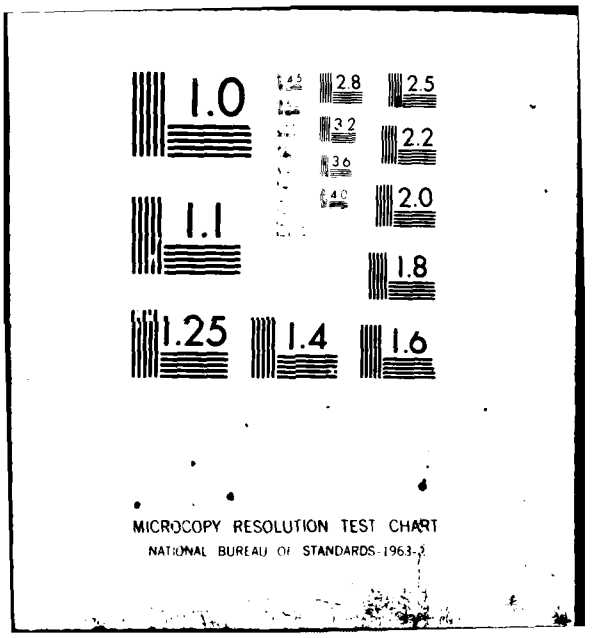
1.0
1.1
1.25
1.4
1.6
1.8
2.0
2.2
2.5
2.8
3.2
3.6
4.0
MICROCOPY RESOLUTION TEST CHART
NATIONAL BUREAU OF STANDARDS-1963-A

1 mm on retina = ? visual angle

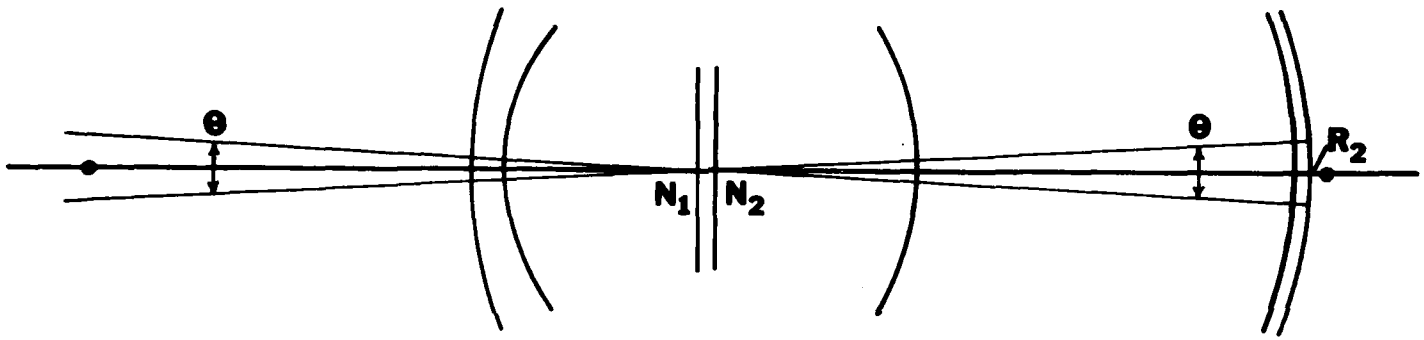

$$\tan(\theta/2) = \frac{0.5\text{mm}}{\overline{N_2 R_2}}$$

$$\overline{N_2 R_2} = 9.398\ \text{mm}$$

$$\theta = 6.09^\circ$$

$$\text{RMF} = 164\ \mu\text{m}/^\circ$$

teleosts has been discussed by Sadler (1973) and Easter et al. (1977). In the juvenile lemon shark, the distance between the lens center and the back focal point ($1/2\ \overline{AV} + \overline{VF_2}$) is 9.606 mm; half of the lens thickness ($\overline{AV}$) is 3.191 mm. Thus the analogous quantity to Matthiessen's ratio in this eye is 9.606/3.191 = 3.01, not 2.55, demonstrating that Matthiessen's ratio should be used for elasmobranchs with the same reservations that Sadler (1973) has advocated for teleosts.

Refractive Error: Schematic Eye vs. Retinoscopy

The resolution achieved by the optical system of an eye fixating a distant object is maximal only if the eye is emmetropic, or if the eye can accommodate to bring distant objects conjugate to (in focus on) the retina. The ametropic unaccommodated eye produces a blurred image of a distant object on the retina, and the amount of blurring depends on the refractive error of the eye and the size of the pupil. The greater the refractive error and the larger the pupil, the more blurred the image becomes.

The refractive error in my schematic eye model for the juvenile lemon shark is +2.76 D, while retinoscopy performed on these animals yielded readings averaging +7.5 D. Before proceeding with a discussion of optical resolution and visual acuity, it is important to consider this discrepancy in refractive state, and attempt to resolve the difference.

Calculations for the schematic eye were based largely on measurements from sections of frozen eyes, which would normally be expected to have undergone some expansion during freezing. The ocular dimension which should have been most affected by freezing is the lens-to-retina distance; the relatively voluminous vitreous, if frozen, would most likely relieve the pressure from expansion by displacing the lens some distance towards the pliable cornea, rather

than towards the cartilagenous sclera. This effectively increases the lens-to-retina distance in the frozen eye over what it truly is in the living eye.

In a hypermetropic eye model, this expansion upon freezing causes the degree of hypermetropia to be reduced, because the back focal point of the lens is brought closer to the photoreceptor layer when the lens-to-retina distance is increased. For this reason, the schematic eye represents a condition of minimum average hypermetropia for the sectioned eyes, and the degree of hypermetropia in the living eye should be expected to be greater, not less, than in the schematic eye.

Is this expansion enough to explain the higher measurements of hypermetropia by retinoscopy? To have changed from a +7.5 D refractive state before freezing to a +2.76 D error after freezing, the distance $\overline{P_2R_2}$ must have increased from a theoretical value of 9.096 mm to the measured value of 9.398 mm, an expansion of 3.32%. This is quite sizable, much larger than the 0.64% expansion that was estimated using caliper measurements of the globe taken prior to freezing. A 0.64% change implies a pre-freezing $\overline{P_2R_2}$ of 9.338 mm; this would yield a refractive error of +3.68 D in the living eye, explaining only about 20% of the discrepancy.

It appears too much to expect the expansion factor to explain all of the discrepancy between retinoscopy and the schematic eye. Neither does the fact that I substituted a homogeneous lens model in the schematic eye for the real multi-refractive lens help the problem, because this would add to, not subtract from, the living refractive state by a small margin in the schematic eye (Hughes, 1979a). Further complicating the issue is the question of the possible effects of disturbing the intraocular pressure after enucleation (Hughes, 1977). In the absence of precise correction factors for these additive and subtractive effects, I

must at this point assume that the frozen sections represent an acceptable portrayal of the dimensions in the living eye of the juvenile lemon shark.

Still remaining, then, is the incidence of high hypermetropia in the retinoscopic measurements. It is possible that chromatic aberration effects may account for some of the error, but my measurements of lens focal lengths indicate that chromatic aberration is not of the magnitude required to produce a five diopter discrepancy. Also, the fact that retinoscopy measures spectacle refraction rather than ocular refraction does not resolve the problem, since the ocular refractive error as calculated in the schematic eye should be slightly greater, not less, than spectacle refractive error measured with the retinoscope.

If, however, the retinoscopic reflex in the shark eye arose not from the level of the photoreceptors at the retinal-choroidal boundary, but rather from a surface layer that is lateral to the photoreceptors, such as the vitreal-retinal boundary, a significant error would be introduced into the retinoscopic measurements of refractive state. Under these conditions, the degree of hypermetropia in the living eye would be overestimated by retinoscopy, because the separation between the eye's back focal point and the reflecting layer would be greater than the actual photoreceptor-to-focal point distance. For the juvenile lemon shark, such an error in the location of the reflecting layer would produce an apparent refractive error (K'), measured relative to the vitreal-retinal boundary, that can be calculated as follows:

$$K' = \frac{n_3}{P_2 R_1} - D_P \qquad (5)$$

Substituting in the known values from the schematic eye on the right side of Equation 5, I obtain an apparent refractive error of +5.85 D, which is well within the range of observed retinoscopic measurements for these eyes and much closer to the mean value of +7.5 D than is the schematic eye value.

The idea of an error in the location of the retinoscopic reflex is not new. Although other workers (e.g. Walls, 1942) had discussed the problem prior to 1970, Glickstein and Millodot's study published that year was the first to quantitatively examine the inexplicable condition of widespread hypermetropia among refracted animals. They discovered that there was a high negative correlation between apparent refractive error measured retinoscopically and the square of eye diameter, such that small eyes exhibited proportionally higher degrees of hypermetropia than large eyes. Using data from a range of mammalian species, Glickstein and Millodot concluded that the apparent reflective layer in retinoscopy was displaced an average of 135 μm vitread to the outer segments, which corresponded with the vitreal-retinal boundary in those animals. Due to the relatively constant thickness of the retina regardless of overall eye size, this displacement has a greater effect on the measured hypermetropia in small eyes vs. large eyes. On the basis of this evidence, it was inferred that retinoscopy added a positive error to the true refractive state of the eye, and that, in fact, most animals have near-emmetropic vision.

Experimental evidence for Glickstein and Millodot's theory has since accumulated and has been reviewed by Hughes (1977; see also Hughes, 1979b). The conclusion that the retinoscopic reflex is dominated by rays originating at the vitreal-retinal boundary has been reached for a number of nonmammalian as well as mammalian species, including teleosts (Schwassmann, 1975), using primarily electrophysiological refractive techniques.

It is logical to assume that the retinoscopic reflex from the shark eye is dominated by rays originating from the tapetum rather than any other surface. However, if this were the case, the actual degree of hypermetropia at the photoreceptors would be even more extreme than the retinoscopic measurements would indicate. This is unacceptable in light of the values derived for the

schematic eye, even though the juvenile sharks that I refracted were moderately dark-adapted with exposed tapeta. If this is an inconsistent set of circumstances, it nevertheless also holds true for kitten and cat eyes (Glickstein and Millodot, 1970), which, like the lemon shark, possess well-developed choroidal tapeta (Walls, 1942).

Table 10 summarizes the various factors that are implicated in the discrepancy between the refractive error of the schematic eye in the juvenile lemon shark and the mean hypermetropia measured retinoscopically in live animals. The more important of these factors are the location of the retinoscopic reflex and the expansion of the eye prior to sectioning. Assuming for the moment that Glickstein and Millodot's hypothesis is correct, and that I have correctly calculated the principal power and focal lengths of the lens for the eye of the living juvenile lemon shark, what does the retinoscopically measured refractive error of +7.5 D indicate? Using Equation 5 and substituting in +7.5 D for K' and +139.82 D for D_P, the theoretical value for $\overline{P_2R_1}$ becomes 9.096 mm. This dimension was actually measured to be 9.199 mm in the frozen sections, implying an expansion upon freezing of 1.13% in $\overline{P_2R_1}$ using the retinoscopic data as a calibration. This amount of expansion due to freezing is plausible. An adjustment of 1.13% in the schematic eye would decrease $\overline{P_2R_2}$ from 9.398 mm to 9.293 mm, yielding an adjusted refractive error of +4.37 D instead of +2.76 D in the final eye model.

In summary, it is evident that my schematic eye model probably represents the optical system of the juvenile lemon shark eye at its optimum level in terms of resolving power; that is, with the consideration of the possible experimental errors, the schematic refractive error of about +3 D is located at the minimum, not the maximum, of the range of probable hypermetropia in the average eye of living juvenile lemon sharks. An analysis of vision in these animals based on my

Table 10. Sources of discrepancy in refractive error of the schematic eye vs. retinoscopic measurements. Only factors (1) and (2) serve to explain the high retinoscopic measurements relative to the lower hypermetropia in the schematic eye. Factors (3) and (4) lead to small errors that are contrary to the observed discrepancy and thus do not help to explain the high retinoscopic measurements. Factor (5) is probably not important in the juvenile lemon shark, based on my in vitro measurements of chromatic aberration in the shark lens.

	Source of Error	Effect
(1)	Retinoscopic reflex from vitreal-retinal boundary	Retinoscopy overestimates hypermetropia
(2)	Expansion of intraocular dimensions during freezing prior to sectioning	Schematic eye underestimates hypermetropia
(3)	Substitution of homogeneous lens model for real multi-refractive lens	Schematic eye overestimates hypermetropia
(4)	Measurement of refractive error at spectacle plane in retinoscopy	Retinoscopy underestimates ocular refractive error
(5)	Chromatic aberration	All methods overestimate hypermetropia in blue light

schematic eye, therefore, will depict juvenile lemon shark vision at its best optical potential for the visual field on or near the shark's optical axis.

B. Image Formation: Visual Acuity

Visual acuity is a general term that refers to an animal's maximum ability to visually resolve the finest detail of an object that is illuminated under certain conditions. Visual acuity is not a concrete specification of a visual system, but rather is an operationally defined feature of an animal's behavior that may vary with measurement conditions, and it is determined by optical as well as neural factors (Hughes, 1977).

With the constants that are supplied in the schematic eye, certain types of visual acuity can be examined on the basis of the morphological design of the eye. With the exception of the incorporation of first level retinal elements (the photoreceptors), these discussions omit the contributions of neural factors, concentrating instead on optical limitations. The type of visual acuity that I will examine using this approach involves that which an animal utilizes to resolve static black/white grating patterns, or to discriminate between two bright points on a uniform dark background.

Because the eye of the juvenile lemon shark apparently suffers from a slight degree of hypermetropia, the effect of this condition on visual acuity must be assesssed concurrently with other structural considerations.

Retinal Blur

When an ametropic eye with a circular pupil looks at a distant object, the out-of-focus retinal image that results can be considered to constitute a field of blur circles corresponding to the individual points in the object (Bennett and Francis, 1962). As a gauge on the negative effect of ametropia on visual acuity, the size of these retinal blur circles can be calculated using the schematic eye,

and this blurriness can be compared with other optical limits on resolving power of the eye. According to Hill and Fry (1974), for a given out-of-focus distance between photoreceptors and the actual plane of focus, and a given position of the eye's exit pupil relative to the plane of focus, the size of the retinal blur circle corresponding to an object point is proportional to the size of the exit pupil. This geometrical relationship based on similar triangles can be expressed as follows (adapted from Hill and Fry, 1974):

$$\frac{b}{p_x} = \frac{\overline{R_2F_2}}{\overline{E_xF_2}} \qquad (6)$$

where b = diameter of retinal blur circle for a single point, p_x = diameter of the exit pupil in the schematic eye, and E_x = position of the exit pupil. $\overline{R_2F_2}$, the out-of-focus distance, equals 0.185 mm in the juvenile lemon shark, and $\overline{E_xF_2}$, the separation between the exit pupil and the back focal point, is 13.831 mm. Thus Equation 6 reduces to

$$b = 0.0134p_x \qquad (7)$$

for the juvenile lemon shark.

Under photopic conditions when acuity is most important, the exit pupil of the juvenile lemon shark eye is a vertical slit measuring approximately 7.20 x 1.44 mm, when the eye is near maximum light adaptation. Under the conditions of +2.76 D hypermetropia with no accommodative compensation, and using Equation 7, this pupil will produce a "blur ellipse" on the retina measuring approximately 96.5 x 19.3 µm. These dimensions far overshadow the diffraction-limited resolution of 6.32 µm, and therefore demonstrate that diffraction effects are not important in limiting visual acuity of this hypermetropic eye.

The size of the retinal blur ellipse can be used to predict the approximate size of the blurred retinal images corresponding to various objects in the shark's visual field. For example, suppose that a thin horizontal line parallel to the

shark's body axis occupies a visual angle of 10^{o} relative to the shark's first nodal point (such a line could be, for example, a 20 cm horizontal stripe on a fish located about 1.14 m away from the shark's eye). Since the RMF of the shark is 164 μm/^{o}visual angle, and treating the stripe's vertical height as being negligible, the shark's retinal image of the stripe would be a thin line 10 x 164 = 1640 μm long if refractive error was zero. But with the +2.76 D hypermetropia, the image of the stripe is defocused so that a blur ellipse exists on the retina for each point in the stripe. Thus, the blurred image is 19.3 μm longer than a focused image would be, and the vertical height of the stripe's image becomes 96.5 μm. The stripe is therefore projected onto the shark's retina as a bar 1659.3 μm long by 96.5 μm high, with the contrast of the stripe correspondingly reduced from what it would be in a clear, focused image.

A retinal blur ellipse measuring 96.5 x 19.3 μm corresponds to visual angles of 35.3' in the vertical meridian and 7.1' in the horizontal meridian. In comparison, the diffraction-limited resolution of 6.32 μm corresponds to a visual angle of 2.3'. These visual angles will be compared with the minimum separable angle (MSA) computed from the intercone spacing in the lemon shark retina, to assess the influence of the +2.76 D hypermetropia on vision in the juvenile lemon shark.

Resolving Power of the Retina

A fundamental limitation on visual acuity that may be predicted using the optical constants of an eye involves the minimum separable angle (MSA) corresponding to the intercone spacing in the retina. The idea that retinal resolving power may be limited by the distance between adjacent cones is attributed to von Helmholtz (1924), and the relatively recent history of applying this Helmholtzian principle to the eyes of fishes has been reviewed by Northmore

et al. (1978). The hypothesis proposes that, if acuity is limited by the grain of the retinal mosaic, the images of the bright bars in a just resolvable grating will fall upon alternate rows of cones. The intercone spacing will thus correspond to a visual angle that represents one half-period of the grating, and this angle is termed the minimum separable angle (Northmore and Dvorak, 1979).

Gruber et al. (1963) published a photograph of a representative tangential section of the juvenile lemon shark retina cut at the level of the cone ellipsoids. Since there is as yet no known heterogeneity in cone density throughout the lemon shark retina, and since no evidence of any double or twin cones has been reported for any elasmobranch species (Gruber and Cohen, 1978), the photograph in Gruber et al. (1963) can be used to estimate the average number of individual cones per unit area of juvenile lemon shark retina. I counted 28 cones within a 40 x 50 μm square measured according to the scale presented in the photograph. This equals 28 cones per 2000 μm^2, or about 14,000 cones/mm^2 in the fixed lemon shark retina. Shrinkage during preparation of the sections must be taken into account, and a figure of 25% linear shrinkage is generally used for retina preparations (Northmore and Dvorak, 1979), although shrinkage factors as high as 36% have been calculated for stained nervous tissue (Konigsmark, 1970).

A convenient formula for the calculation of minimum separable angle from intercone distance has been developed by Northmore and Dvorak (1979) in their work on the goldfish eye. With a few changes in notation, their formula for MSA in min of arc is as follows:

$$MSA = \frac{60{,}000}{(RMF)\,(1 - S)\sqrt{c}} \qquad (8)$$

where RMF = retinal magnification factor in μm/^{o}visual angle, S = shrinkage from histological preparation, and c = number of cones per mm^2 in the fixed

tissue. Substituting in the values for the juvenile lemon shark, Equation 8 becomes:

$$MSA = \frac{60{,}000}{(164)(1-.25)\sqrt{14{,}000}}$$

$$= 4.1' \text{ of visual angle, corresponding to an intercone separation of } 11.3\ \mu m.$$

(Assuming a 36% shrinkage yields an MSA of 4.8' and an intercone separation of 13.2 μm.)

In the absence of good behavioral data on visual acuity in the juvenile lemon shark, it is difficult to judge the validity of the Helmholtzian principle in these animals. However, psychophysical studies on a variety of teleosts have consistently shown that these species are capable of discriminating targets down to threshold visual angles which agree quite well with the MSA predicted from the morphological data (Northmore et al., 1978). This is true regardless of the convergence in retinal wiring from cone to ganglion cell, even though there is nowhere near a one-to-one ratio of cones to ganglion cells in these animals, including foveate species (Schwassmann, 1968). A number of explanations have been propsoed to account for the fact that resolving power is far better than receptive field sizes of ganglion cells would suggest, including the possibilities of overlapping receptive fields or subunits within single receptive fields (Northmore et al., 1978). In the human fovea, where a one-to-one connection of cones to ganglion cells does exist (Walls, 1942), visual acuity is still limited by the retinal mosaic for pupil diameters up to 2 mm (Westheimer, 1970). Concomitant with the need for psychophysical data, the Helmholtzian principle is a valuable tool for the prediction of visual acuity of an animal in which the physiological optics and photoreceptor densities are known, regardless of the animal's higher neural organization.

II. OPTICAL INFLUENCES ON VISUAL FUNCTION IN THE JUVENILE LEMON SHARK

Having now proceeded through the mathematical analyses prerequisite to an optical description of the eye of the juvenile lemon shark, the primary questions posed by my study reduce to the following: Is there a physical refractive error in the average eye of this animal, and if so, what mechanisms might be available to the shark to correct for such an error? Is this refractive error physiologically significant for juvenile lemon shark vision? What are the real limitations imposed by optics on the spatial vision, and, ultimately, the visual behavior, of these sharks?

A. Significance of the Refractive Error: Possible Corrective Mechanisms

The evidence is overwhelming that a measurable positive refractive error, i.e. hypermetropia or far-sightedness, exists in the average juvenile lemon shark eye. And yet, for this animal's eye to be hypermetropic in the resting state is an enigma, for the following reasons. Under the onus of hypermetropia, the image of an optically distant object comes into focus behind the photoreceptors, and the closer the object is brought to the hypermetropic eye, the farther behind the retina the focused image lies. Such an eye, therefore, produces blurred images of objects at optical infinity, and the blurriness <u>increases</u> for objects which are nearer to the eye (without accommodative compensation). This situation is completely counter-productive to the demands of acuity and the specification of object position in space, two attributes which would be expected to be selected for in the evolution of vision in a vertebrate predator such as the lemon shark, which inhabits a well-illuminated photic environment.

In addition, the relatively poor range of vision afforded by the lemon shark's aquatic environment restricts vision to the "near" field; such conditions should select for emmetropic eyes with a moderate range of accommodation, or

myopic eyes with a small accommodative capability. Myopia can actually be beneficial to an animal in which the majority of its visual tasks concern objects in the near field: with moderate myopia, much of the burden on the accommodative apparatus for visualizing near objects is relieved. No such analogous benefit exists for the hypermetropic eye, leading to Hughes's (1977) pronouncement that "emmetropia or myopia is teleologically more comprehensible" (p. 668).

It is logical, therefore, to question the conclusiveness of the finding of about +3 D refractive error in the juvenile lemon shark eye. Before examining the functional impact of this refractive error on visual acuity, it is necessary to consider the possible physical mechanisms for correcting this refractive error prior to the photoreceptor level. Those corrective mechanisms that are potentially available to the juvenile lemon shark can be divided into two groups: "static" corrective mechanisms, and "dynamic" corrective mechanisms. I will first consider the various static mechanisms which could serve to reduce the hypermetropia in the lemon shark eye.

Static Corrections of Refractive Error

a) Visual axis other than optical axis. Utilizing a longer axis in the eye rather than the optical (medio-lateral) axis would reduce the amount of hypermetropia, if such an axis exists. Pupil constriction under photopic conditions, however, when resolution is most important, restricts the long visual axes through the crystalline lens to the central dorso-ventral zone of the eye. Frozen vertical sections through this zone demonstrate that the central geometric axis, i.e. the optical axis, is probably the longest axis within this zone (see Fig. 7). However, Sivak's (1974b) retinoscopic refractions of two juvenile lemon sharks indicated somewhat lesser degrees of hypermetropia for the ventral

cornea-to-dorsal retina axis than for the optical axis of each animal, the difference being about 1-1.5 D. My vertical section data does not explain this difference, although there is a possibility that the power of the crystalline lens is increased enough in this oblique ventral-dorsal meridian to compensate for the shorter visual axis. A ventrally-directed visual axis might be beneficial to the juvenile lemon shark, which feeds to some extent on benthic crustaceans (Springer, 1950); visual axis has previously been shown to be correlated with the predominant direction of feeding in many species of teleosts (Tamura, 1957; Tamura and Wisby, 1963; Kimura and Tamura, 1966; Sivak and Howland, 1973).

Because sharks are generalized as possessing retinas lacking an area centralis, these animals are currently believed to function without a visual axis per se, monitoring all regions within their visual fields relatively equally. However, this characterization may be due simply to the lack of thorough histological studies of ganglion cell and photoreceptor densities in the retinas of these animals. Preliminary observations of rod:cone ratios across the retinas of juvenile lemon sharks have revealed that the photoreceptor organization may be more heterogeneous than the relatively uniform count of 12:1 reported by Gruber et al. (1963) and Wang (1968), possibly reaching densities of 5:1 in certain areas of the retina (Cohen, 1980). Clearly, histological studies as well as comprehensive investigations of possible accommodative movements are called for, in order to firmly establish the existence or nonexistence of a precise visual axis in the lemon shark. The results of such studies would certainly influence the course of all future studies of vision in these animals.

b) Chromatic aberration. Any amount of chromatic aberration in a hypermetropic eye would serve to reduce refractive error for blue light as opposed to white light, since shorter wavelengths are focused in front of longer wavelengths in optical systems with chromatic aberration (Bennett and Francis,

1962). The crystalline lens of the juvenile lemon shark cannot be assumed to be completely free of chromatic aberration, but I could not measure a compensatory shift in lens focal length for blue light (490 nm) that would significantly reduce this eye's hypermetropia. Sivak (1978b) and Nuboer et al. (1979) have advocated that the spectral nature of an aquatic animal's environment, as well as the animal's spectral sensitivity, should be established before assigning a particular refractive state to that animal's eye. This is unquestionably correct, but for the juvenile lemon shark, this chromatic adjustment will not in itself significantly reduce the measured hypermetropia of +2.76 D.

c) The retina as a refractive element. Vertebrate photoreceptors have been variously proposed to act as wave guides or light funnels (Enoch, 1963; Weale, 1974), by virtue of their high refractive index (approximately 1.4; Sidman, 1957), orientation, thickness, and other optical featurs. As refractive light funnels, the photoreceptor inner segments could aid in further focusing image points on the outer segments, thereby reducing some of the eye's hypertropia. As wave guides, however, the photoreceptors would actually enhance the ocular hypermetropia, by adversely interfering with the convergence of light rays toward the outer segments. Treated as a single high refractive index element, the overall retina would likewise increase the eye's hypermetropia, due to its concavity and thus its acting as a negative lens. In the absence of comprehensive studies of the optics of the shark retina, therefore, the precise retinal influence on the estimated ocular hypermetropia cannot be assessed for the juvenile lemon shark.

d) Mirror optics. Is it possible that the elasmobranch tapetum could act similarly to the argenteum of the scallop eye (Land, 1965), that is, as a focusing mirror? The requirements for such an image-forming optical device in the shark eye would be: (1) the reflector must be specular, which the elasmobranch

tapetum is; and (2) the mirror or mirror plates must reflect light rays back along the same optical paths from which they entered the choroid, which the elasmobranch tapetum does (Gruber and Cohen, 1978; Denton, 1970). I have determined the out-of-focus distance behind the photoreceptor outer segments in the juvenile lemon shark to be approximately 185 μm, while the average separation between the outer segments and the tapetal plates in Negaprion brevirostris is about 50 μm (derived from Kuchnow and Gilbert, 1967). A tapetal focusing mirror in this animal would therefore contribute about 2 x 50 = 100 μm of additional optical axis along which light rays could converge further; in other words, approximately 100/185 = 54% of the dioptric "overshoot" could be eliminated by a focusing tapetum. Such a mechanism would significantly reduce the measured hypermetropia in these eyes.

This notion is based purely on speculation, but several inferences emerge if such a mechanism were to exist in the shark eye. First, image-forming eyes that depend on mirror optics suffer a loss of image contrast (Land, 1978), but this result will be inevitable in a hypermetropic shark eye, regardless of whether or not the tapetum acts as a focusing mirror. Second, and this is a pivotal point, the lemon shark tapetum is occlusible (Gilbert, 1963), so that the reflecting plates are exposed only under conditions of dim illumination. But cone function, and therefore acuity, are operative only under photopic conditions, and with this realization we seem to have reached a dead end with the theoretical mechanism of a focusing tapetum. Could the tapetal reflector be an effective acuity-modulator during the photochromatic interval between rod and cone thresholds (Graham, 1965), when the pupillary aperture, and thus the retinal blur, are large? No evidence presently exists for such a mechanism.

None of these four static corrective mechanisms appear particularly viable in eliminating all of the juvenile lemon shark's hypermetropia of around +3 D. I

will next consider the possible dynamic mechanisms which may serve to reduce the hypermetropia.

Dynamic Corrections of Refractive Error

a) Active accommodation. Despite the 50-year history of speculation on the accommodative system of sharks, beginning with Franz (1931), the reality is that no firm evidence exists of a dynamic accommodative capability in sharks which corrects for the ocular hypermetropia measured in these animals in the unanesthetized state. Sivak and Gilbert (1976) have produced retinoscopic evidence of accommodatory changes in the nurse shark (Ginglymostoma cirratum), under the conditions of tricaine methanesulfonate anesthesia and electrical stimulation of the oculomotor nerve. Although the direction of these changes was consistent with a logical model of accommodation in sharks, however, emmetropia (or surpassing that, myopia) was never achieved through accommodation in two out of three of these hypermetropic animals. Sivak and Gilbert also tested sandbar sharks (Carcharhinus milberti), which, like the lemon shark, is a carcharhinid, but the results were completely inconclusive. In agreement with those results was Sivak's (1974b) finding of no change in the refractive state of juvenile lemon sharks before and after administration of tricaine methanesulfonate or pilocarpine hydrochloride.

Therefore, regardless of the theoretical mechanism of accommodation for sharks, be it the type elucidated by Walls (1942) involving lens movements, or changes in globe depth similar to those of the frog eye (du Pont and de Groot, 1976), no experimental evidence of corrective accommodative adjustments yet exists for sharks. My studies of juvenile lemon sharks have not altered this situation, although I have mentioned my ophthalmoscopic observations of apparent movements of dioptric elements in these animals' eyes on two

occasions. In any case, the question of what benefit for the shark is afforded by hypermetropia under any visual circumstances (resting/fixating, anesthetized/unanesthetized, etc.) will continue to haunt all attempts to demonstrate an accommodatory mechanism in this group of animals.

b) Developmental adjustments. A final type of "dynamic" correction to the hypermetropia measured in the juvenile lemon shark eye is the possibility of developmental adjustments in the principal points of the eye, as the animal grows to maturity. This of course will not explain how the juvenile copes with hypermetropia, but the concept that the juvenile eye represents an uncompleted state of optical development deserves consideration.

The line of evidence providing the greatest, if not the only, support for this hypothesis concerns the observations of the juvenile and adult lemon sharks' optical media in vivo. I have noted the irregular opacities and general translucence common in the juvenile eyes, and the apparent clearing of this condition in the adults as evidenced by preliminary ophthalmoscopic examinations (S. Spielman and S. Gruber, personal communication). If this developmental process is accompanied by a nonisometric growth of the ocular components (the growth of the ocular components is isometric with increase in body length throughout the range of juvenile sharks that I examined), it is conceivable that older age groups could be emmetropic, or even myopic. However, preliminary retinoscopic measurements of refractive error in adult lemon sharks have to date revealed the same degree of hypermetropia as in the juveniles (S. Spielman and S. Gruber, personal communication).

The visual effects of the apparently poor optical quality in the juvenile shark eye are difficult to assess. An analogous condition exists in the kitten eye, and the developmental progression of optical quality in that eye has been studied in depth (Bonds and Freeman, 1978; Freeman and Lai, 1978; Freeman et al.,

1978). The translucence of the optical media displayed in kittens between the period of eyelid opening (six to ten days after birth) and about four weeks of age has been attributed to a vascular tunic surrounding the crystalline lens; this tunic is normally absorbed by about the 25th day after birth (Freeman and Lai, 1978). The finding of importance in these studies, however, was that the relatively poor optical quality of the kitten eye does not significantly limit either optical performance or visual development (Bonds and Freeman, 1978). Visual acuity does improve rapidly in the kitten during the first few post-natal weeks, but this is mainly due to the development of the neural pathways, not to the clearing of the optical media.

In light of these findings, and in the absence of modulation transfer function (MTF) or line-spread data for either juvenile or adult lemon sharks, as well as firm refractive error data for the adults, the subject of developmental changes in the eyes of these animals is flooded with questions lacking answers. Regardless of the potential for developmental adjustments in refractive state for the species, however, the inevitable question remains: What are the limits imposed by hypermetropia on the vision of the free-living, predatory juveniles?

In summary, there is as yet no evidence to support the assumption that juvenile lemon sharks possess the capability to correct for their moderate hypermetropia of about +3 D. This refractive error is a physical reality for these animals, and with this conclusion emerge the final aspects of discussion: the physiological significance of the hypermetropia; the real optical limitations on resolving power; and the role of optics and vision in the behavior and ecology of the juvenile lemon shark.

B. Optical Limitations on Spatial Vision

Two of the dioptric factors that could limit visual resolution in the juvenile lemon shark (diffraction and refractive error), and the theoretical MSA based

solely on the estimated average distance between adjacent cones, are represented schematically in Fig. 15. This illustration, and the discussion of visual acuity that follows, are applicable only for maximum photopic conditions (total pupillary constriction, full cone operation). Under less than maximum light adaptation, retinal blur ellipses will be larger due to larger pupillary aperatures, so that resolving power will be more severely limited by optical factors. In addition, my analysis is restricted to resolution of the horizontal visual field that is perpendicular to the shark's optical axis; this type of visual acuity is exemplified by the resolution of vertical black/white gratings. Because the lemon shark's pupil is larger along the dorso-ventral axis than along the rostro-caudal axis, optical resolving power of horizontal gratings should be less than that of vertical gratings, based on blur circle size. My analysis, therefore, concentrates on the optimum acuity of the juvenile lemon shark in the lateral visual field.

The diffraction-limiting Airy image under photopic conditions limits visual resolution to a retinal image no smaller than 6.3 μm (2.3' visual angle) in the horizontal field. This dimension is about twice as large as the maximum diameter of the cone outer segments (approximately 3.0 μm/1.1'; derived from Gruber et al., 1963), but considerably smaller than the intercone spacing (11.3 μm/4.1') and somewhat less than the retinal distance between borders of adjacent cones (8.3 μm/3.0'). The Airy image is much smaller than the retinal blur of a point source caused by the hypermetropia (19.3 μm/7.1'). The conclusion from all of these dimensions is that diffraction is not a limiting factor in optical resolving power of the juvenile lemon shark eye.

By-passing the influence of the hypermetropia for the moment, what are the limits on visual acuity imposed by the retinal mosaic? Solely on the basis of

Fig. 15. Morphological and dioptric factors affecting horizontal visual resolution in the retina of the juvenile lemon shark. a--Schematic diagram of approximate relationships between outer segments of three typical neighboring cones sectioned tangentially. Average cone diameter and intercone distance derived from Gruber et al. (1963) and Equation 8. b--Diffraction-limiting Airy image of a single point source centered on the middle cone under photopic conditions. c--Theoretical minimum resolvable grating of shark retina under photopic and emmetropic conditions. The width of the illuminated bar, corresponding to the average intercone distance, defines one half-period of the grating, and is equal to the theoretical minimum separable angle (MSA). d--Horizontal blur on the retina of a single point source, due to a hypermetropia of +2.76 D under photopic conditions. Each illuminated point of an object in the hypermetropic shark's visual field is represented by such a blurred image on the shark's retina.

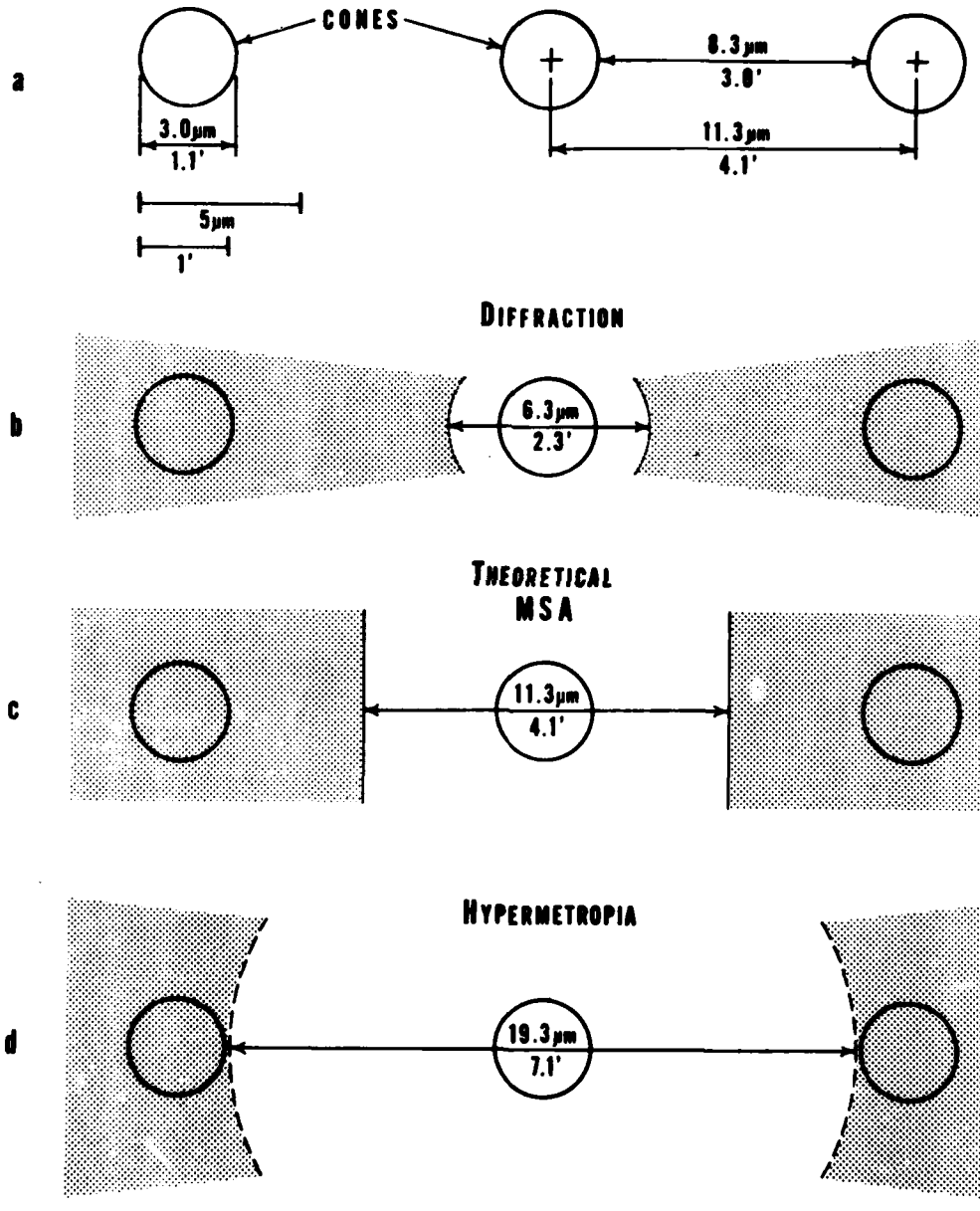
a
CONES
8.3μm
3.0'
3.0μm
1.1'
11.3μm
4.1'
5μm
1'
DIFFRACTION
b
6.3μm
2.3'
THEORETICAL
MSA
c
11.3μm
4.1'
HYPERMETROPIA
d
19.3μm
7.1'

the theoretical MSA, the juvenile lemon shark should be capable of discriminating a light/dark grating pattern down to a visual angle of 4.1' (or two illuminated dots separated by an angle of 2 x 4.1 = 8.2'). This is a valid prediction even though the receptive fields in these animals generally occupy visual angles of about 5-9° (Cohen, 1980), about two orders of magnitude greater than the MSA. An angle of 8.2' corresponds with a theoretical ability to resolve at a distance of 10 m two points that are 2.4 cm apart, or at a distance of 1 m two points that are 2.4 mm apart.

The theoretical MSA of the juvenile lemon shark is about one-third that of the goldfish, which is approximately 13' (Northmore and Dvorak, 1979); this is not due so much to a significant difference in cone density, which is about 12,000 cones per mm^2 in the fixed goldfish retina, but rather to an increase in eye size and hence a larger retinal magnification factor in the juvenile lemon shark.

Tamura (1957) and Tamura and Wisby (1963) calculated MSAs for a number of engybenthic (what Tamura calls "littoral") and epineritic (called "pelagic" by Tamura and Wisby) species of marine teleosts inhabiting continental shelf waters; the formula that they used, however, actually yields twice the MSA, or the threshold angle of discrimination between two illuminated points (Northmore and Dvorak, 1979). Their results are further compromised by an across-the-board invocation of Matthiessen's ratio, as pointed out by Sadler (1973). Nevertheless, it appears that the actual MSAs of most of the relatively small, engybenthic teleosts studied by Tamura (1957) are comparable to the 4.1' theoretical MSA of the juvenile lemon shark, which is itself an engybenthic species. Those teleosts investigated by Tamura included small tetraodontids, serranids, sparids, and scorpaenids. On the other hand, the ten large epineritic species investigated by Tamura and Wisby (1963), including dolphin (Coryphaena hippurus), three species of tunas (Euthynnus and Thunnus spp.), white marlin (Tetrapturus albidus), and

great barracuda (Sphyraena barracuda), all displayed an MSA that was less than that of the juvenile lemon shark, ranging from 0.9 to 2.1'. Though this is in part due to larger eye size, most of the ten epineritic teleosts also have specialized retinal areas with higher cone densities than that of the juvenile lemon shark (Tamura and Wisby, 1963).

A final comparison can be made with the human eye, which in this case differs in the greatest respect from the juvenile lemon shark eye in its possession of an all-cone fovea. The density of cones in the human fovea is approximately 150,000 per mm^2 (Hughes, 1977). The posterior nodal distance in the unaccommodated human eye is 17.055 mm (von Helmholtz, 1924), yielding a retinal magnification factor of 298 $\mu m/^{o}$, compared with 164 $\mu m/^{o}$ in the juvenile lemon shark. This results in a theoretical MSA of 31.2" for the human eye; actual measurements of resolution of the human eye, utilizing interference fringes to experimentally bypass the spatial degradation by the eye's optics, reveal limits of approximately 30 to 35" of visual angle (Westheimer, 1979). Therefore, since the human MSA is about 1/8 that of the juvenile lemon shark, the resolving power of the human eye is at least eight times that of the juvenile lemon shark eye under equal conditions. This disparity is due primarily to the presence of the cone-dense fovea in the human eye.

The preceding statements concerning MSA for the juvenile lemon shark disregard any confounding effects of the +2.76 D average hypermetropia on resolving power. There is no question that refractive error adversely affects resolving power and visual acuity. In the human eye, for example, a one diopter defocus reduces threshold visual angle to about 30% of that of the emmetropic eye (Westheimer, 1979). What, then, is the quantitative role of the hypermetropia in the theoretical acuity of lemon sharks? By working backward from the retinal image of the theoretical "just resolvable" grating, and by

examining the effects of the hypermetropic blur on that image, the answer to this question can be obtained.

According to the Helmholtzian theory, the minimum threshold of resolution of the juvenile lemon shark should be achieved in resolving a vertical grating with a half-period equivalent to the visual angle between two of the shark's adjacent cones, which is 4.1' or 11.3 μm on the shark retina (Fig. 15). Suppose such a grating was presented to a subject shark with average dioptrics under photopic conditions. Because of the animal's hypermetropia, this grating will not be imaged in optimum focus on the retina; each white (illuminated) bar in the grating will be blurred, so that light quanta will intercept the retina in the supposedly non-illuminated areas of the retinal image. The borders of each white bar in the image will therefore be spread laterally into the black bar regions, by a distance equal to one-half of the diameter of the retinal blur ellipse, or 19.3/2 = 9.7 μm/3.6'. The increment by which the overall width of each illuminated bar will be increased on the retina is equal to the total diameter of the retinal blur ellipse, or 19.3 μm/7.1'. This is represented diagrammatically in Fig. 16a. Due to the blurring, all illuminated bars in the image will be spread out to overlap the neighboring cones, which would have been in the dark in a focused image. The amount of overlap is 2.5 μm/0.9' beyond each adjacent cone. All retinal areas are thus illuminated to some extent, and no cones are left unstimulated, so the shark will not be able to resolve the 4.1' half-period grating.

Suppose next that a grating with a half-period equal to the distance between three consecutive cones is chosen and tested. The focused images of the illuminated bars in this grating should each subtend 22.6 μm on the retina, or 8.3' of visual angle. With the blurring caused by the hypermetropia, however, the illuminated bars will spread out as in Fig. 16b. Once again, all cones are stimulated, and the 8.3' half-period grating is not resolvable by the shark's eye.

Fig. 16. Effect of +2.76 hypermetropia on otherwise perfect images of vertical square-wave gratings at the level of the photoreceptors in the juvenile lemon shark retina. a--Defocus of grating image with 4.1' half-period, corresponding to theoretical MSA, illuminates all adjacent cones. b--Similar result obtained with 8.3' half-period grating. c--Grating with a half-period of 12.4' (corresponding to the distance between four consecutive cones) leaves one cone in every six not illuminated; grating is now resolvable. See text for details.

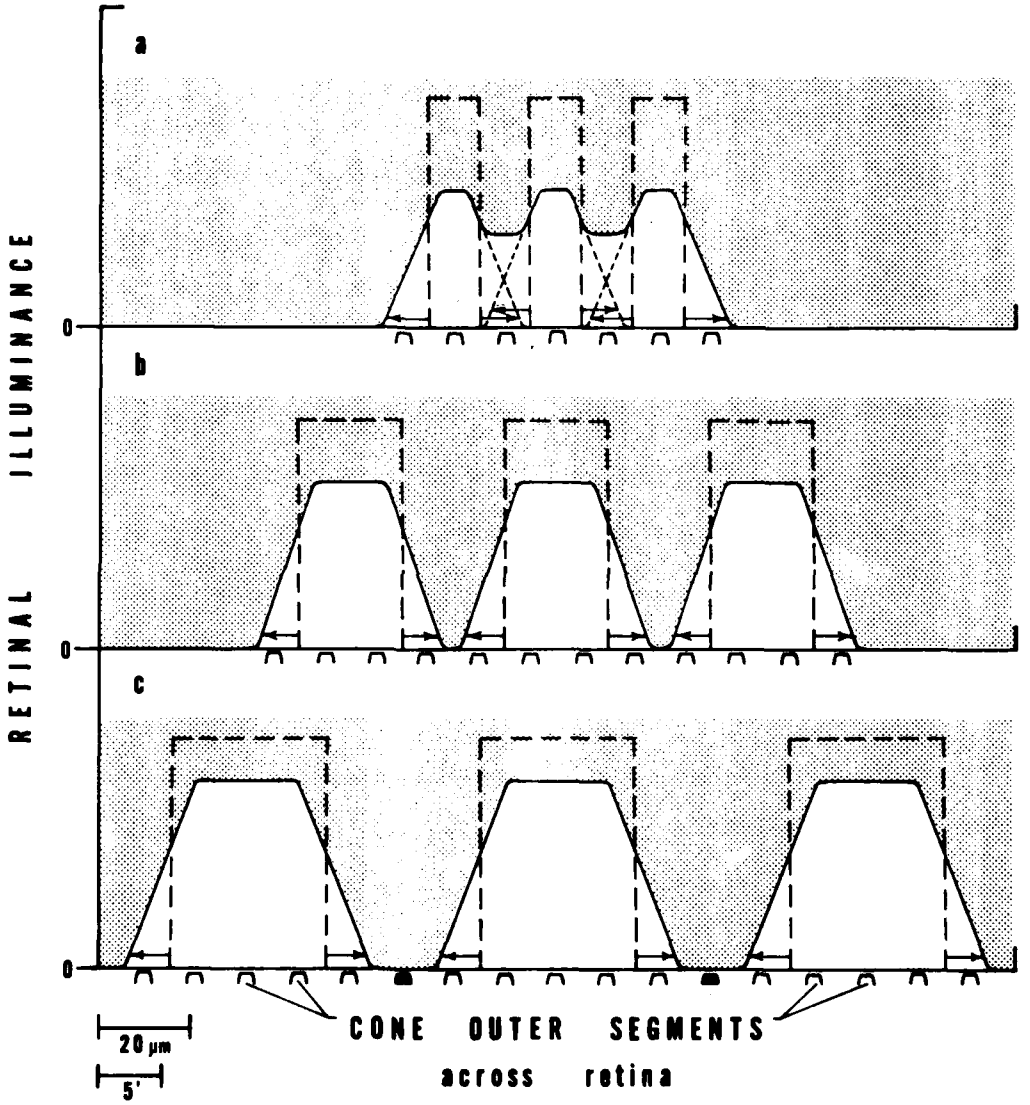
a
b
c
RETINAL ILLUMINANCE
0
0
0
20 μm
5'
CONE OUTER SEGMENTS
across retina

Carrying this demonstration one step further, suppose that a grating with a half-period equal to the distance between four consequtive cones is now tested. The image of this grating on the retina, with the effect of the hypermetropia, would be as in Fig. 16c. In this case, at least one cone in every six is not stimulated, and theoretically, the shark should now be able to detect the nature of the grating pattern.

Therefore, the half-period of the just resolvable grating for this animal should be 12.4', which is three times the optimum visual angle predicted from the MSA calculations. This decrease in resolving power is entirely due to the shark's hypermetropia; an animal that has been corrected for the refractive error should be able to resolve down to a 4.1' half-period grating. A grating angle of 12.4' corresponds with a theoretical ability to resolve at a distance of 10 m two points that are 7.2 cm apart, or at a distance of 1 m two points that are 7.2 mm apart.

These calculations quantify the limitations imposed on the juvenile lemon shark's spatial vision by the cone density and the refractive error. The predicted minimum resolvable angles from my morphological and dioptric data could now be tested using suitable psychophysical procedures. The accuracy of my resolution predictions is sensitive to deviations in photoreceptor density and intercone separation, which I estimated from only one sample photograph, so that the predictions could be further refined from this basis. Furthermore, my simplistic analysis is conducted in the absence of data on the Rayleigh criterion and Weber-Fechner fraction (Campbell et al., 1974) for the lemon shark. There is no doubt that such physiological considerations will ultimately be required to better understand the results of psychophysical testing of shark vision.

With these qualifications, the primary conclusion that emerges from my calculations is that the juvenile lemon shark, which under emmetropic conditions should have a conventional resolving power similar to those of engybenthic,

nearshore fishes, suffers a significant loss of visual acuity due to its hypermetropia averaging +2.76 D. This shark's resolving power, with the refractive error unchecked, is on the order of 1/24 that of the emmetropic human eye under equal conditions.

C. Spatial Vision and the Aquatic Environment of the Juvenile Lemon Shark

Over fifteen years ago, at a time when basic studies of shark biology were beginning a decade of unprecedented expansion, Gilbert (1963) summarized the visual apparatus of sharks as being "poorly adapted for distinguishing the details and color of an object" but "well equipped . . . for differentiating an object, particularly a moving one, from its background" (p. 321). Since that time, the characterization of sharks as possessing all-rod retinas has been soundly refuted (Gruber, 1975), so that Gilbert's conclusions on the capability of sharks for color vision were based entirely on the misinformation of that period. But what of the capability of sharks to spatially differentiate the objects of its visual environment?

The juvenile lemon sharks of my study function in a habitat which is, from an optical standpoint, relatively poor. The turbidity of Florida Bay water is generally high; throughout the bay, steady winds of about 25 km/h or more are sufficient to turn the water so turbid that the bottom is not visible from the surface in depths of 1.8 m (Ginsburg, 1956). The 2 m-deep floors of the broad, shallow basins known locally as "lakes," which constitute the predominant subenvironment of Florida Bay, are visible from the surface only after calm periods lasting a day or more. Turbidity varies locally according to bottom type, but under average conditions the water of Florida Bay is characteristically a "translucent milky-green color" (Enos and Perkins, 1979; p. 61).

This turbid condition is most prevalent between November and April, when winds are stronger (Ginsburg, 1956), and the juvenile lemon sharks in fact appear

to be less abundant in the shallows of Florida Bay during that time of the year than in the spring and summer months (Springer, 1950). On the other hand, it is relevant that Ginsburg (1956) made special mention of unusually turbid water produced by the activities of the abundant schools of mullet in Florida Bay. According to Ginsburg, "these streaks of white water, or fish muds as they are called locally, are a common feature of the Bay" (p. 2398). Interestingly, Springer (1950) states that the young lemon sharks of Florida Bay are frequently found following these schools of mullet on which they apparently feed at times.

In light of these environmental factors, the selective pressures required for the development of high resolving power in the lemon shark, at least in the juvenile stage, may not be operational in the Florida Bay population. Under the conditions of high scattering and loss of contrast, which increase with rising turbidity, many visual functions associated with spatial acuity are impaired (Duntley and Kinney, 1970). It may be quite difficult, if not impossible, for an aquatic animal to calibrate its ocular developement for emmetropia, when that animal must function under generally turbid conditions, fixating on targets of frequently poor optical quality.

If it were not for the juvenile lemon shark's hypermetropia, the potential acuity of this shark would be comparable to that of fishes with similar ecological niches--feeding on or close to the bottom, in nearshore habitats that are subject to episodic turbid conditions. Very little reliable information exists on the dioptrics and refractive states of these fishes, so that detailed comparisons can not yet be made. The scant data providing some insight on the potential acuity of active, epineritic teleosts (tunas, billfishes, etc.) suggest that the spatial resolving power of the eyes of these species is relatively well developed. These active predators generally function in a clear visual environment that is wide in range, completely uniform, and devoid of detail; in such an environment, the

detection of the slightest disruption in the uniformity of the spatial visual field would be highly desirable. For the engybenthic animal, on the other hand, the baseline visual environment already contains detail, much of which is irrelevant visual stimulus; investigating every detail would be inefficient. In the juvenile lemon shark, therefore, it may not be the spatial organization of detail that is keyed on, but rather the relevant changes in that organization over time--the detection of motion, calling for dynamic visual acuity. Gilbert's summary statements of 1963 echo this very scheme.

The influence of hypermetropia on visual function in the lemon shark remains a problem. I have already mentioned the conspicuous lack of benefit that hypermetropia affords an animal's optical system, compared with emmetropia or even myopia. But considering the poor optical quality of the juvenile lemon shark's environment, perhaps it is too much to expect the refractive states of these animals to cluster tightly around emmetropia.

The juvenile lemon sharks of Florida Bay are free-living, actively hunting predators, with few, if any, natural predators of their own. Their visual world is limited in range to a few meters, by virtue of the shallowness of their habitat and the turbid nature of their optical environment; it may be limited in resolution to a visual angle of about 12 minutes of arc, based on the morphology of their eyes. These eyes appear to contain flaws, both in the clarity of the optical media and in the positioning of the focused image. Though these findings may be unsettling to a teleological view of visual function, they are not dramatic when weighed against the constraints of the photic environment of these sharks. Since these animals are known to move out of Florida Bay into clearer waters as they mature (Springer, 1950), much of my data will doubtless be shuffled into a different perspective with the investigation of the physiological optics of the adults. Information concerning the eyes of another population of lemon sharks

that are born and mature in clearer, more tropical waters, such as over the Bahama Bank, would also be enlightening.

SUMMARY OF CONCLUSIONS

1) The physiological optics of the eyes of juvenile lemon sharks inhabiting Florida Bay were investigated. Data were collected from a total of 23 sharks averaging less than one year of age.

2) The cornea of the juvenile lemon shark eye is optically absent, since its refractive index is equivalent with that of seawater, the aqueous, and the vitreous (1.340).

3) The crystalline lens is the sole refractive element in this eye, and its overall equivalent refractive index (n_{EL}) is 1.664. The principal power of the lens, and thus the total power of the eye, is +139.82 D. The lens is ellipsoidal (lenticular) in shape, not spherical.

4) The schematic eye for the juvenile lemon shark is characterized by a hypermetropia of +2.76 D and an out-of-focus distance ($\overline{R_2F_2}$) of 185 μm between the photoreceptors and the back focal point.

5) The medial nodal distance ($\overline{N_2R_2}$) is 9.398 mm in the schematic eye; retinal magnification factor (RMF) is 164 μm/°visual angle, and 1 mm on the retina corresponds to a visual angle of 6.09°.

6) Growth of the ocular components in the juvenile lemon shark eye is isometric with increase in body length throughout the range of sharks examined (60 to 90 cm total length).

7) The optic disc in this eye is located approximately 30° ventral and 10° rostral to the optical axis.

8) Chromatic aberration or diffraction do not limit resolving power of the dioptrics in the juvenile lemon shark eye.

9) Minimum separable angle (MSA) predicted from the RMF and average intercone distance is approximately 4.1', which is comparable to MSAs reported for engybenthic, nearshore teleosts. MSA, however, is severely affected by the

juvenile lemon shark's hypermetropia, which may decrease visual acuity to a MSA of as much as 12.4' of visual angle.

10) Retinoscopically measured refractive error in juvenile lemon sharks averages +7.5 D; the major source of discrepancy in refractive error of the schematic eye vs. retinoscopy is attributed to the retinoscopic reflex arising principally from the vitreal-retinal boundary.

11) No capability for accommodation in the juvenile lemon shark has been observed.

12) The eyes of living juvenile lemon sharks are typically characterized by opacities and a general translucence in the optical media.

13) The slight hypermetropia and ocular opacity of the juvenile lemon sharks of Florida Bay are related to the poor photic quality of their environment. It is probable that further decrease of the hypermetropia in these sharks would have no appreciable effect on increasing their visual acuity within this habitat.

14) Future studies of the physiological optics and spatial vision of these animals are recommended to concentrate on the following areas: electrophysiological assessments of refractive state, accommodative capability, and visual acuity; determination of visual axis from organization of the retina and optic tectum; spectrophotometric studies of the ocular media; psychophysical testing of spatial vision in the Florida Bay sharks; comparative studies on adult lemon sharks and juveniles from clear water habitats; utilization of retinoscopy only as a secondary qualitative check on refractive state of vertebrate eyes; and development of more precise optical techniques for rapidly determining refractive state in the intact aquatic eye.

APPENDIX

RETINOSCOPY OF AQUATIC EYES

Introduction

The technique of retinoscopy has long been used to determine the refractive state of vertebrate eyes, since it offers a relatively easy means of objectively measuring refractive error in the living animal. Recently, this technique has been scrutinized for inconsistencies between retinoscopic measurements and other experimental determinations of refractive state. For example, the question of which ocular surface gives rise to the principal retinoscopic reflex was foreshadowed in Beer's (1894) discussion of ophthalmoscopy, but the issue did not draw significant attention until Glickstein and Millodot's views appeared in 1970; Hughes (1977) has reviewed this question in detail. The role of chromatic aberration in retinoscopy has also been examined (Millodot and Sivak, 1978; Nuboer and van Genderen-Takken, 1978; Hughes, 1979b).

Retinoscopy has been heavily relied upon in studies of refractive error in aquatic and semi-aquatic animals. The list of such animals includes elasmobranchs (Sivak, 1974b, 1976b; Sivak and Gilbert, 1976); teleosts (Baylor and Shaw, 1962; Baylor, 1967; Charman and Tucker, 1973; Sivak, 1973, 1974a, 1975, 1976a); sea birds (Sivak, 1976c; Sivak and Millodot, 1977; Sivak et al., 1977); and marine mammals (Piggins, 1970; Dawson et al., 1972; Sivak and Piggins, 1975). The standard procedure for measuring underwater refractive error in these studies is of two types: (1) immersing the whole animal or animal's head in a water chamber, and refracting an eye either through the air-water interface or through a glass wall of the chamber; or (2) fitting the animal's eye with a water-filled cup that simulates underwater conditions, with

retinoscopy performed through a plano surface of the cup that is perpendicular to the eye's optical axis. Trial lenses for neutralization of the retinoscopic reflex are positioned in the air space between the retinoscopist and the water, as close to the animal's immersed eye as possible.

In the majority of these studies, it is assumed that the optics of the retinoscopic technique as practiced on aerial eyes are unchanged when the technique is used for aquatic eyes. Only two of these reports (Piggins, 1970; Charman and Tucker, 1973) note that a correction was made for changes in vergence of the retinoscopic reflection as it traverses the air-water interface; however, these workers did not explain the basis of their corrections. The other reports make no mention of such an adjustment, correcting only for the working distance between retinoscopist and subject eye.

My retinoscopic measurements of the underwater ametropia in juvenile lemon sharks have been significantly greater than that computed for the schematic eye (see Results and Discussion). To explain this inconsistency, I conducted some tests utilizing a model eye, to measure the effect of the air-water interface on retinoscopy of aquatic eyes.

Methods

A simulated aquatic "eye" was constructed using an optical crown glass lens (Melles Griot), a cylindrical plastic tube, and a circular piece of metal foil that served as a diffuse reflector. The arrangement of these elements is shown in Fig. A1. The biconvex lens (n = 1.523; radii of curvature = $\pm$30.7 mm; thickness = 12.9 mm) was sealed onto the plastic tube with a strip of paraffin film, which additionally acted as an iris in limiting the retinoscopic beam to the central axial optics of the lens. The foil screen, simulating a retina, was mounted on a flat plate, and its distance from the lens vertex could be varied within the tube. The

Fig. A1. Aquatic model eye used for retinoscopic tests. The eye is shown adjusted for emmetropia, such that the back focal point of the lens coincides with the reflector screen. P_2, second principal plane of the lens; V, lens vertex.

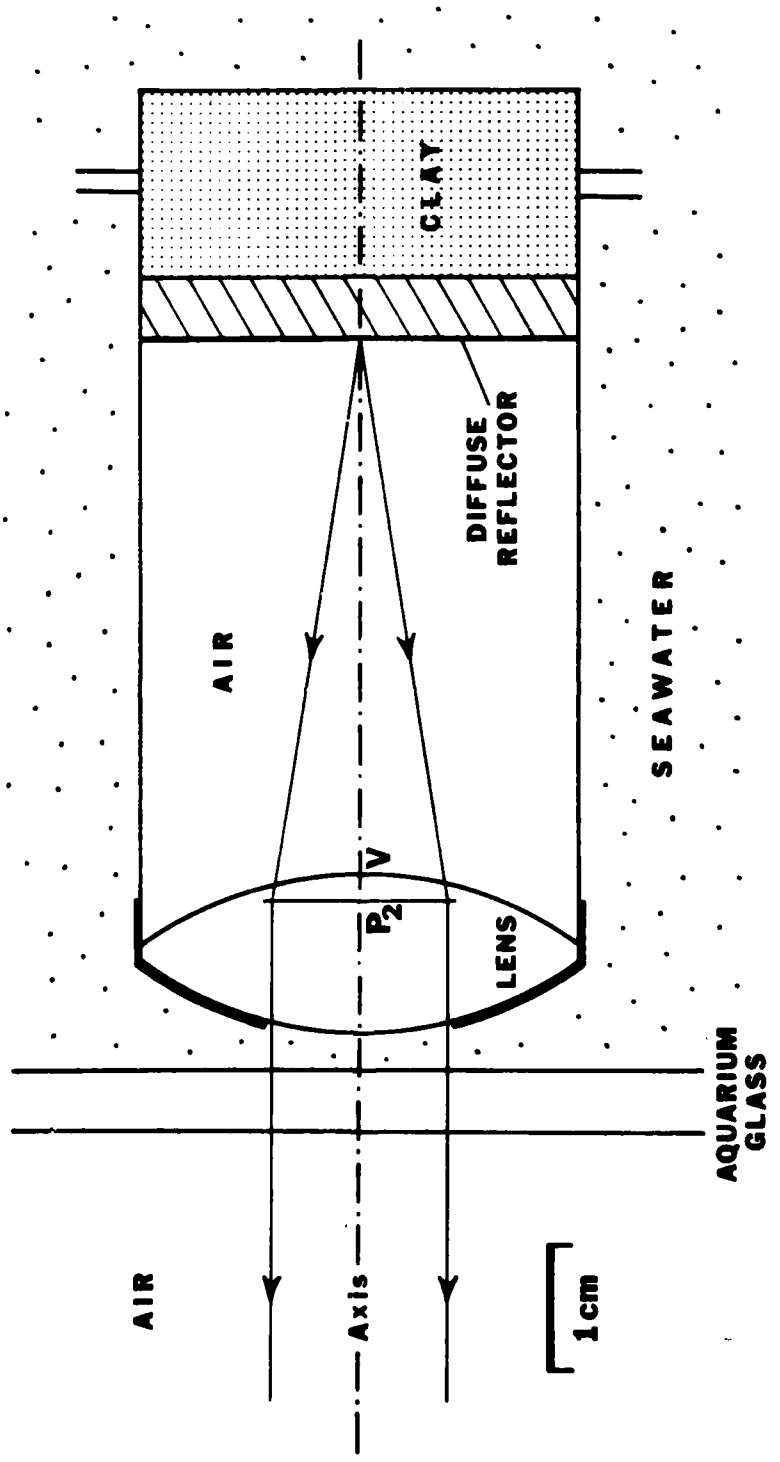
CLAY
DIFFUSE REFLECTOR
AIR
SEAWATER
V
P2
LENS
AQUARIUM GLASS
AIR
Axis
1cm

"intraocular" medium was air, chosen to keep the back focal length of the lens relatively short.

The model eye was immersed in an aquarium containing seawater with a salinity of 35°/oo (n = 1.340; Jerlov, 1976), and was positioned with its optical axis perpendicular to the glass. A few mm separated the aquarium glass from the lens of the model eye. The optical characteristics of this system were computed using thick-lens and physiological optics theory (Bennett and Francis, 1962). The principal power of this eye was +22.14 D, yielding a principal focal length of 45.2 mm and a vertex focal length of 42.9 mm. Knowing the separation between the second principal plane and the lens vertex, I could adjust the lens-to-screen distance to simulate a number of different refractive errors.

Five refractive states were chosen and tested, one simulating emmetropia, and two pairs of hypermetropic and myopic cases. Because there was a 20 mm separation between the trial lens and the model eye's second principal plane, spectacle ametropias corresponding to the five ocular ametropias were calculated according to the methods of Bennett and Francis (1962). This factor becomes increasingly important with higher degrees of ametropia.

A streak retinoscope (Keeler), adjusted to give a divergent plano mirror effect, was used in the tests. Retinoscopy was performed on the immersed eye from a working distance of 50 cm; trial lenses were interposed about 2 mm in front of the aquarium glass, in air. Refractive errors were measured to the nearest 0.5 D.

Results and Discussion

Retinoscopic readings of refractive error in the aquatic ametropic eyes were consistently greater than the calculated ametropias, while retinoscopic readings of the emmetropic eye were correct (Table A1). The test readings

Table A1. Retinoscopic readings of an aquatic model eye set at five degrees of ametropia.

Condition	Model Eye Lens Vertex-to-Screen Distance (mm)	Calculated Ocular Ametropia (D)	Calculated Spectacle Ametropia (D)	Test Retinoscopic Readings (D)
Emmetropia	42.9	0	0	0.0
Hypermetropia	37.5	+3	+2.83	+4.0
	33.2	+6	+5.36	+7.0
Myopia	49.9	-3	-3.19	-4.5
	59.7	-6	-6.82	-9.0

reported in Table A1 are corrected for the 50 cm working distance, i.e., 2 D have been subtracted from the power of the trial lens required for neutralization.

Therefore, retinoscopy performed on an aquatic eye overestimates the eye's true ametropia, be it ocular or spectacle. The source of this error arises from the trial lens being located in air while the eye is in water, with an air-water interface existing between the two. This situation is depicted diagrammatically in Fig. A2. In retinoscopy, the optics of the incoming beam from the retinoscope to the subject's retina can be ignored, and the retina can be treated as a light source (Bennett and Francis, 1962). In an emmetropic eye, the retina lies at the back focal point of the eye's optical system, so that light originating from the retina will pass through the dioptric elements and emerge from the eye as a parallel beam. The only trial lens required in this case is a positive lens of sufficient power to refocus the parallel beam for the retinoscopist's eye. In emmetropia, therefore, the effect of the air-seawater interface is nil, because the emerging beam is collimated and passes perpendicularly through the interface. Thus the retinoscopic reading is accurate in this case.

In a hypermetropic aquatic eye, the emerging beam is divergent, because the dioptrics are not strong enough to match the lens-to-retina distance. When this divergent beam encounters the air-water interface, physical refraction occurs, rendering the beam more divergent. Thus the trial lens required for neutralization does not measure the vergence of the beam emerging from the eye, but instead measures the beam's vergence after refraction at the air-water interface. Retinoscopy in this case overestimates the amount of hypermetropia.

In myopia, the beam emerging from the aquatic eye is convergent, and refraction at the air-water interface will cause the beam to converge further. Retinoscopy performed on this eye will therefore overestimate the amount of

Fig. A2. Schematic diagram of the effect of the air-water interface in retinoscopy of an aquatic eye. The interface does not affect refraction of an emmetropic eye, but it leads to overestimation of the degree of ametropia in a hypermetropic or myopic eye. (Retinoscope and incoming beam into the subject aquatic eye not shown.) See text for details.

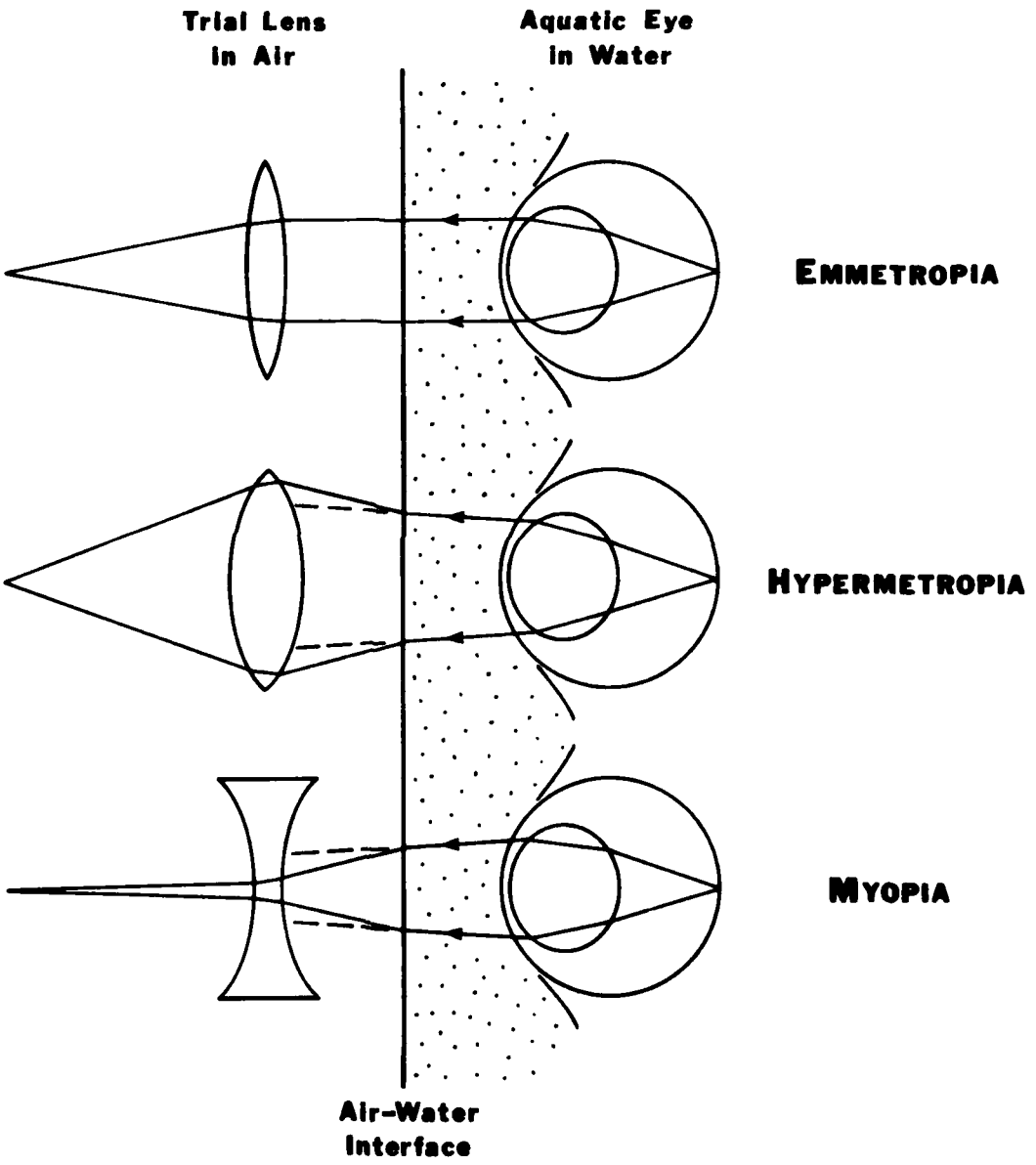
Trial Lens
in Air
Aquatic Eye
in Water
EMMETROPIA
HYPERMETROPIA
MYOPIA
Air-Water
Interface

myopia as well. In either case, the error factor is the ratio of the refractive indices of water to air (about 1.34:1 for seawater and 1.33:1 for freshwater), since the vergence change of light upon passing from one medium to another is proportional to the ratio of the two refractive indices (Bennett and Francis, 1962).

Retinoscopic readings should therefore be divided by 1.34 for marine animals and 1.33 for freshwater animals, after the adjustment for working distance has been made. (This is contingent upon the retinoscopy being performed perpendicular to the air-water interface; for an oblique axis, the change in vergence will be different.) The correction brings my test readings of the model eyes into close agreement with the calculated spectacle ametropias, when the test readings are divided by 1.34 (see Table A1). If the amount of ametropia is not excessive, the effect of the aquarium glass on the vergence of the reflex beam is negligible: the thickness of the glass, and the small shifts in vergence of the beam due to the glass, are insignificant relative to the position of the far point in a moderately ametropic eye. The important effects are therefore limited to the water-to-air transition.

Piggins (1970) incorporated the air-water correction of 1.33:1 in his retinoscopic readings of immersed seal eyes, and presumably Charman and Tucker (1973) similarly adjusted their readings of goldfish eyes "for refraction at the air-glass and glass-water interfaces" (p. 4). Sivak (1973, 1976b) refracted an aquatic model eye to assess the discrepancies between spectacle and ocular ametropia, but he did not examine the effects of the air-water interface.

Clearly, future retinoscopic measurements of refractive state in aquatic eyes should be corrected for this physical error. The adjustment will help to reduce the high ametropias previously reported for some of these eyes (e.g. Baylor and Shaw, 1962). It may also help to explain some of the discrepancy

found between retinoscopic measurements and other methods of evaluating refractive state, such as electrophysiological techniques (Schwassmann, 1975), which have been used for aquatic eyes.

REFERENCES

Babkin B.P., Bowie D.J., and Nicholls J.V.V. (1933) Structure and reactions to stimuli of arteries (and conus) in the elasmobranch genus Raja. Contr. Can. Biol. Fish., New Series VIII: 207-225.

Baldridge H.D. (1974) Shark attack: a program of data reduction and analysis. Contrib. Mote Marine Lab. 1(2): 1-98.

Baron J. and Verrier M.L. (1951) Réfraction et cerveau des poissons a fovea: contribution à l'étude des corrélations organiques. Bull. Biol. Fr. Belg. 85: 105-111.

Bauer N., Fajans K., and Lewin S.Z. (1960) Refractometry. In Technique of Organic Chemistry (3rd ed.), Vol. I: Physical Methods of Organic Chemistry, Part II (ed. by Weissberger A.), pp. 1139-1281. Interscience, New York.

Baylor E.R. (1967) Vision of Bermuda reef fishes. Nature 214: 306-307.

Baylor E.R. and Shaw E. (1962) Refractive error and vision in fishes. Science 136: 157-158.

Beer T. (1894) Die Accommodation des Fischauges. Pflügers Arch. ges. Physiol. 58: 523-650.

Bennett A.G. and Francis J.L. (1962) Visual optics. In The Eye, Vol. 4: Visual Optics and the Optical Space Sense (ed. by Davson H.), pp. 3-208. Academic Press, New York.

Bigelow H.B. and Schroeder W.C. (1948) Sharks. In Fishes of the Western North Atlantic, I/1 (ed. by Tee-Van J., Breder C.M., Hildebrand S.F., Parr A.E., and Schroeder W.C.), pp. 59-546. Sears Found. Mar. Res., Yale Univ., New Haven.

Block M.T. (1969) A note on the refraction and image formation of the rat's eye. Vision Res. 9: 705-711.

Bonds A.B. and Freeman R.D. (1978) Development of optical quality in the kitten eye. Vision Res. 18: 391-398.

Campbell C.J., Koester C.J., Rittler M.C., and Tackaberry R.B. (1974) Physiological Optics. Harper & Row, Hagerstown, Maryland.

Charman W.N. and Tucker J. (1973) The optical system of the goldfish eye. Vision Res. 13: 1-8.

Cohen J.L. (1980) Functional organization of the retina of the lemon shark (Negaprion brevirostris, Poey): an anatomical and electrophysiological approach. Ph.D. diss., Univ. Miami, Coral Gables, Florida.

Cohen J.L., Gruber S.H., and Hamasaki D.I. (1977) Spectral sensitivity and Purkinje shift in the retina of the lemon shark, Negaprion brevirostris (Poey). Vision Res. 17: 787-792.

Compagno L.J.V. (1977) Phyletic relationships of living sharks and rays. Amer. Zool. 17: 303-322.

Compagno L.J.V. and Vergara R. (1978) Sharks: Carcharhinidae: Negaprion brevirostris (Poey, 1868). In FAO Species Identification Sheets for Fishery Purposes. Western Central Atlantic (Fishing Area 31), Vol. V (ed. by Fischer W.), p. CARCH Neg 1. FAO, Rome.

Dawson W.W., Birndorf L.A., and Perez J.M. (1972) Gross anatomy and optics of the dolphin eye (Tursiops truncatus). Cetology 10: 1-11.

Denton E.J. (1970) On the organization of reflecting surfaces in some marine animals. Phil. Trans. Roy. Soc. Lond. B 258: 285-313.

Duke-Elder W.S. (1958) System of Ophthalmology, Vol. 1: The Eye in Evolution. Henry Kimpton, London.

DuPont J. and de Groot P.J. (1976) A schematic dioptric apparatus for the frog's eye (Rana esculenta). Vision Res. 16: 803-810.

Easter S.S. Jr., Johns P.R., and Baumann L.R. (1977) Growth of the adult goldfish eye—I: Optics. Vision Res. 17: 469-477.

Enoch J.M. (1963) Optical properties of the retinal receptors. J. Opt. Soc. Am. 53: 71-85.

Enos P. and Perkins R.D. (1979) Evolution of Florida Bay from island stratigraphy. Geol. Soc. Amer. Bull. 90: 59-83.

Franz V. (1905) Zur Anatomie, Histologie und funktionellen Gesaltung des Selachierauges. Jena. Z. Naturw. 40: 697-840.

Franz V. (1931) Die Akkommodation des Selachierauges und seine Abblendungsapparate, nebst Befunden an der Retina. Zool. Jb. Physiol. 49: 323-462.

Franz V. (1934) Vergleichende Anatomie des Wirbeltierauges. In Handbuch der vergleichenden Anatomie der Wirbeltiere, Vol. 2 (ed. by Bolk L., Göppert E., Kallius E., and Lubosch W.), pp. 989-1292. Urban & Schwarzenberg, Berlin.

Freeman R.D. and Lai C.E. (1978) Development of the optical surfaces of the kitten eye. Vision Res. 18: 399-407.

Freeman R.D., Wong S., and Zezula S. (1978) Optical development of the kitten cornea. Vision Res. 18: 409-414.

Gauss J.K.F. (1841) Dioptrische Untersuchungen. Göttingen.

Gilbert P.W. (1963) The visual apparatus of sharks. In Sharks and Survival (ed. by Gilbert P.W.), pp. 283-326. D.C. Heath, Boston.

Gilbert P.W. and Wood F.G. Jr. (1957) Method of anesthetizing large sharks and rays safely and rapidly. Science 126: 212-213.

Ginsburg R.N. (1956) Environmental relationships of grain size and constituent particles in some South Florida carbonate sediments. Bull. Amer. Assoc. Petrol. Geol. 40: 2384-2427.

Glickstein M. and Millodot M. (1970) Retinoscopy and eye size. Science 168: 605-606.

Graham C.H. (1965) Vision and Visual Perception. Wiley, New York.

Gruber S.H. (1967) A behavioral measurement of dark adaptation in the lemon shark, Negaprion brevirostris. In Sharks, Skates, and Rays (ed. by Gilbert P.W., Mathewson R.F., and Rall D.P.), pp. 479-490. Johns Hopkins Press, Baltimore.

Gruber S.H. (1969) The physiology of vision in the lemon shark, Negaprion brevirostris (Poey): a behavioral analysis. Ph.D. diss., Univ. Miami, Coral Gables, Florida.

Gruber S.H. (1975) Duplex vision in the elasmobranchs: histological, electrophysiological and psychophysical evidence. In Vision in Fishes: New Approaches to Research (ed. by Ali M.A.), pp. 525-540. Plenum Press, New York.

Gruber S.H. (1977) The visual system of sharks: adaptations and capability. Amer. Zool. 17: 453-469.

Gruber S.H. (1979) The role of the lemon shark, Negaprion brevirostris (Poey), as a predator in the tropical marine ecosystem. Res. proposal to NSF, Univ. Miami, Miami, Florida.

Gruber S.H. (1980) Keeping sharks for research. In Keeping Fish for Research (ed. by Hawkins A.D.). Academic Press, London (in press).

Gruber S.H. and Cohen J.L. (1978) Visual system of the elasmobranchs: state of the art 1960-1975. In Sensory Biology of Sharks, Skates, and Rays (ed. by Hodgson E.S. and Mathewson R.F.), pp. 11-105. ONR, Dept. Navy, Arlington, Virginia.

Gruber S.H., Hamasaki D.I., and Bridges C.D.B. (1963) Cones in the retina of the lemon shark (Negaprion brevirostris). Vision Res. 3: 397-399.

Gruber S.H. and Scheiderman N. (1975) Classical conditioning of the nictitating membrane response of the lemon shark (Negaprion brevirostris). Behav. Res. Meth. Inst. 7: 430-434.

Hill R.M. and Fry G.A. (1974) Retinal blur circle calculations based on the Hughes schematic eye for the rabbit. Vision Res. 14: 1037-1038.

Hirschberg J. (1882) Zur Dioptrik und Ophthalmoskopie der Fisch- und Amphibienaugen. Arch. Anat. Physiol. Lpz. 6: 493-526.

Holden M.J. (1974) Problems in the rational exploitation of elasmobranch populations and some suggested solutions. In Sea Fisheries Research (ed. by Harden Jones F.R.), pp. 117-137. Logos Press, London.

Hughes A. (1972) A schematic eye for the rabbit. Vision Res. 12: 123-138.

Hughes A. (1975) A quantitative analysis of cat retinal ganglion cell topography. J. Comp. Neurol. 163: 107-128.

Hughes A. (1977) The topography of vision in mammals of contrasting life style: comparative optics and retinal organisation. In Handbook of Sensory Physiology, Vol. VII/5: The Visual System in Vertebrates (ed. by Crescitelli F.), pp. 613-756. Springer-Verlag, Berlin.

Hughes A. (1979a) A schematic eye for the rat. Vision Res. 19: 569-588.

Hughes A. (1979b) The artefact of retinoscopy in the rat and rabbit eye has its origin at the retina/vitreous interface rather than in longitudinal chromatic aberration. Vision Res. 19: 1293-1294.

Jerlov N.G. (1976) Marine Optics. Elsevier, Amsterdam.

Kennedy D. and Milkman R.D. (1956) Selective light absorption by the lenses of lower vertebrates, and its influence on spectral sensitivity. Biol. Bull. 111: 375-386.

Kimura K. and Tamura T. (1966) On the direction of the lens movement in the visual accommodation of teleostean eyes. Bull. Jap. Soc. Sci. Fish. 32: 112-116.

Konigsmark B.W. (1970) Methods for the counting of neurons. In Contemporary Research Methods in Neuroanatomy (ed. by Nauta W.J.H. and Ebbesson S.O.E.), pp. 315-340. Springer-Verlag, New York.

Kuchnow K.P. (1970) Threshold and action spectrum of the elasmobranch pupillary resonse. Vision Res. 10: 955-964.

Kuchnow K.P. and Gilbert P.W. (1967) Preliminary in vivo studies on pupillary and tapetal pigment responses in the lemon shark, Negaprion brevirostris. In Sharks, Skates, and Rays (ed. by Gilbert P.W., Mathewson R.F., and Rall D.P.), pp. 465-477. Johns Hopkins Press, Baltimore.

Land M.F. (1965) Image formation by a concave reflector in the eye of the scallop, Pecten maximus. J. exp. Biol. 45: 433-447.

Land M.F. (1978) Animal eyes with mirror optics. Sci. Am. 239: 126-134.

Listing J.B. (1845) Beitrag zur physiologischen Optik. Göttingen.

Locket N.A. (1977) Adaptations to the deep-sea environment. In Handbook of Sensory Physiology, Vol. VII/5: The Visual System in Vertebrates (ed. by Crescitelli F.), pp. 67-192. Springer-Verlag, Berlin.

Luria S.M. and Kinney J.A.S. (1970) Underwater vision. Science 167: 1454-1461.

Marshall J., Mellerio J., and Palmer D.A. (1973) A schematic eye for the pigeon. Vision Res. 13: 2449-2453.

Massof R.W. and Chang F.W. (1972) A revision of the rat schematic eye. Vision Res. 12: 793-796.

Matthiessen L. (1879) Die Differentialgleichungen der Dioptrik der geschichteten Krystallinse. Pflügers Arch. ges. Physiol. 19: 480-562.

Matthiessen L. (1880) Untersuchungen über den Aplanatismus und die Periscopie der Kristallinsen in den Augen der Fische. Pflügers Arch. ges. Physiol. 21: 287-307.

Matthiessen L. (1882) Über die Beziehungen, welche zwischen dem Brechungsindex des Kerncentrums der Krystallinse und den Dimensionen des Auges bestehen. Pflügers Arch. ges. Physiol. 27: 510-523.

Matthiessen L. (1886a) Beiträge zur Dioptrik der Krystallinse I. Z. vergl. Augenheilk. 4: 1-39.

Matthiessen L. (1886b) Über den physikalisch-optischen Bau des Auges der Vögel. Pflügers Arch. ges. Physiol. 38: 104-112.

Matthiessen L. (1886c) Über den physikalisch-optischen Bau des Auges der Cetaceen und der Fische. Pflügers Arch. ges. Physiol. 38: 521-528.

Matthiessen L. (1887a) Beiträge zur Dioptrik der Krystallinse II. Z. vergl. Augenheilk. 5: 21-44.

Matthiessen L. (1887b) Beiträge zur Dioptrik der Krystallinse III. Z. vergl. Augenheilk. 5: 97-126.

Matthiessen L. (1887c) Über den physikalisch-optischen Bau des Auges von Cervus alcesmos. Pflügers Arch. ges. Physiol. 40: 314-323.

Matthiessen L. (1893) Über den physikalisch-optischen Bau des Auges von Knölwal (Megaptera boops, Fabr.) und Finwal (Balaenoptera musculus Comp.). Z. vergl. Augenheilk. 7: 77-101.

Meyer D.L. and Schwassmann H.O. (1970) Electrophysiological method for determination of refractive state in fish eyes. Vision Res. 10: 1301-1303.

Millodot M. and Sivak J. (1978) Hypermetropia of small animals and chromatic aberration. Vision Res. 18: 125-126.

Nakao S., Fujimoto S., Nagata R., and Iwata K. (1968) Model of refractive-index distribution in the rabbit crystalline lens. J. Opt. Soc. Am. 58: 1125-1130.

Nicol J.A.C. (1978) Studies on the eye of the stingaree Dasyatis sabina, with notes on other selachians I. Eye dimensions, cornea, pupil and lens. Cont. Mar. Sci. 21: 89-102.

Northmore D.P.M. and Dvorak C.A. (1979) Contrast sensitivity and acuity of the goldfish. Vision Res. 19: 255-261.

Northmore D., Volkmann F.C., and Yager D. (1978) Vision in fishes: color and pattern. In The Behavior of Fish and Other Aquatic Animals (ed. by Mostofsky D.I.), pp. 79-136. Academic Press, New York.

Nuboer J.F.W., Bos N., van Genderen-Takken H., van den Hoeven H., and van Steenbergen J.C. (1979) Retinoscopy and chromatic aberration. Experientia 35: 1066-1067.

Nuboer J.F.W. and van Genderen-Takken H. (1978) The artifact of retinoscopy. Vision Res. 18: 1091-1096.

O'Gower A.K. and Mathewson R.F. (1967) Spectral sensitivity and flicker fusion frequency of the lemon shark, Negaprion brevirostris. In Sharks, Skates, and Rays (ed. by Gilbert P.W., Mathewson R.F., and Rall D.P.). Johns Hopkins Press, Baltimore.

Oswaldo-Cruz E., Hokoç J.N., and Sousa A.P.B. (1979) A schematic eye for the opossum. Vision Res. 19: 263-278.

Parrish R.K. (1972) An Introduction to Visual Optics. Am. Acad. Ophthal. Otolar., Rochester, Minnesota.

Penzlin H. and Rönicke H. (1976) Zur Dioptrik des Teleosteerauges [Towards the dioptric of the teleostean eye]: Untersuchungen am Flußbarsch (Perca fluviatilis Linnaeus 1758), an der Regenbogenforelle (Salmo gairdneri Richardson 1836) und am Goldfisch (Carassius auratus auratus Linnaeus 1758). Zool. Jb. Physiol. 80: 413-431.

Phillipson B. (1969) Distribution of protein within the normal rat lens. Invest. Ophthal. 8: 258-270.

Piggins D.J. (1970) Refraction of the harp seal, Pagophilus groenlandicus (Erxleben, 1777). Nature 227: 78-79.

Polyak S. (1957) The Vertebrate Visual System. Univ. Chicago Press, Chicago.

Pumphrey R.J. (1961) Concerning vision. In The Cell and Organism (ed. by Ramsay J.A. and Wigglesworth V.B.), pp. 193-208. Cambridge Univ. Press, London.

Riggs L.A. (1965) Visual acuity. In Vision and Visual Perception (ed. by Graham C.H.), pp. 321-349. Wiley, New York.

Rochon-Duvigneaud A. (1943) Les Yeux et la Vision des Vertébrés. Masson et Cie, Paris.

Sadler J.D. (1973) The focal length of the fish eye lens and visual acuity. Vision Res. 13: 417-423.

Schwassmann H.O. (1968) Visual projection upon the optic tectum in foveate marine teleosts. Vision Res. 8: 1337-1348.

Schwassmann H.O. (1975) Refractive state, accommodation, and resolving power of the fish eye. In Vision in Fishes: New Approaches to Research (ed. by Ali M.A.), pp. 279-288, Plenum Press, New York.

Schwassmann H.O. and Meyer D.L. (1971) Refractive state and accommodation in the eye of three species of Paralabrax (Serranidae, Pisces). Vidensk. Meddr dansk naturh. Foren. 134: 103-108.

Sidman R.L. (1957) The structure and concentration of solids in photoreceptor cells studied by refractometry and interference microscopy. J. biophys. biochem. Cytol. 3: 15-30.

Sivak J.G. (1973) Interrelation of feeding behavior and accommodative lens movements in some species of North American freshwater fishes. J. Fish. Res. Board Can. 30: 1141-1146.

Sivak J.G. (1974a) The refractive error of the fish eye. Vision Res. 14: 209-213.

Sivak J.G. (1974b) Accommodation of the lemon shark eye (Negaprion brevirostris). Vision Res. 14: 215-216.

Sivak J.G. (1975) Accommodative lens movements in fishes: movement along the pupil axis vs movement along the pupil plane. Vision Res. 15: 825-828.

Sivak J.G. (1976a) Optics of the eye of the "four-eyed fish" (Anableps anableps). Vision Res. 16: 531-534.

Sivak J.G. (1976b) The accommodative significance of the "ramp" retina of the eye of the stingray. Vision Res. 16: 945-950.

Sivak J.G. (1976c) The role of a flat cornea in the amphibious behavior of the blackfoot penguin (Spheniscus demersus). Can. J. Zool. 54: 1341-1345.

Sivak J.G. (1978a) Refraction and accommodation of the elasmobranch eye. In Sensory Biology of Sharks, Skates, and Rays (ed. by Hodgson E.S. and Mathewson R.F.), pp. 107-116. ONR, Dept. Navy, Arlington, Virginia.

Sivak J.G. (1978b) Optical characteristics of the eye of the spiny dogfish (Squalus acanthias). Rev. Can. Biol. 37: 209-217.

Sivak J.G. (1978c) Errata to Sivak (1976b). Vision Res. 18: 613.

Sivak J.G. and Bobier W.R. (1978) Chromatic aberration of the fish eye and its effect on refractive state. Vision Res. 18: 453-455.

Sivak J.G. and Gilbert P.W. (1976) Refractive and histological study of accommodation in two species of sharks (Ginglymostoma cirratum and Carcharhinus milberti). Can. J. Zool. 54: 1811-1817.

Sivak J.G. and Howland H.C. (1973) Accommodation in the northern rock bass (Ambloplites rupestris rupestris) in response to natural stimuli. Vision Res. 13: 2059-2064.

Sivak J.G., Lincer J.L., and Bobier W. (1977) Amphibious visual optics of the eyes of the double-crested cormorant (Phalacrocorax auritus) and the brown pelican (Pelecanus occidentalis). Can. J. Zool. 55: 782-788.

Sivak J.G. and Millodot M. (1977) Optical performance of the penguin eye in air and water. J. comp. Physiol. 119: 241-247.

Sivak J.G. and Piggins D.J. (1975) Refractive state of the eye of the polar bear (Thalarctos maritimus Phipps). Norw. J. Zool. 23: 89-91.

Somiya H. and Tamura T. (1973) Studies on the visual accommodation in fishes. Japan. J. Ichthyol. 20: 193-206.

Springer S. (1950) Natural history notes on the lemon shark, Negaprion brevirostris. Texas J. of Sci. 2: 349-359.

Sroczyński S. (1976a) Die chromatische Aberration der Augenlinse der Regenbogenforelle (Salmo gairdneri Rich.) [Chromatic aberration of crystalline lens in rainbow trout (Salmo gairdneri Rich.)]. Zool. Jb. Physiol. 80: 432-450.

Sroczyński S. (1976b) Untersuchungen über die Wachstumsgesetzmäßigkeiten des Sehorgans beim Hecht (Esox lucius L.) [Investigations on the growth regularity of the organ of sight on pike (Esox lucius L.)]. Arch. Fisch Wiss. 26: 137-150.

Sroczyński S. (1977) Spherical aberration of crystalline lens in the roach, Rutilus rutilus L. J. comp. Physiol. 121: 135-144.

Tamura T. (1957) A study of visual perception in fish, especially on resolving power and accommodation. Bull. Jap. Soc. Sci. Fish. 22: 536-557.

Tamura T. and Wisby W.J. (1963) The visual sense of pelagic fishes especially the visual axis and accommodation. Bull. Mar. Sci. Gulf Carib. 13: 433-448.

Tscherning M. (1898) Optique Physiologique. Paris.

Vakkur G.J. and Bishop P.O. (1963) The schematic eye in the cat. Vision Res. 3: 357-381.

Verrier M.L. (1927) Sur la réfraction statique de l'oeil chez les poissons. Comptes Rendus Hebdom. des Séances Acad. Sci. 185: 1070-1072.

Verrier M.L. (1928) Recherches sur les yeux et la vision des poissons. Bull. Biol. Fr. Belg. Suppl. XI: 1-222.

Verrier M.L. (1930) Contribution à l'étude de la vision chez les sélaciens. Ann. Sci. Nat. Zool. XIII: 5-54.

Verrier M.L. (1934) La réfraction de l'oeil des poissons. Bull. Soc. Zool. Fr. 59: 535-538.

Von Helmholtz H. (1924) Treatise on Physiological Optics (trans. from 3rd German ed. of 1909 by Southall J.P.C.). Amer. Opt. Soc.

Walls G.L. (1942) The Vertebrate Eye and its Adaptive Radiation. Cranbrook Inst. Sci., Bloomfield Hills, Michigan.

Wang C.S.J. (1968) The eye of fishes with special reference to pigment migration. Ph.D. diss., Cornell Univ., Ithaca, New York.

Weale R.A. (1974) Natural history of optics. In The Eye, Vol. 6: Comparative Physiology (ed. by Davson H. and Graham L.T. Jr.), pp. 1-110. Academic Press, New York.

Westheimer G. (1970) Image quality in the human eye. Optica Acta 17: 641-658.

Westheimer G. (1972) Optical properties of vertebrate eyes. In Handbook of Sensory Physiology VII/2: Physiology of Photoreceptor Organs (ed. by Fuortes M.G.F.), pp. 449-482. Springer-Verlag, Berlin.

Westheimer G. (1979) The spatial sense of the eye. Invest. Ophthalmol. Visual Sci. 18: 893-912.

Zar J. (1974) Biostatistical Analysis. Prentice-Hall, Englewood Cliffs, New Jersey.

Zigman S. and Gilbert P.W. (1978) Lens colour in sharks. Exp. Eye Res. 26: 227-231.

SECURITY CLASSIFICATION OF THIS PAGE (When Data Entered)

REPORT DOCUMENTATION PAGE

READ INSTRUCTIONS BEFORE COMPLETING FORM

1. REPORT NUMBER

2. GOVT ACCESSION NO. AD-A084 847

3. RECIPIENT'S CATALOG NUMBER

4. TITLE (and Subtitle)
Physiological Optics of the Eye of the Juvenile Lemon Shark (Negaprion brevirostris).

5. TYPE OF REPORT & PERIOD COVERED
Technical Rept. 1979-1980

6. PERFORMING ORG. REPORT NUMBER

7. AUTHOR(s)
Robert Edward Hueter

8. CONTRACT OR GRANT NUMBER(s)
N00014-75-C-0173

9. PERFORMING ORGANIZATION NAME AND ADDRESS
Rosenstiel School of Marine and Atmospheric Science, University of Miami, 4600 Rickenbacker Causeway, Miami, Florida 33149

10. PROGRAM ELEMENT, PROJECT, TASK AREA & WORK UNIT NUMBERS
NR 083-060

11. CONTROLLING OFFICE NAME AND ADDRESS
Commander Ronald C. Tipper
Biological Oceanography (Code 484), Dept. of Navy, ONR, NSTL Station, Mississippi 39524

12. REPORT DATE
1980

13. NUMBER OF PAGES
145

14. MONITORING AGENCY NAME & ADDRESS(if different from Controlling Office)

15. SECURITY CLASS. (of this report)
Unclassified

15a. DECLASSIFICATION/DOWNGRADING SCHEDULE

11 May 80

16. DISTRIBUTION STATEMENT (of this Report)
Approved for public release, distribution unlimited

12 156

17. DISTRIBUTION STATEMENT (of the abstract entered in Block 20, if different from Report)
Approved for public release, distribution unlimited

18. SUPPLEMENTARY NOTES
14 UM-RSMAS-80003

19. KEY WORDS (Continue on reverse side if necessary and identify by block number)
Vision, shark biology, schematic eye, physiological optics, refractive state, visual acuity, aquatic eye, Negaprion brevirostris

20. ABSTRACT (Continue on reverse side if necessary and identify by block number)
A schematic eye for the eye of the average juvenile lemon shark inhabiting Florida Bay, a shallow marine environment marked by high turbidity, was constructed. The crystalline lens in this eye is the sole refractive element, with an overall equivalent refractive index of 1.664 and a principal power of approximately +140 diopters. The eye is hypermetropic by nearly +3 diopters in seawater, although retinoscopic measurements of the refractive state of this eye average +7.5 diopters. Sources of this discrepancy are evaluated.

over

DD FORM 1 JAN 73 1473 EDITION OF 1 NOV 65 IS OBSOLETE
S/N 0102-014-6601

405515

SECURITY CLASSIFICATION OF THIS PAGE (When Data Entered)

4.1 ft

MICROMETERS PER DEG

20. Retinal magnification factor (RMF) in this eye is 164 μm/° visual angle; minimum separable angle (MSA) predicted from the RMF and average intercone distance is approximately 4.1' but this type of visual acuity will be adversely affected by the hypermetropia. Even so, the slight hypermetropia and observed intraocular opacity of these eyes are probably secondary to the poor quality of their photic environment.